Analysis of immunity signalling pathways in rice (*Oryza sativa*)

Inaugural-Dissertation

zur

Erlangung des Doktorgrades

der Mathematisch-Naturwissenschaftlichen Fakultät

der Universität zu Köln

vorgelegt von

Joel Fernandes

aus Goa

Köln, December 2022

Diese Arbeit wurde durchgeführt am Max-Planck-Institut für Pflanzenzüchtungsforschung in Köln in der Abteilung für Pflanze-Mikroben Interaktionen (Direktor: Prof. Dr. P. Schulze-Lefert), Arbeitsgruppe Prof. Dr. Jane Parker, angefertigt.

The work described in this thesis was conducted under the supervision of Prof. Dr. Jane Parker at the Max Planck Institute for Plant Breeding Research (Department of Plant-microbe interactions, Director: Prof. Dr. P. Schulze-Lefert)

Gutachter*innen:	Prof. Dr. Jane E. Parker
	Prof. Dr. Stanislav Kopriva
Prüfungsvorsitzender:	Prof. Dr. Gunther Döhlemann
Tag der mündlichen Prüfung:	15 February 2023

Summary

Major crop innovations in agriculture rely on understanding how crop immune systems are controlled and how immunity receptors defend against pathogens. Plant pathogens translocate effectors (virulence factors) into plant cells to dampen immunity and increase pathogen growth inside the plant. Research efforts are focused mainly on understanding defence networks in the model plant *Arabidopsis thaliana (A. thaliana).* Probing and verifying the conservation of *A. thaliana* gene networks in crop genomes is an important step towards generating the next generation of crops that are resilient to environmental changes and not compromising on yield.

Polymorphic nucleotide-binding leucine-rich repeat (NLR) receptors control effector triggered immunity (ETI) [1]. NLRs are divided into coiled-coil (CC) domain NLRs (CNLs) and Toll-Interleukin1 Receptor (TIR) domain NLRs (TNLs) [2]. The EDS1 lipase-like protein family (EDS1, PAD4 and SAG101) is well studied in *Arabidopsis thaliana* (*A. thaliana*) as essential signal transducers for TNLs and to transcriptionally reprogram defence and stress hormone pathways in ETI. *TNL*s and the downstream immunity genes *SAG101* and *NRG1s* which act as a helper NLRs, have a central role in eudicot immunity but have been lost in monocots [3–5]. Why co-functioning immunity genes (*ADR1*, *EDS1*and *PAD4*) are retained with only CNL sensors and some TIR-domain proteins in monocots, such as *Oryza sativa* (*O. sativa*), is not understood and represents the central research question I addressed in my PhD project .

Rice has a diverse CNL receptor repertoire to defend against pathogens such as the blast fungus *Magnaporthe oryzae pv oryzae* (*Mo*), and other pathogens such as *Xanthomonas oryzae* to test my PhD question. Based on knowledge from *A. thaliana* immunity hubs, I generated rice CRISPR-Cas9 mutants in *OsEDS1*, *OsPAD4*, *OsADR1* and *OsICS1* genes. These mutant lines were crossed to generate combinatorial mutants in order to investigate immunity networks in rice. I first assessed

physiological and developmental traits of my mutants under non-triggered conditions (unstressed greenhouse grown plants). *Oseds1pad4* double mutant lines exhibited stunting and autoimmunity, which is not observed in *A. thaliana eds1pad4* double mutants. I performed RNA-seq analysis of the rice mutants which revealed immunity gene modulation (CNLs and phytohormone pathway genes) as well as genes affecting development in *Oseds1pad4* plants. Basal immunity to virulent *Mo* and *Xanthomonas oryzae* isolates required *EDS1* and *PAD4* as demonstrated by infection assays of single mutants. All tested CRISPR-Cas9 mutants were not compromised in CNL ETI to *Mo* effector AVRPia but were susceptible to a weakly recognized effector variant AVRPiaR43G, suggesting that the *OsEDS1, OsPAD4* and *OsADR1* genes are needed for full tissue-level immunity. Heterologous expression of OsEDS1, OsPAD4 and OsADR1 did not cause host cell death was not observed when these proteins were expressed. The results presented in this thesis provide new insights into the genetic and molecular architecture of a conserved hub (*EDS1*-family genes with *ADR1*) in rice innate immunity. Functional, structural and molecular insights and identification of upstream and downstream processes are important to understand this module better towards engineering sustainable crops

Table of Contents

Acknowledgements

Thanks a lot Jane for accepting me as your PhD student, I still celebrate the day you agreed to my proposal (20th of September). You have always been there whenever I have needed your support emotionally when experiments did not go right (by saying "it's going to be fine Joel!!!"), professionally ("let me know what you need Joel and I will make it happen") and personally (by saying "if I were you, I would not do that").

I would like to thank my thesis committee Prof. Dr. Stanislav Kopriva and Prof. Dr. Gunther Doehlemann for taking your time out to critically evaluate my thesis and give your valuable inputs.

Thanks a lot, to all my JP group members. Thank you, Jaqueline, for all your help, support and patience every time I asked "Where do I find this or where can I find this mutant/plasmid". Thanks to all the past members, Deepak, Dmitry, Jingde Xinhua, Friedrike and Patrick who helped me ease seamlessly into the lab. Thanks a lot, to all the current members, Fede, Junli, Fei, Giuliana, Henni, Anthony Charles, Lara and Oliver. You being there saved me a lot of money on therapy!! Thanks a lot for amazing working atmosphere, patience and a lot of feedback in the various JP group meetings which I always managed to overshoot the allotted time. I would also like to thank Zarah and Paul for agreeing to be supervised by me.

I would also like to thank Dr. Thomas Kroj for your supervision and constant support, critical advice and allowing me to carry a part of my work at your lab. I am truly honored to have you supervise me and thank you for being there via zoom, phone call when I am in Cologne, or just a knock away when I am there at your lab. To all Kroj lab and INRAE members, Marie, Nutthalak, Stella, Mael, Veronique, Karine, Yuxuan, Celine and Isabelle, thanks for all the experimental help, advice and also integrate me into French culture, I definitely have you to blame for all the cheese and wine bills at the end of the month. Thanks Marie Brevet for your patience in translating the so called "Inglish" to French, you definitely made my stay in Montpellier easier! Thanks to Thomas for staying in touch and see a different perspective in life when I was in Montpellier.

Thanks to DAAD Scholarship for supporting PhD studies and thanks to PSL department for the amazing scientific community and resources to conduct my research.

A big thanks to Prof. Dr. Haitao Cui for helping me with my research by guiding me through my research questions and being very transparent with your research.

Thanks a lot, to department office staff, Sabine, Megan and Jutta, as well the administrative office staff, Priska and Heike for helping me with all the approvals, contracts and also planning the itinerary for conferences and research visits. A special thanks to Dr. Stephan Wagner for helping me integrate into the institute and guiding me through "German bureaucracy" for university matters.

Thanks to the greenhouse staff especially Aristeidis, Frank and Andreas for providing me with all the support to carry out my research.

I would like to thank Fredster Antilla for bearing with me whenever I said "Good morning" or the "ina mo" moments. Thanks for all your scientific advice, coffee discussions and above all your friendship.

Thanks to all other PSL and IMPRS colleagues for your constant support. Stephan, Noah and Pascal for the various chess sessions. Lucas for keeping my table tennis skills going. Katarina and Simone for beers at the TATA bar.

I would also like to thank the Indian community at MPIPZ, it was an honor to organize TATA-bars with you introducing our culture to MPIPZ. Thanks to Nitika, Athul, Swati and Ranju for your advice, support and generous Indian servings during lunchtime during my PhD.

A special thanks to Aarti and Ranjita for believing in me and guiding me through my PhD applications. This PhD would not have been possible if not for your constant words asking me to believe in my dream. Thanks to my friends Clive, Joylen and Raisa, though we are seas apart you have truly inspired me to better myself day after day.

Frency, thanks for being there and providing the moral support getting my PhD over the line, without your constant reminders and words of encouragement during the thesis writing process I would not have been able to do this!

Last but not the least I would like to thank my family for your support. Thanks Dad, Mom, Levette, Leona, Jonathan, Lars, Phani. I would like to thank my German mother Birgitt for all your support, your love and support definitely made my life in Cologne enjoyable. Thank you all, I would not have been able to reach this far without your support, I am truly grateful to have you in my life.

I wish Mai (MP Dias) was alive to see her grandson graduate but am sure she was always up there praying for me. I would forever hold your saying in my heart to help inspire me

"Phusko marlole pavti bhonk dhyunlear dorea udok kabar zatolem"

Abbreviations

%	percent
°C	degree Celsius
µL	microlitre(s)
µm	micrometre(s)
aa	amino acid(s)
ADP	adenosine diphosphate
ADR1	ACTIVATED DISEASE RESISTANCE 1
At	*Arabidopsis thaliana*
ATP	adenosine triphosphate
Avr-protein	avirulence protein
BLAST	Basic Local Alignment Search Tool
bp	base pair(s)
Ca^{2+}	Calcium
Cas9	CRISPR-associated protein 9
CC	coiled-coil domain
cDNA	complementary DNA
CDS	coding sequence
CFU	colony-forming unit(s)
cm	centimetre(s)
CNL	CC-domain NLR
Col-0	*Arabidopsis thaliana* accession "Columbia 0"
CRISPR	Clustered Regularly Interspaced Short Palindromic Repeats
C-terminus	carboxyl terminus
cv.	cultivar
ddH_2O	double-distilled water
DMSO	dimethyl sulfoxide
DNA	deoxyribonucleic acid
dNTP	deoxynucleoside triphosphate
dpi	day(s) post infection
DTT	dithiothreitol
EDS1	ENHANCED DISEASE SUSCEPTIBILITY 1
EDTA	ethylenediaminetetraacetic acid
EP-domain	EDS1-PAD4 domain
epss	*eds1a/pad4/sag101a/sag101b*
ETI	effector-triggered immunity
EV	empty vector
flg22	22 amino acid epitope of flagellin
fw	forward

gDNA	genomic DNA
GFP	green-fluorescent protein
gRNA	guide RNA
GW	Gateway® cloning
h	hour(s)
HA	hemagglutinin
HeLo	Fungal domain; PFAM database: PF14479
HF	High Fidelity
hpi	hour(s) post infection
HR	Hypersensitive cell death responses
HRP	horse radish peroxidase
HRT	HR to TCV
HSD	honestly significant difference
ICS1/SID2	ISOCHORISMATE SYNTHASE 1
IgG	Immunoglobulin G
IP	immunoprecipitation
JA	Jasmonic Acid
JAZ1/4	JASMONATE ZIM DOMAIN 1/4
kb	kilobase(s)
kDa	kilo Dalton
kV	kilo Volt(s)
l	litre(s)
LRR	leucine-rich repeat domain
M	molar
MAMP	Microbe-Associated Molecular Pattern
MHD	Methionine_Histidine_Aspartic Acid
MAPK	mitogen-activated protein-kinase
mg	milligram(s)
min	minute(s)
mL	millilitre(s)
MPIPZ	Max Planck Institute for Plant Breeding Research
mm	millimetre(s)
mM	millimolar
Mo	*Magnaporthe oryzae pv. oryzae*
mRNA	messenger RNA
ms	millisecond(s)
MYA	Million years ago
Nb	*Nicotiana benthamiana*
NB-ARC	nucleotide-binding, shared by Apaf-1, R-proteins and CED-4
NB	nucleotide-binding domain
ng	nanogram(s)

NLR	nucleotide-binding and leucine-rich repeat
nm	nanometre(s)
nM	nanomolar
NOD	nucleotide-binding-oligomerization domain
NPR1/3/4	NON-EXPRESSOR OF PR GENES 1/3/4
NRG1	N REQUIREMENT GENE 1
nt	nucleotide(s)
N-terminus	amino terminus
o/n	overnight
OD_{600}	optical density at 600 nm
Os	*Oryza sativa*
p35S	35S promoter from *Cauliflower Mosaic Virus*
PAD4	PHYTOALEXIN-DEFICIENT 4
PAGE	polyacrylamide gel electrophoresis
PAMP	pathogen-associated molecular pattern
PCR	polymerase chain reaction
PR1	PATHOGENESIS RELATED1
PRR	pattern-recognition receptor
Pst	*Pseudomonas syringae* pv. *tomato*
PTI	pattern-triggered immunity
pv.	pathovar
RBOHD	RESPIRATORY BURST OXIDASE HOMOLOGUE D
RNA	ribonucleic acid
RNA seq	RNA-sequencing
RNL	RPW8-like CNL
ROS	reactive oxygen species
RGA4/RGA5	RESISTANCE GENE ANALOG 4/5
Roq1	RECOGNITION OF XOPQ 1
RPP8	RECOGNITION OF *PERONOSPORA PARASITICA*8
rpm	round(s) per minute
RPM1	RESISTANCE TO *P. SYRINGAE PV. MACULICOLA* 1
RPS2	RESISTANT TO *P. SYRINGAE* 2
RPS4	RESISTANCE TO *P. SYRINGAE* 4
RPW8	RESISTANCE TO POWDERY MILDEW 8
RRS1	RESISTANT TO *RALSTONIA SOLANACEARUM* 1
RT	room temperature
RT-PCR	reverse-transcriptase PCR
rv	reverse
SA	Salicylic Acid
SAG101	SENESCENCE-ASSOCIATED GENE 101
SARM1	STERILE ALPHA AND TIR MOTIF CONTAINING 1

SDM	Site directed mutagenesis
SDS	sodium dodecyl sulphate
sec	second(s)
SNC1	SUPPRESSOR OF NPR1-1, CONSTITUTIVE 1
TBS	TRIS-buffered saline
T-DNA	Transfer DNA from *Agrobacterium tumefaciens*
TEMED	tetramethyl ethylenediamine
TGW	Thousand grain weight
TIR	Toll/interleukin-1 receptor
tpm	transcripts-per-kilobase-million
TPR	Tetratricopeptide repeat
TRIS	tris(hydroxymethyl)aminomethane
UV	ultraviolet light
V	Volt(s)
v/v	volume per volume
w/v	weight per volume
WT	wild type
x	times
xg	relative centrifugal force
Xoo	*Xanthomonas oryzae pv. oryzae*
Xoc	*Xanthomonas oryzae pv. oryzicola*
YFP	yellow-fluorescent protein
ZAR1	HOPZ-ACTIVATED RESISTANCE 1

Chapter 1: Introduction

1.1 Surface and intracellular immune receptors in plants

In the environment plants interact with a plethora of microbes, pathogenic microbes reduce the plant growth while the plant growth and development are better with beneficial microbes (for example to help nutrient uptake) [6–8]. The perception predicament of beneficial vs pathogenic microbes led to the evolution of an intricate immune system that allows mutualistic interactions while defending against pathogens. Plants sense conserved pathogen-associated microbial patterns (PAMPs) such as bacterial flagellin, lipopolysaccharides, peptidoglycans, chitin and chitin derivatives in the extracellular space using plasma membrane localized pattern recognition receptors (PRRs) [9–11]. Upon PAMP perception the PRRs initiate an array of signal transduction cascades involving phosphorylation of RESPIRATORY BURST OXIDASE HOMOLOGUE PROTEIN D (RBOHD) leading to apoplastic reactive oxygen species (ROS) burst, cytosolic Ca^{2+} signalling and Mitogen-activated protein kinases (MAPKs) to induce transcriptional reprogramming leading to various physiological changes that limit pathogen growth) [9–11]. Taken together PRR-induced responses form an effective barrier against a broad range of opportunistic pathogens, classically termed as pattern- triggered immunity (PTI).

Rapidly evolving professional host adapted pathogens can thwart PTI responses by secreting virulence factors called effectors, which manipulate the host to aid pathogen colonization. In order to combat such professional pathogens, plants have evolved a second immune defense layer centered around intracellular nucleotide-binding leucine-rich repeat (NLR) receptors to recognize these secreted effectors and trigger local and systemic immune responses [12]. To this end, activated NLRs induce transcriptional reprogramming to induce immunity pathway. In addition to transcriptional re-programming, NLR-induced pathways also frequently trigger localized cell

death pathways leading to localized hypersensitive response (HR) in pathogen-infected tissues to limit host-adapted pathogen growth. Together, these NLR-dependent defense pathways against professional pathogens are termed effector triggered immunity (ETI) [13,14].

In the dicot model species *Arabidopsis thaliana (A. thaliana)*, basal immunity consisting of a weak immune response which delays virulent pathogen disease progression operates in parallel with ETI. Although basal immunity shares ETI signalling components, how basal immunity is activated and the resistance mechanism limiting pathogen growth remains elusive. Basal immunity is thought to be the combined outcome of residual PTI (after effector interference) and weak ETI [1].

1.2 NLR triggered ETI

The NLRs are a family of multidomain receptor proteins that are present in both plants and animals. These proteins share many structural features, including a central nucleotide-binding domain which is required for receptor activation and a series of C-terminal leucine-rich repeat (LRR) domain which mediate effector-recognition. Upon NLR activation, the NLR switches from a closed ADP-bound "off" state to an open ATP-bound "on" state by releasing ADP and binding ATP [14,16,17]. NLRs are divided into two major clades (together known as sensor NLRs) based on their variable N-terminal domain, toll/interleukin1 receptor (TIR) NLRs (referred to as TNLs), and coiled-coil (CC) NLRs (referred to as CNLs) [18]. CNLs (CC_R), also referred to as "helper NLRs" are a special sub-class of CNLs characterized by the presence of an N-terminal RESISTANCE TO POWDERY MILDEW 8 (RPW8) domain (also called RNLs) is required for downstream pathway signalling upon effector recognition[5,19]. NLRs were shown to harbour one/several non-canonical domains

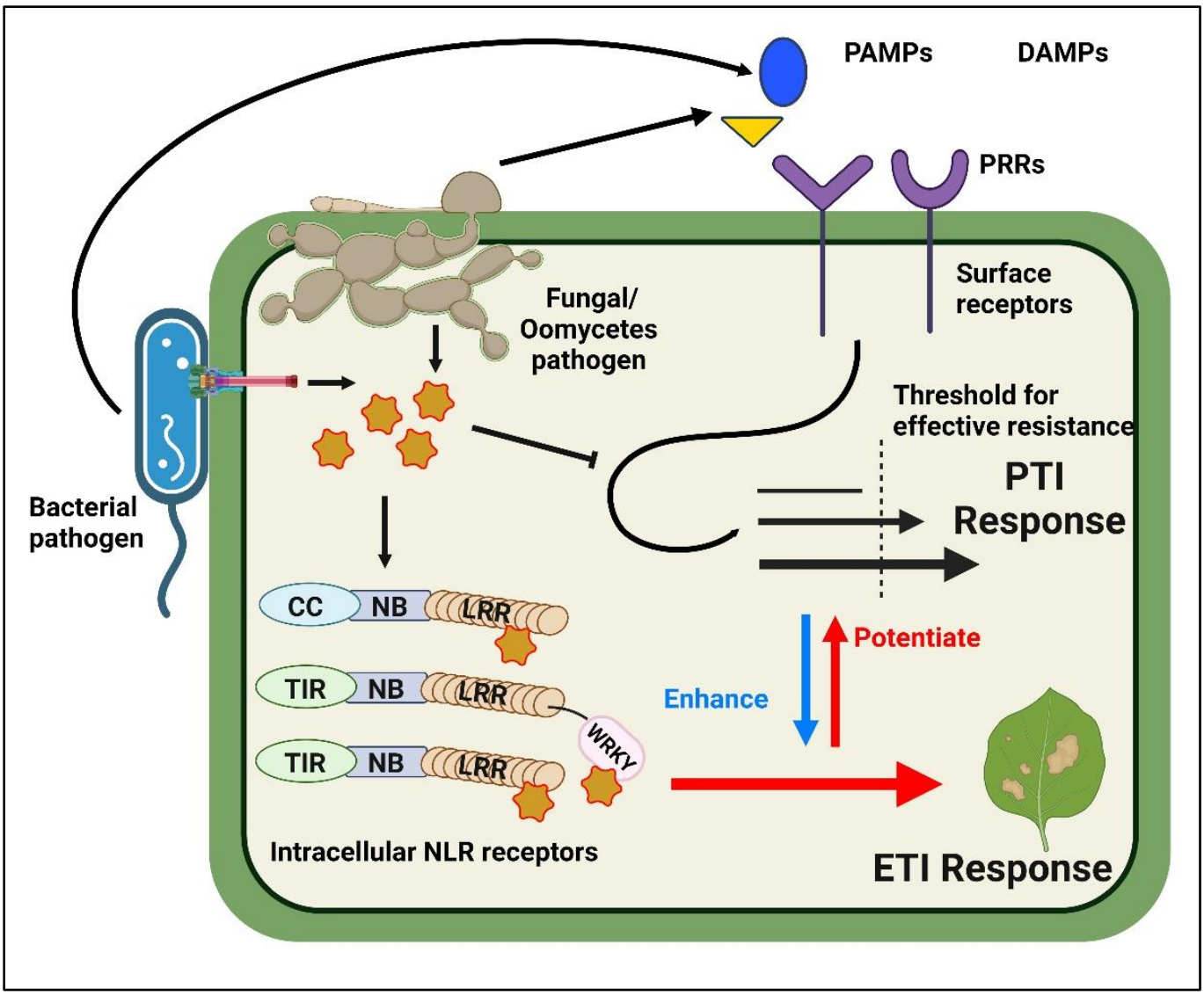

Figure 1: Plant immune system

Conserved PAMPs Bacterial, fungal and Oomycete are perceived by surface receptors recognizing conserved PAMPs crossing the threshold for an effective defence response triggering PTI. Host-adapted pathogens release effectors into the cells using type 3 secretion systems which dampens PTI responses below the threshold increasing pathogenicity. NLRs majorly classified as TNLs (N-terminal TIR domain) and CNLs (N-terminal CC domain) detect effectors with the help of LRR domains or through a guard, decoy or integrated decoy (as in the case of RESISTANCE TO PSEUDOMONAS SYRINGAE 4 (*At*RPS4) with the help of WRKY domain detecting PopP2 effector) triggers a downstream immune response termed as ETI. Effective ETI responses require a functional PTI machinery potentiating the PTI response and consequently enhancing ETI responses.

called integrated domains (IDs) which might be present between different domains (between CC and NB domain or NB and LRR domain or at the N- or C- terminus) [2].

The mechanism of effector recognition by the NLRs is not universal, however distinct molecular mechanisms have been defined. The effector-NLR interaction can be direct where a physical interaction was present. Other strategies involved the NLRs perceiving changes induced by the effector on specific plant target (explained by the guard model) or a decoy protein that mimics the actual effector target thereby serving as an effector trap (explained by the decoy model).

The IDs discussed earlier contained decoy domains of proteins targeted by effectors to recognize effectors [20–25]. These ID containing NLRs often genetically and functionally cluster together with another NLR (called paired NLRs) that is important for signalling and executing downstream defence responses such as cell death.

Different NLRs can form homo-complexes or co-operate to recognize a wide array of effectors. Paired NLRs consists of genetically linked NLR pairs in which one NLR facilitates effector recognition with the help of IDs and the other activates downstream signalling[2]. A well-studied receptor pair is the CNL-receptor pair RESISTANCE GENE ANALOG 4/5 (RGA/5). RGA4/5 function together in rice to detect *Mo* effectors AVR-Pia and AVR1-CO39 [20,26,27]. In normal plant conditions, RGA4's activity is suppressed by RGA5, but in the absence of RGA5, RGA4 induces host cell death. . RGA5 effector binding leads to a conformational change releasing RGA4 inhibition leading to a cell death response [27].

NLR-mediated signalling beyond genetically-linked pairs (sensor – executor NLRs) involves "helper NLRs" that integrates signals from multiple sensor NLRs [28]. The RNL family consisting of ACCELERATED DISEASE RESISTANCE 1 (ADR1) and N REQUIREMENT GENE 1

(NRG1) function as helper NLRs [29–35] NRG1 functions in *A. thaliana* towards TNL-ETI triggering cell death while ADR1 functions in downstream signalling towards TNL-triggered, CNL-triggered and basal immunity. In conclusion, boosting SA by ADR1 is part of a finely balanced stress hormone network [29,30,36].

1.3 TIR and CC NLRs resistosome formation drives immune signalling

Orthologs of the TIR-domains of plant TNLs are conserved across the kingdoms of life, appearing in both bacterial and archaeal genomes. possesses a NAD hydrolase which can hydrolyse nicotinamide adenine dinucleotide (NAD^+). The expression of TIR domain alone of TNLs can induce cell death in plant tissue suggesting that the domain is an important for signalling in HR responses [18]. The plant TIR domains are similar to animal and bacterial TIRs which are highlighted by the structural studies of animal STERILE ALPHA AND TIR MOTIF CONTAINING 1 (SARM1) which were similar to that of plant TIRs. SARM1 requires a conserved glutamate residue for NADase activity which when mutated had a lower NADase activity. TIR tertiary structure consists of a core β-sheet and several surrounding loops and α-helices that help interactions with other TIR domains in plants [37]. The importance of AE interfaces involving the αA and αE helices which were previously shown to be essential for oligomerization. Mutations of residues at the AE interface impaired the ability of several TIR domains and TNLs to self-associate and induce hypersensitive response (HR) [38–43]. Full length in-vitro studies of TNLs RECOGNITION OF XOPQ 1 (ROQ)1 and RECOGNITION OF *PERONOSPORA PARASITICA* 1 (RPP1) (WsB variant) bound to their cognate effectors XopQ and ATR1 (Emoy2 variant) respectively forming a tetrameric resistosome explained previous AE and other interface observations. The AE interface as shown by previous functional studies is the key interface which

is important for the two dimer formations within the tetramer. The other interface also called the "BE interface" consists of the BB-loop and the "DE surface" consisting of αD and αE helices [38]. The BB-loop in an active state is tucked in allowing a larger NAD+ binding region at the NAD+ binding site which is highly conserved and is highlighted by the impairment of NAD+ hydrolysis and HR responses upon mutations [18,39,44–48]. Upon recognition of the effectors, the TNLs oligomerize into a tetramer through the NB-ARC domains, exposing the NADase catalytic sites previously not accessible to hydrolyse NAD+ generating a variant-cyclic-ADP-ribose products (v-cADPR) towards downstream immune signalling. Some TIRs were also found to function independent of NADase, the L7TIR and RESPONSE TO HOPBA1 (RBA1) caused TIR-mediated immune responses by hydrolysing DNA/RNA using 2′,3′-cAMP/cGMP synthetases [49].

In contrast to the tetrameric TIR ROQ1 and RPP1, the CC ZAR1 resistosome in the active state forms a wheel-like pentamer complex. In the non-active state, the ZAR1 is ADP bound, upon *Xanthomonas* effector AvrAC recognition via a decoy protein kinase PBS1-like protein 2 (PBL2) detected by RKS1 pseudo kinase molecule that is bound to ZAR1 LRR domain, a conformational change occurs that releases ADP and binds ATP[16].

ATP binding induces active pentameric resistosome formation with the N-terminal α1 helix of CC domain forming a funnel shaped structure which on association to the PM acts as Ca2+ channel towards cell death responses. Mutations of the negatively charged residues involved in funnel shaped structure abolished ion transport and subsequently cell death responses highlighting the importance of this structure in immunity activation. Recent structural insights of wheat resistosome Sr35 bound to its cognate effector AvrSr35 reveal a similar pentameric resistosome formation as that of *At*ZAR1 required similar negative residues in the CC domain forming a non-selective Ca2+ channel at the PM for cell death induction [16,50]. Interestingly, the isolated CC domain of the helper

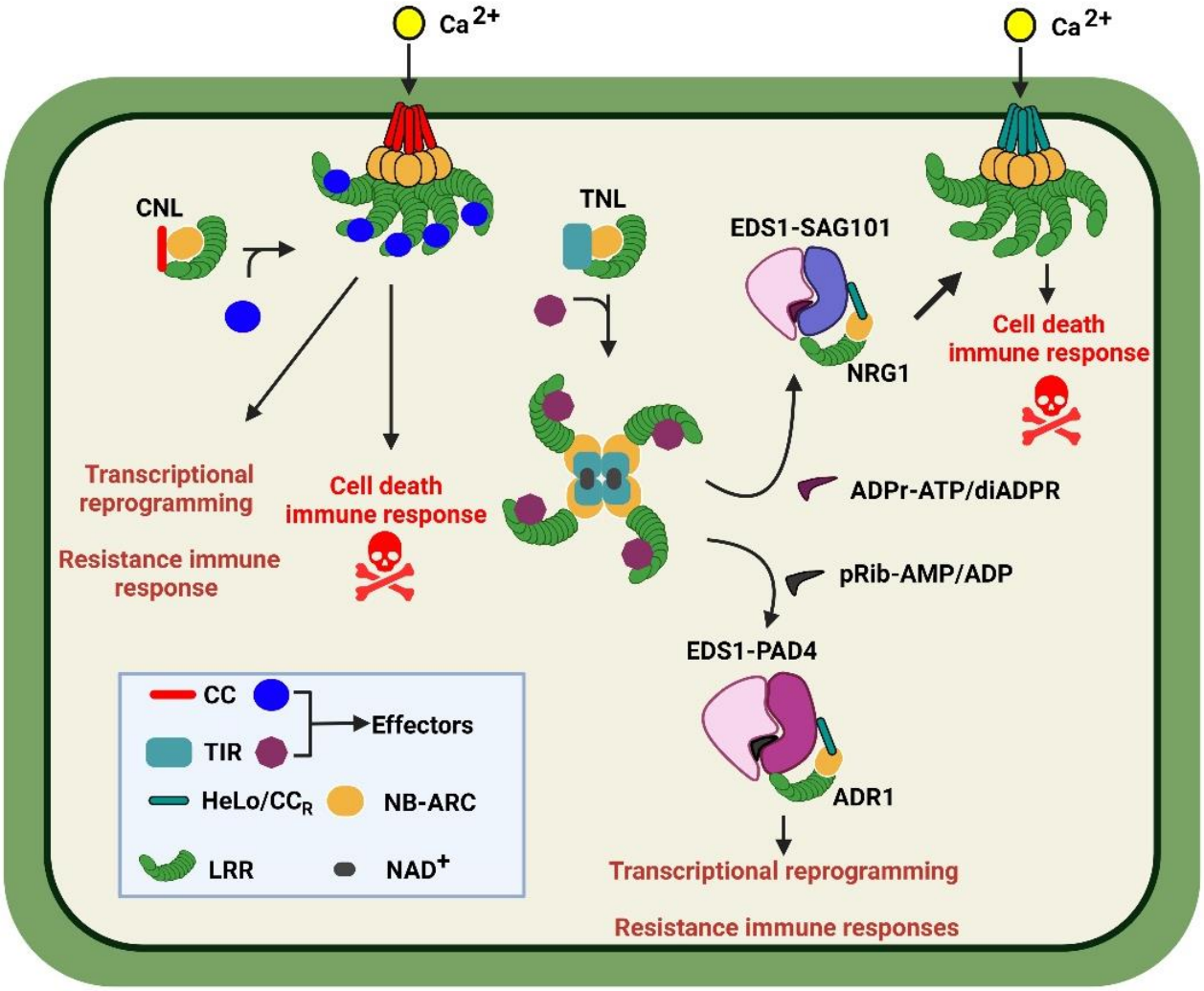

Figure2: TNL and CNL resistosome formation drives ETI

CNLs (based on ZAR1 and Sr35) oligomerize upon effector recognition by direct/indirect binding to form a pentameric resistosome in-vitro [16,50]. The resistosome has been shown to be a non-selective cationic Ca^{2+} channel which induces transcriptional reprogramming or cell death responses. The TNL resistosome in contrast to CNL resistosome forms a tetrameric structure requiring the EDS1-family proteins (EDS1, PAD4 and SAG101) signalling towards a resistance immune response or cell death responses. pRib-AMP/ADP resistosome generated small molecules activate EDS1-PAD4 heterodimer formation, activating the downstream helper NLR ADR1 while the ADPr-ATP/diADPR small molecules activate the EDS1-SAG101 heterodimer formation activating helper NLR NRG1.

CC_R *At*NRG1A formed a similar structure as that of *At*ZAR1 forming a funnel shaped tetrameric structure and required similar residues in N-terminal regions of the CC domains for channel activity and cell death induction [51].The Ca2+ influx mechanism upon Oligomerization, localization at the PM and induction of cell death was similar to *At*ZAR1 suggesting a common resistance mechanism of CNLs [51].

1.4 *EDS1* gene family signals downstream NLR activation in *A. thaliana*

In *A. thaliana* all tested TNLs [52,53] and some CNLs (RPS2, HRT and RPP8) [54] required *EDS1* for immune signalling. The EDS1-family comprising of EDS1, PHYTOALEXIN-DEFICIENT 4 (PAD4) and SENESCENCE-ASSOCIATED GENE 101 (SAG101) is a set of sequence-related immune regulators containing an N-terminal α/β-hydrolase (class-3 lipase) domain and a unique C-terminal 'EP' domain [31,55–58]. The EDS1 proteins form mutually exclusive heterodimers with its two interacting partners PAD4 or SAG101[58].

Distinct functions towards immunity for EDS1-PAD4 and EDS1-SAG101 have been genetically and biochemically defined [13,55,57–59]. EDS1–SAG101 functioning exclusively in TNL triggered ETI requires the downstream coevolved NRG1 group RNLs to regulate cell death responses while the EDS1-PAD4 requires the coevolved ADR1 group RNLs to regulate TNL and CNL triggered ETI and basal immunity responses [5,13,29,32,33,60,61]. The EDS1-PAD4 together with the ADR1 RNLs transcriptionally boosts the genetically parallel SA pathway (which can be targeted by effectors) to mediate local and systemic defences[5,61,62]. Several recent reports in our lab (Parker lab at MPIPZ) have revealed a role of EDS1-SAG101 and NRG1 RNLs towards cell death responses in TNL ETI[31,63]. Interestingly, *Atpad4* mutants phenocopy *Atadr1* mutants in ETI and basal immunity while *Atsag101* and *Atnrg1* phenocopy in ETI cell death responses [31,33,63].

Thus, EDS1-SAG101 functioning together with NRG1s and EDS1-PAD4 with ADR1s constitutes two distinct nodes that signal downstream activated NLRs [31,33,64].

1.5 Effective modulation of phytohormone pathways decides pathogen resistance

The *A. thaliana* EDS1-PAD4 node functions in parallel with the SA phytohormone pathway in resistance to biotrophic/hemi-biotrophic pathogens [57,65–67]. The major SA-biosynthesis gene *ISOCHORISMATE SYNTHASE 1 (ICS1)* accounting for ~95% pathogen induced SA accumulation partially requires EDS1-PAD4 node [13,61,68,69]. SA is produced in the chloroplasts and requires ENHANCED DISEASE SUSCEPTIBILTY 5 (EDS5, also known as *SID1*) for extrusion out of the chloroplasts. *A. thaliana eds1* and *pad4* mutants exhibited a defective pathogen activated *ICS1* and *EDS5* expression suggesting an upstream function of *EDS1* and *PAD4* to that of SA. SA accumulation in *A. thaliana* is monitored by the SA receptor NON-EXPRESSOR OF PR GENES 1 (NPR1). NPR3/4 function antagonistically to NPR1 by repressing SA responsive genes under low SA conditions. High SA levels prompt SA binding to NPR3/4 to inhibit their gene repression. A recent report showed physical binding of SA to NPR1 induced an open domain to help bind to TGACG-binding factor to stimulate SA-responsive genes) [70–74].

In *A. thaliana*, it has been demonstrated that the synthesis and signaling of jasmonic acid (JA) are upregulated and essential for mounting resistance against necrotrophic pathogens.[75,79]Necrotrophy induces biologically active jasmonoyl isoleucine (JA-Ile) production which degrade JAZs (JASMONATE ZIM DOMAIN) and CORONATINE INSENSITIVE 1 (COI1) to release the JAZ repressed JA pathway signalling master regulator MYC2 [75–77]. MYC2

binds to MEDIATOR COMPLEX 25 (MED25) to induce JA signalling genes. MYELOCYTOMATOSIS ONCOGENE HOMOLOG 2 (MYC2) was shown to suppress SA biosynthesis by binding to NAC TF[78–80]. MYC TFs induce gene transcription changes that stimulate resistance to necrotrophic pathogens and antagonize EDS1-PAD4 and SA immune pathways [13,61,81,82].

The hormonal crosstalk between SA-JA in *A. thaliana* is utilized by pathogens to increase virulence. Coronatine (COR) which is functionally similar to JA-Ile, is produced by various *Pseudomonas syringae* strains to upregulate JA signalling which downregulates SA pathways [83–85]. COR has also been shown to open stomata which aid in the bacterial infection [86]

1.6 Distribution of NLR classes and *EDS1*-family genes across seed plants

NLR-triggered-pathway functional conservation exists between monocot and eudicot though divergence occurred between 120-180 MYA. A barley (*Hordeum vulgare*) CNL, *CNL MILDEW LOCUS A* (*MLA*) when transferred to *A. thaliana* was still functional [87]. Despite this functional conservation, several differences occur between monocot and eudicot genomes, the major being the loss of *TNLs*, helper NLR family *NRG1* and *SAG101* [4,5,88,89]. The role of EDS1-SAG101 and NRG1 in TNL-triggered ETI appears to be limited to eudicot lineages because monocot and gymnosperm genomes lack these genes. In contrast, conserved *EDS1*, *PAD4*, *ADR1*, *ICS1* genes in eudicots and monocots, suggest a role in CNL ETI and/or basal immunity.

1.7 The model monocot rice to study CNL-mediated and basal immunity

Rice is consumed by more than half of the world making it an important crop. A variety of pathogens invade rice at different developmental stages such as fungi, viruses and bacteria thereby greatly reducing yields. *Mo, Xanthomonas oryzae pv oryzae (Xoo)* and *Xanthomonas*

oryzae pv. oryzicola (Xoc) represents one of the major deadly diseases in rice causing up to 100%, 50% and 32% yield losses respectively. The resistances and genes required for resistance towards these pathogens have been widely studied which gives an excellent resource to study basal and ETI. The rice Kitaake variety developed in the INRAE, Montpellier containing two NLR pairs RGA4/5 and Pikp1/2 provides an excellent resource to study rice ETI [20,26,27,90–92].

1.8 JA as the major contributor to disease resistance in rice?

In *A. thaliana* TNL-mediated ETI, the stress network is steered towards salicylic acid (SA) and against jasmonic acid JA (a hormone needed in resistance to necrotrophic pathogens and chewing insects) and abscisic acid (ABA) (needed for response to drought/osmotic stress) [13,93]. SA levels and associated defence related pathways in *A. thaliana* are strongly induced (250-1000 ng/g fw basal SA to ~20x levels of basal SA) upon hemi/biotrophic pathogen inoculation [94]. In contrast, *Oryza sativa* contains 20-30 times the basal level of SA detected in *A. thaliana* and in rice SA does not significantly increase upon pathogen inoculation (*Mo* or *Rhizoctonia solani*) [94–96]. The high level of SA in rice is attributed to oxidative stress protection [96]. Several publications have highlighted a role of JA in rice defence response pathways towards hemi-biotrophic pathogens *Mo, Xoo and Xoc*[97–101]. *Mo* effectors have also been shown to target the active components of the JA pathway which suggests that in rice the innate immunity defence response pathways might be steered towards JA phytohormone and not SA [97].

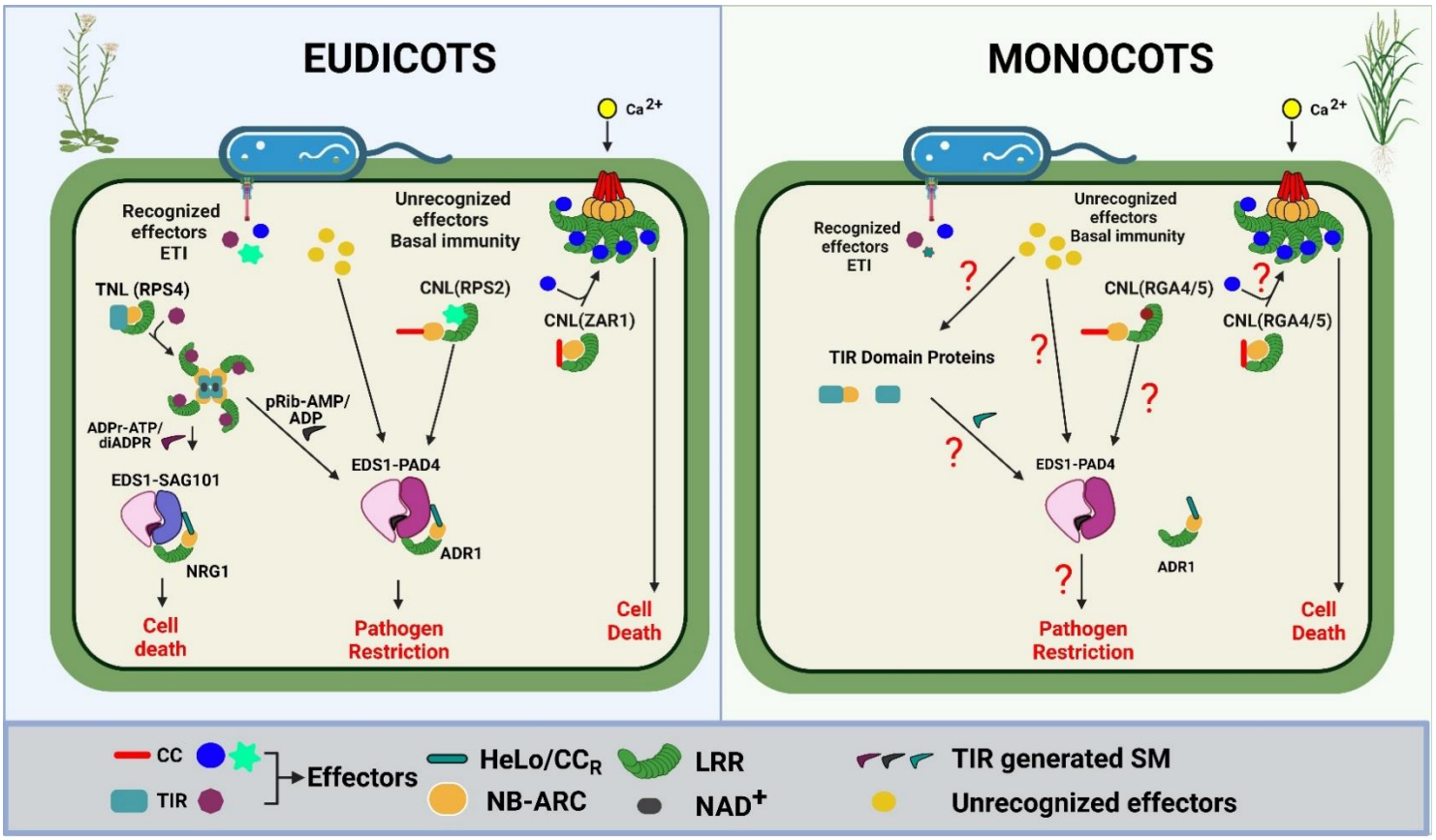

Figure 3: *TNLs, SAG101* and *NRG1* are lost while *CNLs, EDS1, PAD4* and *ADR1* are maintained in monocots

Functional studies in eudicot genomes have shown the requirement of *EDS1*-family genes upon TNL and some CNL-mediated ETI responses in *A. thaliana*. The EDS1-SAG101-NRG1 module is required for cell death responses while the EDS1-PAD4-ADR1 module is required for pathogen restriction. Though some CNLs require EDS1 family genes towards basal and ETI responses, a majority of the CNL-mediated responses were independent of EDS1-family genes. CNL *At*ZAR1 upon effector recognition oligomerizes into a pentamer, localizes to the plasma membrane inducing host cell death.

Phylogenetic studies between eudicot and monocot genomes reveal a loss of SAG101, NRG1 and TNLs in monocots while a conservation of EDS1, PAD4, ADR1 and CNLs. Using a rice cultivar containing the integrated RGA4/5 and Pikp1/2 CNL paired NLRs, the major question remains "Could *Os*EDS1, *Os*PAD4 and *Os*ADR1 function in rice basal and CNL-mediated immunity?" The presence of TIR domain containing protein could possibly produce small molecules aiding heterodimer formation signalling to pathogen restriction. Based on *A. thaliana* ZAR1 and wheat Sr35 structural insights, CNLs in rice could function independently of EDS1-family and OsADR1 proteins.

1.9 Thesis aims

In the evolutionary arms race between plants and pathogens, plants have evolved receptors to recognize pathogens while plant-adapted pathogens translocate effectors (virulence factors) into plant cells to dampen immunity. *EDS1* gene family forms a crucial signalling hub between pathogen effector recognition by NLR proteins and downstream transcriptional reprogramming [102–104]. It has been demonstrated that EDS1 is essential for plant basal defence and TNL-mediated ETI. EDS1 physically interacts with PAD4 or SAG101 to form signalling competent dimers. For various R protein-mediated ETI, distinct EDS1-PAD4 and EDS1-SAG101 complexes are required. Phylogenetic and molecular studies provide strong evidence for a TNL-specific ETI function of an EDS1-SAG101 heterodimer which cooperates with the NRG1 sub-family of signalling HeLo-NLRs to induce host cell death (HR) at infection sites [31,58]. The role of EDS1-SAG101 and NRG1 in TNL-triggered ETI appears to be limited to eudicot lineages because monocot and gymnosperm genomes lack these genes (Wagner 2013). In contrast, conserved EDS1, PAD4 and ADR1 genes in eudicots and monocots, suggest a role in CNL ETI and/or basal immunity [31,58,89].

The primary research goal for my PhD is to understand the function of *EDS1, PAD4* and *ADR1* genes in monocots utilizing rice as a model species because it is a well-established and genetically editable monocot for studying ETI and basal immunity. Using a reverse genetic approach with the help of Clustered Regularly Interspaced Short Palindromic Repeats (CRISPR)-CRISPR-associated protein 9 (Cas9) (CRISPR-Cas9) system, I created single and combinatorial mutants of the rice *OsEDS1*, *OsPAD4*, and *OsADR1* genes. I have divided up my thesis results into two sections. The first section examines the effects of *OsEDS1*, *OsPAD4*, and *OsADR1* single and combinatorial mutants on rice physiology and development. No prior information was provided for these

mutants, thus parameters such plant height, leaf emergence, flowering time, seed characteristics, photosynthetic parameters, and leaf conductance were measured. The second part of the first section examines transcriptional changes in non-triggered tissues of the mutant lines. In the second section I address the question "How are the rice combinatorial mutants of *OsEDS1*, *OsPAD4* and *OsADR1* genes affected in basal immunity and/or CNL-mediated ETI?". Here, I test the mutants for basal immune responses utilizing the *Mo*, *Xoo*, and *Xoc* pathogens as well as CNL-mediated ETI toward defined *Mo* effectors.

Chapter 2: Results

2.1 *EDS1, PAD4* and *ADR1* genes are conserved and might work as a module in rice physiology and development

One of the goals of my research is to determine how the EDS1-family of genes affects monocot immunity. Phylogenetic analysis performed on published eudicot and monocot genomes reveal a conservation of *EDS1*, *PAD4*, *ADR1* and CNLs while a loss of *SAG101*, *NRG1* and *TNLs*[4,58,89]. Though these genes share sequence similarity to corresponding *A. thaliana* genes, their role in rice physiology and development remains elusive. In this section in order to acquire a deeper understanding of the molecular function of these genes, I have knocked out these genes in rice using reverse genetic techniques, and subsequently investigated physiological and developmental traits.

2.1.1 CRISPR-Cas9 mediated knock-outs of *OsEDS1, OsPAD4* and *OsADR1* genes in rice and crossing to generate combinatorial mutants

Gene annotation was performed using online resources such as the rice genome annotation project (RGAP) (https://rice.plantbiology.msu.edu), Arabidopsis Information Resource (TAIR) (https://www.arabidopsis.org/) and Ensemble Plants (https://plants.ensembl.org/index.html). The following genes were found in the *O. sativa* genome using the above-mentioned pipeline: *OsEDS1* (LOC Os09g2245), *OsPAD4* (LOC Os11g09010), and *OsADR1* (LOC Os12g39620). These genes were confirmed via reciprocal BLAST (https://blast.ncbi.nlm.nih.gov/Blast.cgi) searches to make sure no genes were missed due to potential incomplete protein annotations in the used proteome.

The CRISPR-Cas9 technology, which has been demonstrated to edit plants with great efficiency, was used to target the conserved *OsEDS1*, *OsPAD4*, and *OsADR1* genes individually, or, in the case of *OsEDS1* and *OsPAD4* also in combination in the genome of the rice variety Kitaake (*O. sativa subsp. Japonica*) [105]. The Kitaake accession was selected as it has a fast growth cycle and contains the CNL pairs RGA4/RGA5 and Pikp1/2 which were developed as models to understand CNL-mediated immunity. The specific guide-RNAs for targeted mutagenesis were selected using online CRISPR tool (https://www.genome.arizona.edu/crispr/CRISPRsearch.html) ensuring a high on-target score, targeting the first exon and having no off-targets. *Agrobacterium*-mediated plant transformation was used in calli, and T_0 plants were genotyped using specific PCR primers for each gene. Cas9 free T_1 mutant plants were propagated to the T_2 generations. The resulting T_2 generation single mutants (*OsE1*, *OsE2*, *OsP1*, *OsP2*, *OsA1* and *OsA2*) and double mutant (*OsE3P3*) lines were confirmed using PCR amplification and subsequent Sanger sequencing.

A

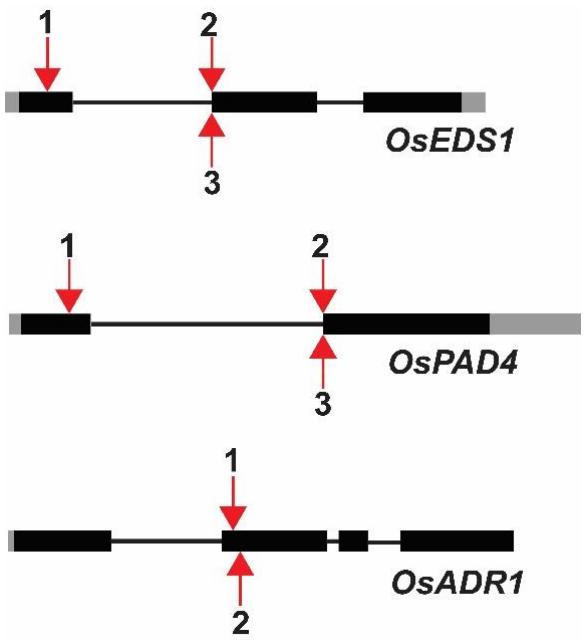

B

Mutant code	Mutant name	Mutant rice variety	Mutant origin	Deletion / Addition	Full length protein (in AA)	Mutant protein length
OsE1	*Oseds1-1*	Kitaake	Kroj/Parker Lab	250bp rearrangement	621	35
OsE2	*Oseds1-2*	Kitaake	Kroj/Parker Lab	-1	621	148
OsE3	*Oseds1-3*	Kitaake	Kroj/Parker Lab	+1	621	60
OsE4	*Oseds1-4*	Kitaake	Cui Lab	-1	621	147
OsP1	*Ospad4-1*	Kitaake	Kroj/Parker Lab	-2	536	125
OsP2	*Ospad4-2*	Kitaake	Kroj/Parker Lab	-1	536	128
OsP3	*Ospad4-3*	Kitaake	Kroj/Parker Lab	+1	536	198
OsP4	*Ospad4-4*	Kitaake	Cui Lab	+1	536	131
OsA1	*Osadr1-1*	Kitaake	Kroj/Parker Lab	+1	870	330
OsA2	*Osadr1-2*	Kitaake	Kroj/Parker Lab	-2	870	331
OsA3	*Osadr1-3*	Kitaake	Cui Lab	-1	870	335

Figure 4: CRISPR-Cas9 mediated mutagenesis of *OsEDS1*, *OsPAD4* and *OsADR1* genes

A: The conserved *OsEDS1*, *OsPAD4* and *OsADR1* genes were knocked out using a CRISPR-Cas9 protocol as described by (Miao et al., 2013). The gene diagrams for each of the edited genes are listed here. Grey box represents UTR regions, black box represents exons and the line represent introns. Each of the red arrows show the regions where a stop codon was generated as a result of a frameshift mutation. The number on the arrow represents the mutant allele generated.

B: Information list of CRISPR-Cas9 mutants generated. A more detailed curated list explains the code for each of the mutant allele, the genetic background, place where the mutants were generated, information of the deletion/addition of mutation to create a frameshift mutation and protein information before and after the CRISPR-Cas9 protocol.

In order to evaluate potential immune functions, I set up preliminary *Mo* (basal and ETI) and *Xoc* assays while genotyping and segregating the CRISPR-Cas9 mutations in the F_2 generation. Based on the preliminary assays, I hypothesized a possible redundant role of these 3 genes, a conundrum that could be addressed during my PhD studies if I quickly setup another CRISPR-Cas9 mutagenesis. Though technically viable, creating a higher order mutant (>2) utilizing the CRISPR-Cas9 gene editing approach would be challenging to segregate mutants that we Cas9-free. Since I only had a single double *OsE3P3* mutant the crossing served a dual role of generating a triple mutant and a genetic backcross (Figure 5). In the F_2 population I segregated multiple segregants of the *Oseds1pad4* (mutant segregants are subsequently named as *OsE3P3-1* and *OsE3P3-2*), *Ospad4adr1* (mutant segregants are subsequently named as *OsP3A1-1* and *OsP3A1-2*), *Oseds1adr1* (mutant segregant is subsequently named as *OsE3A1-1*) and the *Oseds1pad4adr1* (mutant segregants are subsequently named as *OsE3P3A1-1* and *OsE3P3A1-2*).

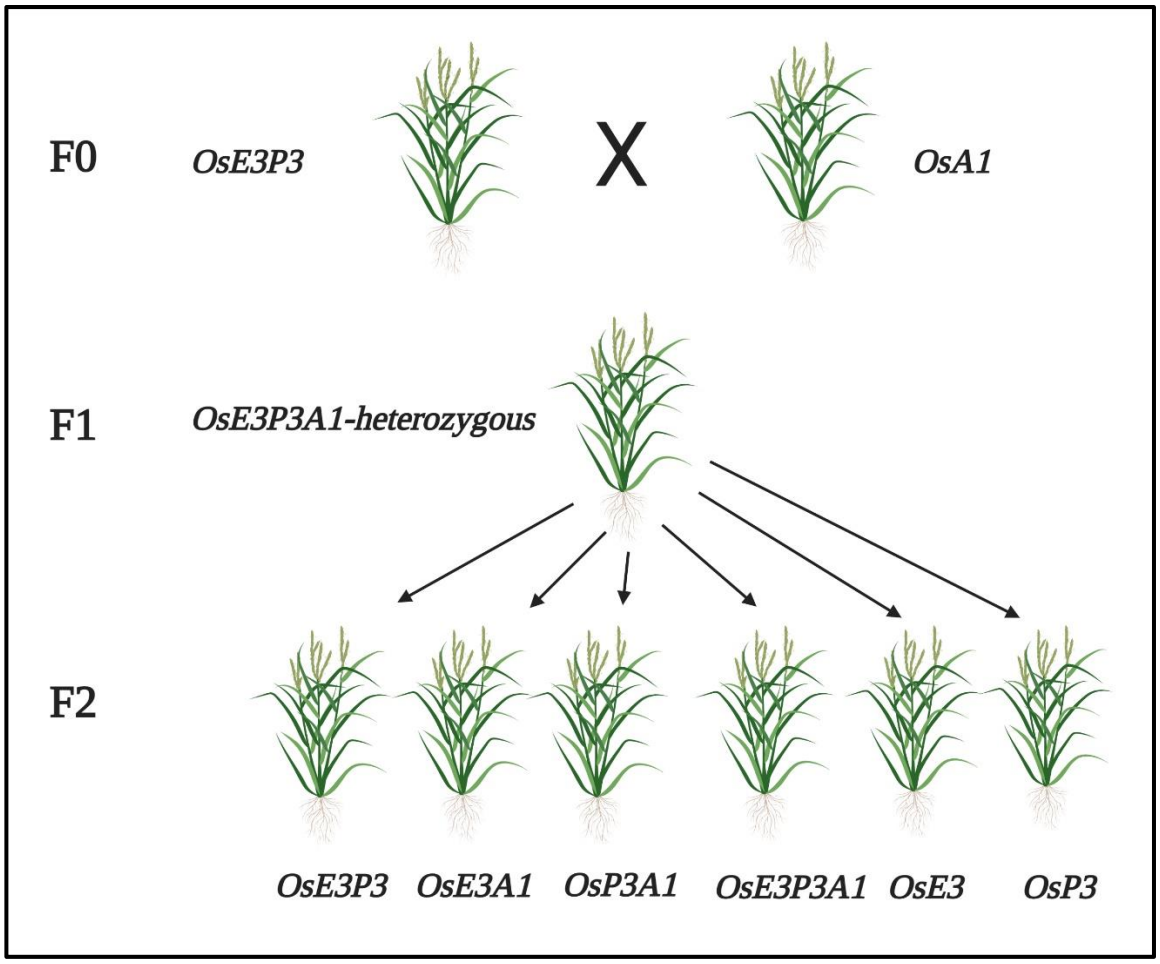

Figure 5: Crossing to generate combinatorial mutants

The double *OsE3P3* mutant was crossed to single *OsA1* mutants. The F1 plants were screened for heterozygosity and propagated for further screening. In the F2 generation the double and triple mutant combinations were confirmed using PCR-based genotyping. Please refer to materials and methods for the crossing protocol. The plants were grown and propagated in a greenhouse using the conditions described in materials and methods.

2.2 Developmental phenotypes of the generated CRISPR-Cas9 mutants

A widely accepted hypothesis on the growth-defence trade-off postulates an inverse relationship between growth and defence networks, where a persistent defence activation demands a significant number of resources. On the other hand, an impaired defence network implies a higher resource allocation towards growth. The role of *AtEDS1* in defence has been widely reported, therefore, it was of interest to assess developmental and physiological traits of healthy growing rice plants. To investigate these, I evaluated growth and yield traits such as plant height, tiller number, seed morphology and characteristics, developmental traits like leaf emergence and flowering time, and physiological traits like leaf conductance and photosystem quantum yield in the generated mutant lines.

2.2.1 *OsE3P3* mutants have various developmental phenotypes that are rescued in the *OsE3P3A1* mutant

I measured the mutant plants' heights at different stages of their growth (3,4,8,12 weeks), and I then repeated the experiment at the specific time point (Week 12). In comparison to WT plants, the single, double (excluding *OsE3P3*), and triple mutants did not exhibit any significant variation in plant height (Figure 6). The *OsE3P3* mutant plants were substantially shorter, pointing to a potential developmental function or auto-immune response associated to these genes. The potential developmental/auto-immunity role is attributed to *Os*ADR1 protein in the absence of both *Os*EDS1 and *Os*PAD4 proteins, an observation strongly supported by the rescue of the phenotype in the *OsE3P3A1* mutants. While the double *OsE3P3* mutants grew less well than the WT ZH11 plants, the single *OsE5* and *OsP5* mutants in the ZH11 rice background exhibited similar plant heights to the WT ZH11 plants (data not shown).

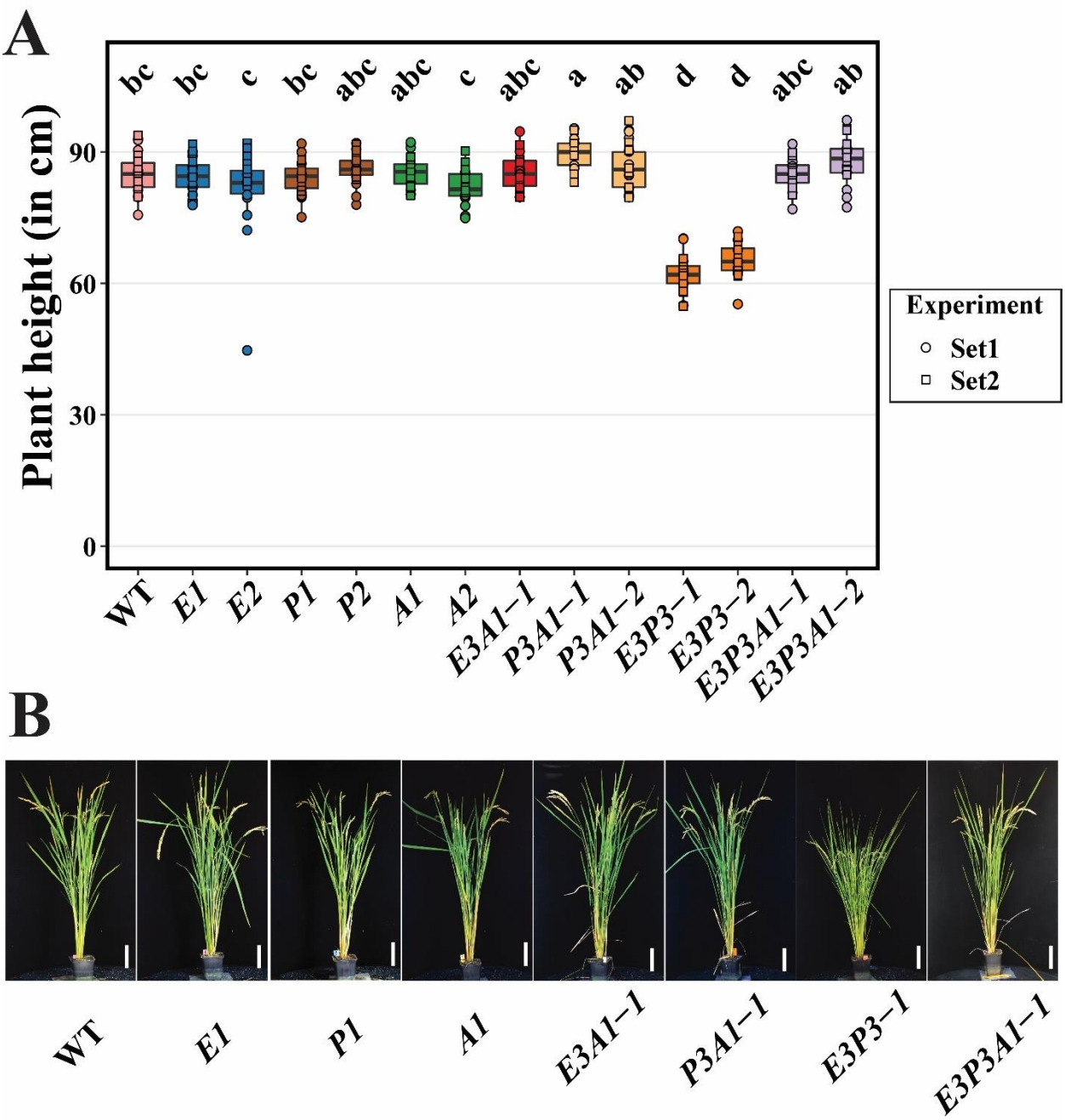

Figure 6: *E3P3* mutant plants are shorter than WT

Plant height of 12-week-old single *Oseds1* (*OsE1* and *OsE2*), *Ospad4* (*OsP1* and *OsP2*) *Osadr1* (*OsA1* and *OsA2*), double *Osedsadr1* (*OsE3A1-1*), *Ospad4adr1* (*OsP3A1-1* and *OsP3A1-2*), *Oseds1pad4* (*OsE3P3-1* and *OsE3P3-2*), triple *Oseds1pad4adr1* (*OsE3P3A1-1* and *OsE3P3A1-2*) mutants and WT (Kitaake) was measured. The plant height was measured from the base of the plant to the highest vegetative tissue.

A) Box plots show plant heights, colours indicate different genotypes. Two independent experiments were performed which are indicated by two different shapes over the box-plots. Each respective shape over the box-plot represents a biological replicate (12/genotype). Genotype-treatment combinations sharing letters above boxplots do not show statistically significant differences (Tukey HSD test, $\alpha = 0.05$, $n = 12$).

B) Photographs of 12-week-old *O. sativa* plants described in **A**. One representative picture was selected for mutants that had 2 alleles. Plants were grown in LD conditions under greenhouse conditions described in the Materials and Methods section. Scale in the bottom-right corner of the images is 10cm.

These results further supported my observations in my Kitaake mutants. Overexpression of disease resistance gene *OsWRKY67* over a certain threshold led to shorter plants and an increased resistance to *Mo* and *Xoo* [106]. In conclusion, the plant height readings in the *OsE3P3* mutants indicates an auto-active role of *Os*ADR1 protein in the absence of *Os*EDS1 and *Os*PAD4 proteins, however it is important to note that the shorter plant phenotype might be linked to an impaired developmental machinery.

2.2.2 Higher tiller number in *OsE3P3* mutants does not correspond to increased yield

The quantity of rice tillers defines plant architecture and ultimately the yield. Immoderate tiller amounts lead to a reduction in leaf area, photosynthetic efficiency and an increase in unproductive tillers while a scarce number of tillers decreases plant biomass, grain filling capacity and grain carbohydrate content [107].Depending on the time of the year the average number of weeks for the plants to fully mature (to harvest) varied from 12 to 16 weeks. I kept track of the tiller count, from week 4 until the plant reached maturity, I observed a gradual increase of tiller number from week to week (data not shown) but when Week 6 was compared to Week 12 a significant increase in the

number of tillers was observed in the *OsE3P3* mutants when compared to WT plants. The tiller number phenotypic rescue in the *OsE3P3A1* from *OsE3P3* mutants was the notable observation (Figure 9). All of the mutants showed similar tiller development except the *OsE3P3* mutants suggesting an impaired growth defect which might lead to higher productivity.

2.2.3 *OsE3P3* mutant seed morphology is in contrast to WT plant

Specific seed morphological characteristics directly affect yield. I measured the length, breadth, and TGW of seeds cultivated under standard greenhouse conditions. While seed width remained constant across WT and mutant plants, seed length changed (Figure 8A, 8B). In line with the other data, the thousand grain weight was significantly decreased in the *OsE3P3* mutants and was restored in the *OsE3P3A1* mutants (Figure 8C). Higher yield should logically follow from having more tillers, but *OsE3P3* mutants had significantly lower grain weight per plant than WT (Figure 8D). The phenotype of *OsE3P3* mutant is rescued in the *OsE3P3A1* mutant plants resembled that of WT plants, suggesting that *OsADR1* plays a role in the growth of the rice tiller.

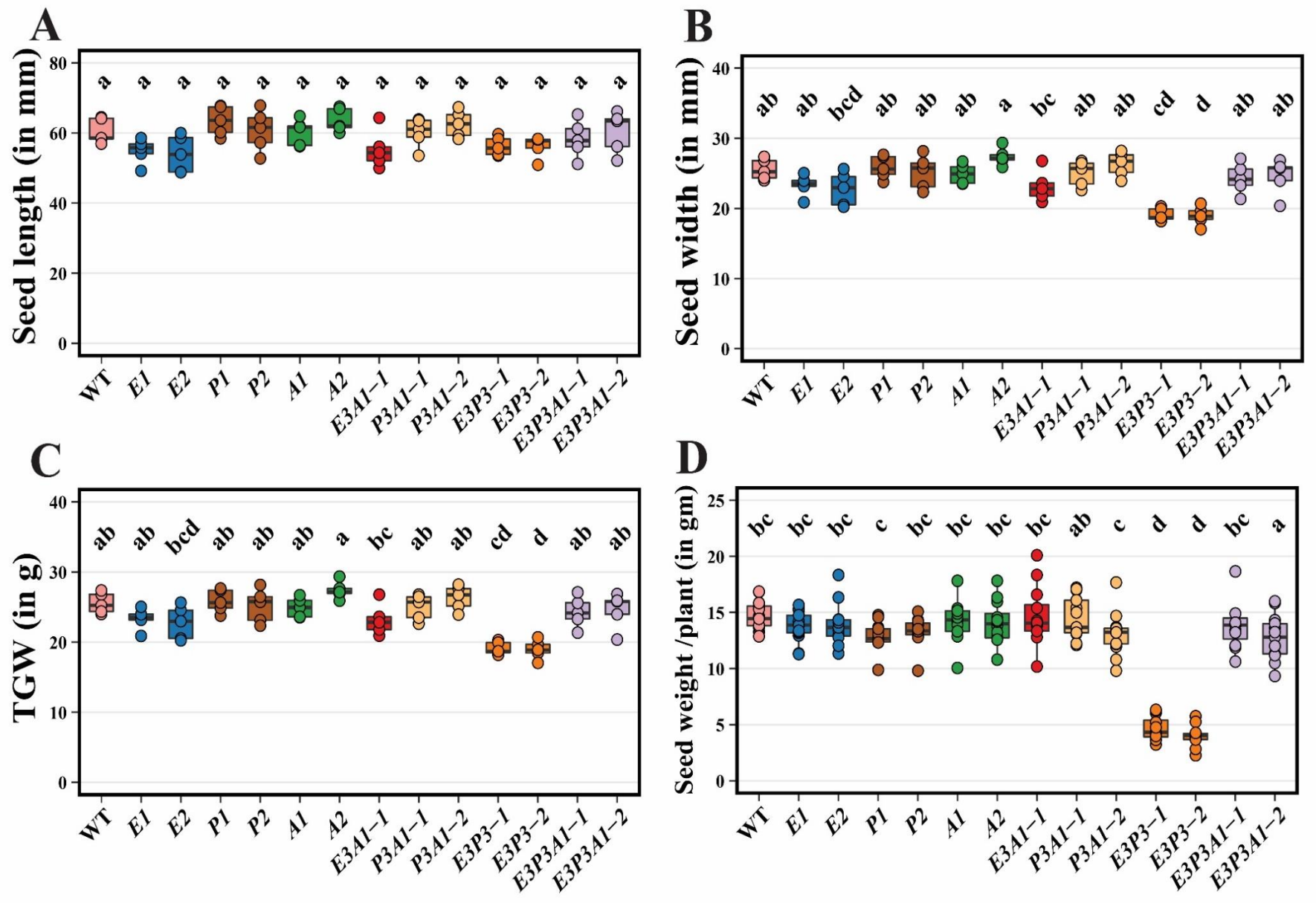
A
Seed length (in mm)
0
20
40
60
80
a a a a a a a a a a a a a a
WT E1 E2 P1 P2 A1 A2 E3A1–1 P3A1–1 P3A1–2 E3P3–1 E3P3–2 E3P3A1–1 E3P3A1–2
B
Seed width (in mm)
0
10
20
30
40
ab ab bcd ab ab ab a bc ab ab cd d ab ab
WT E1 E2 P1 P2 A1 A2 E3A1–1 P3A1–1 P3A1–2 E3P3–1 E3P3–2 E3P3A1–1 E3P3A1–2
C
TGW (in g)
0
10
20
30
40
ab ab bcd ab ab ab a bc ab ab cd d ab ab
WT E1 E2 P1 P2 A1 A2 E3A1–1 P3A1–1 P3A1–2 E3P3–1 E3P3–2 E3P3A1–1 E3P3A1–2
D
Seed weight /plant (in gm)
0
5
10
15
20
25
bc bc bc c bc bc bc bc ab c d d bc a
WT E1 E2 P1 P2 A1 A2 E3A1–1 P3A1–1 P3A1–2 E3P3–1 E3P3–2 E3P3A1–1 E3P3A1–2

Figure 8: Increased tiller numbers of *OsE3P3* mutants do not correspond to an increased yield.

A) Seed length LD grown single *Oseds1* (*OsE1* and *OsE2*), *Ospad4* (*OsP1* and *OsP2*) *Osadr1* (*OsA1* and *OsA2*), double *Osedsadr1* (*OsE3A1-1*), *Ospad4adr1* (*OsP3A1-1* and *OsP3A1-2*), *Oseds1pad4* (*OsE3P3-1* and *OsE3P3-2*), triple *Oseds1pad4adr1* (*OsE3P3A1-1* and *OsE3P3A1-2*) mutants and WT (Kitaake) plants was measured using an infrared seed counter which has a seed length measurement feature. Box plots shows the mean seed length. The mean of 50-100 seeds was calculated in a biological replicate (5 replicates/ genotype). Colours indicate different genotypes, respective shape over the box-plot represents a biological replicate (5/genotype). The genotype combinations sharing letters above boxplots do not show statistically significant differences (Tukey HSD test, $\alpha = 0.05$, $n = 5$).

B) Seed width for mutants described in **A** was measured using an infrared seed counter which has a seed width measurement feature. Box plots shows the mean seed width. The mean of 50-100 seeds was calculated in a biological replicate (5 replicates/ genotype). Colors indicate different genotypes, respective shape over the box-plot represents a biological replicate (5/genotype). The genotype combinations sharing letters above boxplots do not show statistically significant differences (Tukey HSD test, $\alpha = 0.05$, $n = 5$).

C) Thousand grain weight (TGW) was measured for mutant described in **A**. Thousand seeds/genotype were counted using a seed counter and weights measured on weighing scale. Box plots shows TGW. Colors indicate different genotypes, respective shape over the box-plot represents a biological replicate (5/genotype). The genotype combinations sharing letters above boxplots do not show statistically significant differences (Tukey HSD test, $\alpha = 0.05$, $n = 5$).

D) Total seed weight per plant was measured from plants described in A. 16 plants per genotypes were grown in the greenhouse, seeds were collected from each individual plant and weights were calculated. Box plots show total seed weights/plant. Colors indicate different genotypes, respective shape over the box-plot represents a biological replicate (12/genotype). The genotype combinations sharing letters above boxplots do not show statistically significant differences (Tukey HSD test, $\alpha = 0.05$, $n = 12$).

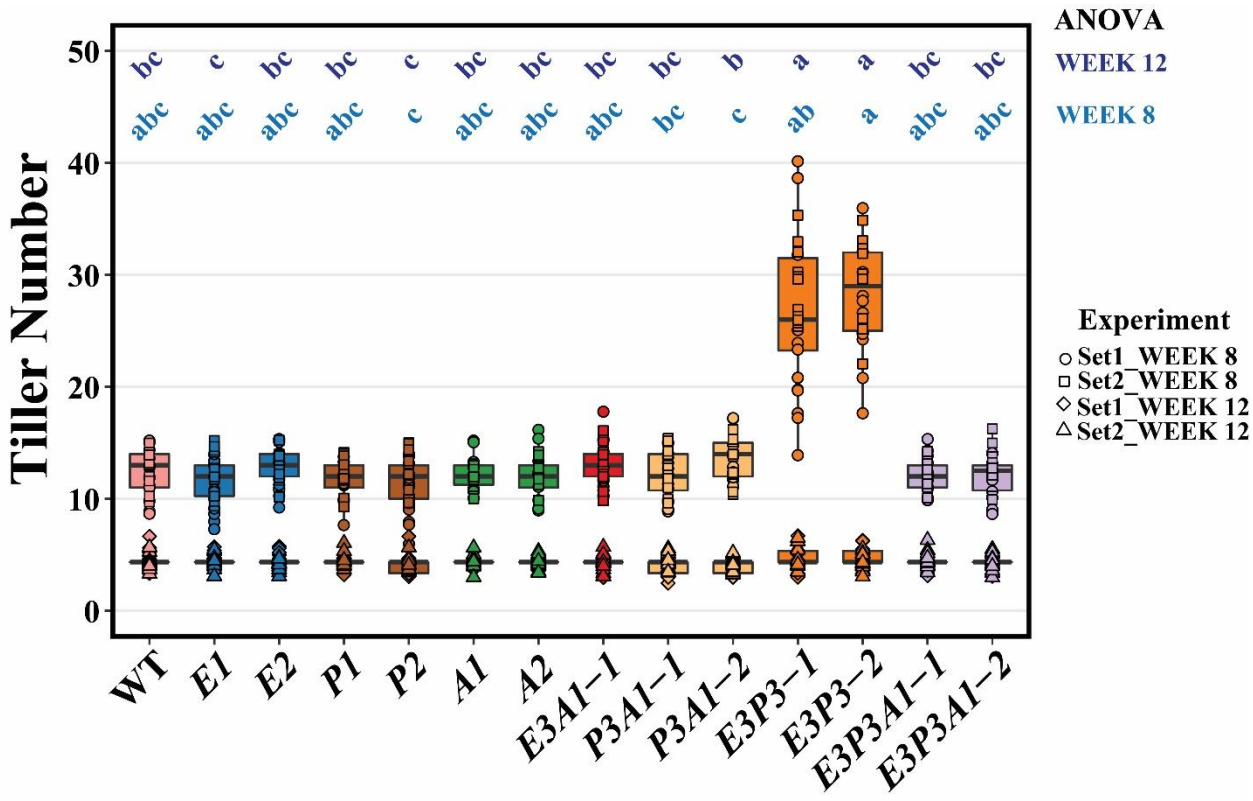

Figure 9: Number of tillers per LD greenhouse grown single *Oseds1* (*OsE1* and *OsE2*), *Ospad4* (*OsP1* and *OsP2*) *Osadr1* (*OsA1* and *OsA2*), double *Osedsadr1* (*OsE3A1-1*), *Ospad4adr1* (*OsP3A1-1* and *OsP3A1-2*), *Oseds1pad4* (*OsE3P3-1* and *OsE3P3-2*), triple *Oseds1pad4adr1* (*OsE3P3A1-1* and *OsE3P3A1-2*) mutants and WT (Kitaake) plant at Week6 and Week12. Box plots show total seed weights/plant. Colours indicate different genotypes, respective shape over the box-plot represents a biological replicate (16/genotype). The genotype combinations sharing letters above boxplots do not show statistically significant differences (Tukey HSD test, $\alpha = 0.05$, $n = 16$).

2.2.4 Flowering time is different in *OsE3P3* mutant and WT plants

The most prevalent trait shared by plants with developmental impairment and autoimmunity is shorter, stunted growth. To attribute a role of the short-stunted phenotype to development/autoimmunity, I assessed the leaf emergence phenotypes (measured by Huan index) in the mutants from Week2 onwards. In contrast to WT plants, there was no variation in leaf emergence in any of the mutants suggesting a uniform developmental stage for all the studied mutants (Figure 7A). Flowering time is one of the most significant agronomic features because it affects rice production and distribution. Genetics and environmental factors are the main determinants of flowering time [108,109]. In contrast to leaf emergence phenotypes, flowering time in *OsE3P3* mutants was significantly shorter as compared to the WT plants. The flowering time of the other mutants did not differ significantly with respect to WT plants. The plants protect deleterious fitness costs during pathogen infection by flowering early which results in early healthy seed production where bacterial infections (*Pseudomonas syringae* and *Xanthomonas campestris*) in *A. thaliana* resulted in early flowering [110]. Studies on different *A. thaliana* ecotypes on pathogens (*Verticillium spp*. and *Fusarium oxysporum)* revealed that resistant ecotype flowered later as compared to the early flowering susceptible ecotypes[111,112]. The shorter flowering time in the *OsE3P3* suggests that the plants might be not auto-immune. Other factors could also flowering time such as nutrient availability, where nitrogen promoted late flowering while phosphorous and potassium application promoted early flowering [113]. In conclusion, based on the leaf emergence measurements all of the CRISPR-Cas9 generated mutants were at the same developmental stage. The shorter flowering time in *OsE3P3* is similar to that of a susceptible plant however, this phenotype might be also due to nutrient deficiency which needs to be investigated further.

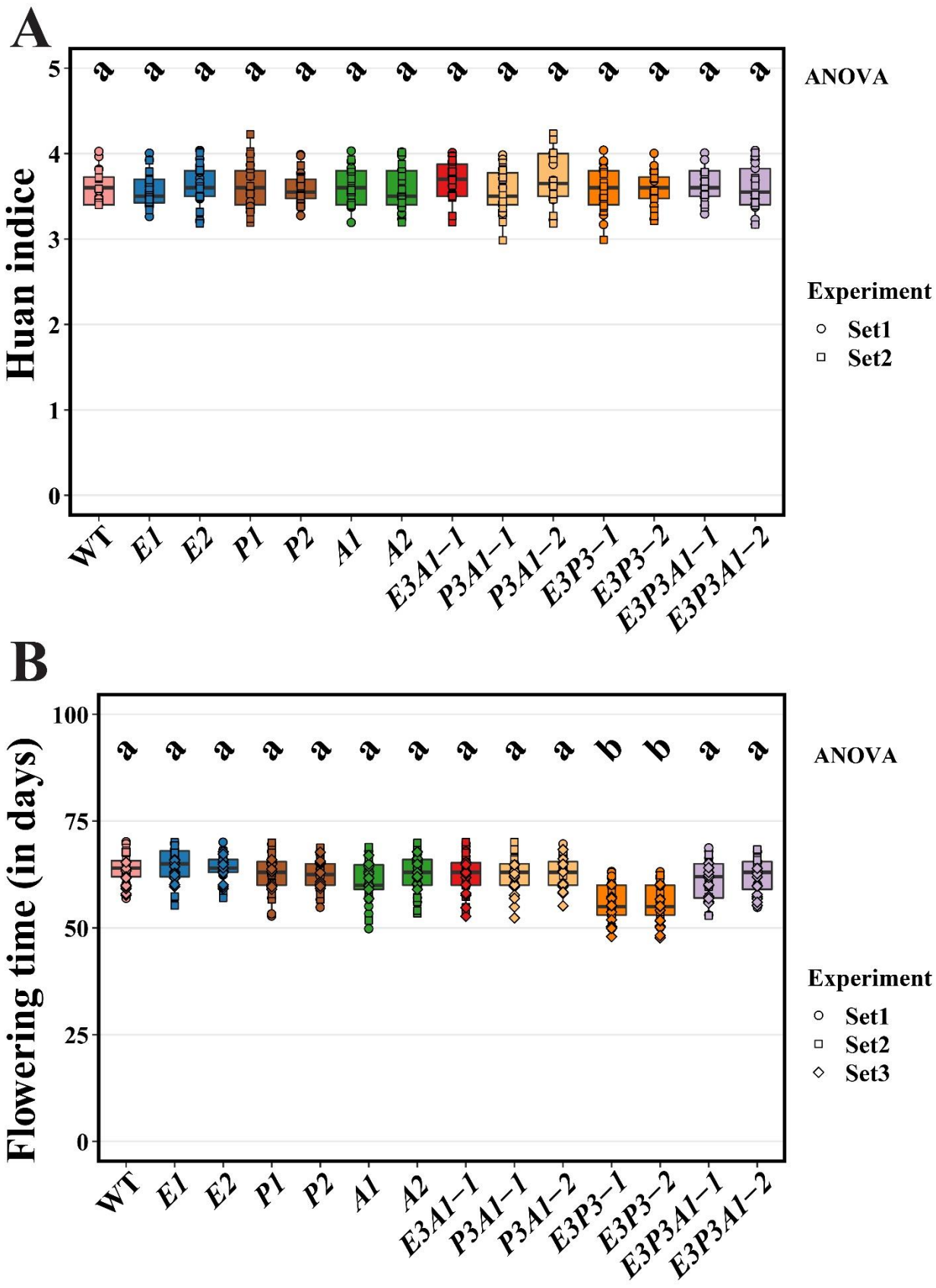
A
Huan indice
5
4
3
2
1
0
a a a a a a a a a a a a a a a
ANOVA
Experiment
Set1
Set2
WT
E1
E2
P1
P2
A1
A2
E3A1−1
P3A1−1
P3A1−2
E3P3−1
E3P3−2
E3P3A1−1
E3P3A1−2
B
Flowering time (in days)
100
75
50
25
0
a a a a a a a a a a b b a a
ANOVA
Experiment
Set1
Set2
Set3
WT
E1
E2
P1
P2
A1
A2
E3A1−1
P3A1−1
P3A1−2
E3P3−1
E3P3−2
E3P3A1−1
E3P3A1−2

Figure 7: Leaf emergence and flowering time plots of the generated rice CRISPR-Cas9 mutants

A) Leaf emergence (Huan index) of 3-week-old LD grown single *Oseds1* (*OsE1* and *OsE2*), *Ospad4* (*OsP1* and *OsP2*) *Osadr1* (*OsA1* and *OsA2*), double *Osedsadr1* (*OsE3A1-1*), *Ospad4adr1* (*OsP3A1-1* and *OsP3A1-2*), *Oseds1pad4* (*OsE3P3-1* and *OsE3P3-2*), triple *Oseds1pad4adr1* (*OsE3P3A1-1* and *OsE3P3A1-2*) mutants and WT (Kitaake) plants was measured. Box plots show plant heights, colours indicate different genotypes. Two independent experiments were performed which are indicated by two different shapes over the box-plots. Each respective shape over the box-plot represents a biological replicate (12/genotype). Genotype-treatment combinations sharing letters above boxplots do not show statistically significant differences (Tukey HSD test, $\alpha = 0.05$, $n = 12$).

B) Flowering time of plants of greenhouse grown plants described in A was calculated. Box plots shows the number of days to flag leaf emergence. Colours indicate different genotypes. Three independent experiments were performed which are indicated by three different shapes over the box-plots. Each respective shape over the box-plot represents a biological replicate (6/genotype). Genotype-treatment combinations sharing letters above boxplots do not show statistically significant differences (Tukey HSD test, $\alpha = 0.05$, $n = 6$).

2.3 Physiological phenotypes of rice single and combinatorial mutants

Analysis of photosynthesis permits characterization of the physiological state of the plant. The photosynthesis reaction involves carbon dioxide and water getting converted into glucose and oxygen. The photosynthetic efficiency can be measured using the quantum efficiency Phi2 values. Photosynthesis can also be quantified by monitoring the quantity of gases exchanged. To evaluate the physiological condition of the plant, I examined the stomatal conductance and the Phi2 values.

2.3.1 Photosystem II quantum yield is unperturbed in the CRISPR-cas9 mutants

Quantum yield assesses the efficiency of the Photosystem II, in a simpler term the amount of light that is converted to the available energy to break down water to be able to produce glucose (the main energy source available to the plant). I measured the Phi2 values of healthy growing rice

plants using a hand-held fluorometer. The photosynthetic machinery was not affected in the generated CRISPR-Cas9 mutants indicated by the similar values to that of the WT plants (Figure 10). I found that the *OsE3P3* mutants had higher photosynthetic efficiency than WT, and like my earlier results, the *OsE3P3A1* plant trend was similar to that of WT plants (Figure 10A). The Phi2 values of the other single mutants and the double mutants (*OsE3A1* and *OsP3A1*) did not differ significantly from those of the WT plants. There was no defect in PSII machinery which suggests that all of the mutants could photosynthesize efficiently barring *OsE3P3* mutants which had a higher efficiency which needs to be investigated further.

2.3.2 Stomatal conductance is impaired in *OsE3P3* mutant vs WT plant

To determine how actively the plant is photosynthesizing, stomatal conductance (mmol m^{-2} s^{-1}), measures the quantity of gases exchanged (mostly as H_20 vapour). When compared to WT plants, the *OsE3P3* mutants' stomatal conductance was noticeably lower. The impairment of the stomatal conductance observed in *OsE3P3* mutants was rescued in the *OsE3P3A1* mutants (Figure 10B). The stomatal conductance of the other single and double mutants (*OsE3A1* and *OsP3A1*) was comparable to that of WT plants. In conclusion the lower stomatal conductance in the *OsE3P3* mutants suggests that these plants prioritize other responses possibly immunity and not photosynthesis.

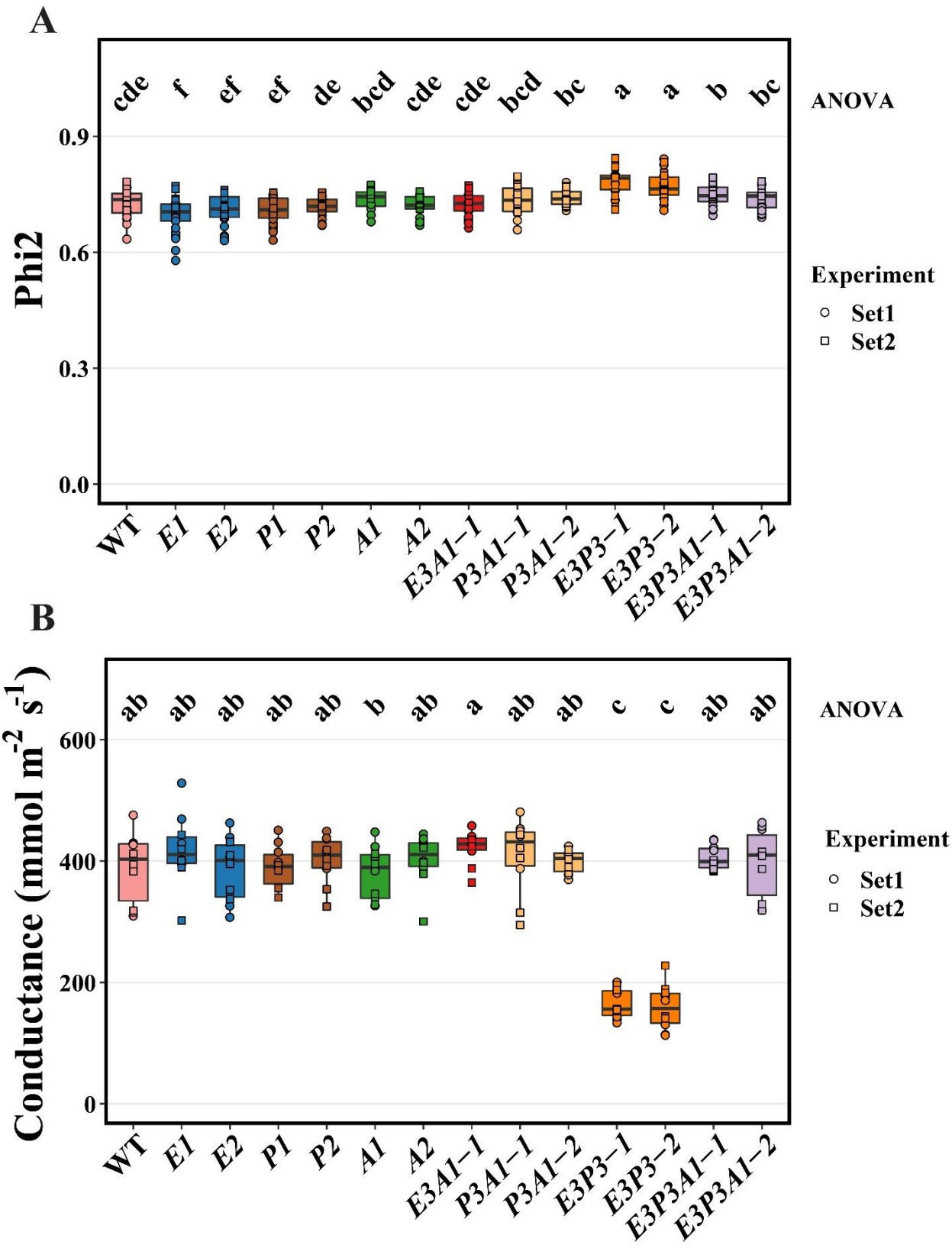
A
cde f ef ef de bcd cde cde bcd bc a a b bc
ANOVA
Phi2
0.9
0.6
0.3
0.0
Experiment
Set1
Set2
WT E1 E2 P1 P2 A1 A2 E3A1−1 P3A1−1 P3A1−2 E3P3−1 E3P3−2 E3P3A1−1 E3P3A1−2
B
ab ab ab ab ab b ab a ab ab c c ab ab
ANOVA
Conductance (mmol m-2 s-1)
600
400
200
0
Experiment
Set1
Set2
WT E1 E2 P1 P2 A1 A2 E3A1−1 P3A1−1 P3A1−2 E3P3−1 E3P3−2 E3P3A1−1 E3P3A1−2

Figure 10: Physiological phenotyping of the mutants to photosynthesis and stomatal conductance

A) Quantum yield of Photosystem II/ Phi2 values were measured for of 8-week-old LD grown single *Oseds1* (*OsE1* and *OsE2*), *Ospad4* (*OsP1* and *OsP2*) *Osadr1* (*OsA1* and *OsA2*), double *Osedsadr1* (*OsE3A1-1*), *Ospad4adr1* (*OsP3A1-1* and *OsP3A1-2*), *Oseds1pad4* (*OsE3P3-1* and *OsE3P3-2*), triple *Oseds1pad4adr1* (*OsE3P3A1-1* and *OsE3P3A1-2*) mutants and WT (Kitaake) plants using the MultispeQ V 2.0 handheld fluorometer. Box plots show Phi2 values, colours indicate different genotypes. Two independent experiments were performed which are indicated by two different shapes over the box-plots. Each respective shape over the box-plot represents a biological replicate (5/genotype). Genotype-treatment combinations sharing letters above boxplots do not show statistically significant differences (Tukey HSD test, $\alpha = 0.05$, $n = 5$).

B) Stomatal conductance was measured in 8-week-old mutants using the SC-1 leaf porometer. Box plots show porometer readings measured from 15:00 hrs during the summer season in Cologne, colours indicate different genotypes. Two independent experiments were performed which are indicated by two different shapes over the box-plots. Each respective shape over the box-plot represents a biological replicate (5/genotype). Genotype-treatment combinations sharing letters above boxplots do not show statistically significant differences (Tukey HSD test, $\alpha = 0.05$, $n = 5$).

2.3.3 *Os*EDS1 forms a complex with *Os*PAD4 but not with *Os*ADR1

Our genetic investigation has revealed that the genes *OsEDS1*, *OsPAD4*, and *OsADR1* appear to have a unique association to rice growth and development. My next objective was to determine whether these proteins could interact with one another. Using an established *Agrobacterium*-mediated *N. benthamiana* protocol in our lab (refer materials and methods section), I expressed the proteins *Os*EDS1, *Os*PAD4 and *Os*ADR1 to verify possible interactions between these proteins. The results of the input westerns confirmed that the protein expression was successful. I performed the immunoprecipitation (IP) protocol by pulling down the proteins using anti-HA and anti-GFP beads. Previous studies have shown the interaction of *Os*EDS1 and *Os*PAD4 but have not been able to comment on the possible *Os*EDS1-*Os*PAD4-*Os*ADR1 module. The IP results support the interaction between *Os*EDS1 and *Os*PAD4 (Figure 11A), however *Os*ADR1 did not

interact with either *Os*EDS1 or *Os*PAD4 in any combination (Figure 11B). *Os*EDS1 and *Os*PAD4 interacted when *Os*EDS1, *Os*PAD4, and *Os*ADR1 were expressed together (Figure 11B), but *Os*ADR1 did not interact with these combinations, which is observed when *Os*EDS1 or *Os*PAD4 GFP-pulled proteins showed *Os*EDS1 and *Os*PAD4 interaction (Figure 11B) but the HA-pulled *Os*ADR1 did not show any *Os*EDS1 or *Os*PAD4 interaction (data not shown but assay was performed). Importantly, these protein interactions were identified in tissue that was not immune-triggered. It is therefore plausible that *Os*EDS1, *Os*PAD4, and *Os*ADR1 may assemble to create a module under triggered conditions. Another possibility is that *Os*ADR1 might be activated by a by-product of *Os*EDS1 and *Os*PAD4 interaction. It's also crucial to remember that these proteins were produced in *N. benthamiana*, raising the risk of interference by native *N. benthamiana* proteins. Studies in my lab here at MPIPZ have shown that buffer conditions also play a huge role and possibly changing buffers during IP assays might help better understand the interactions. The last theory could be verified in rice protoplast assays using these tagged proteins.

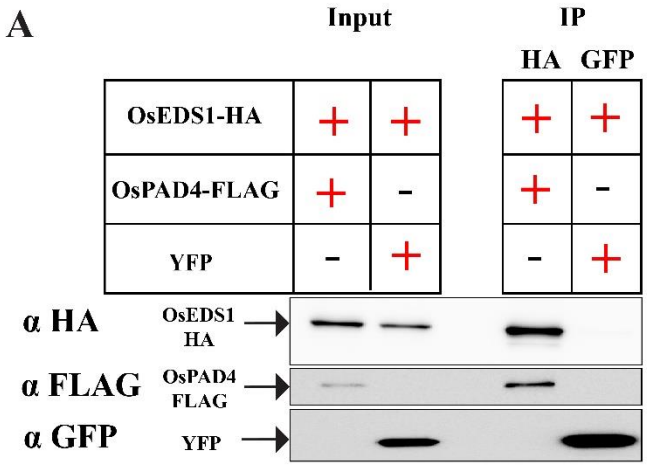
A
Input
IP
HA GFP
OsEDS1-HA
OsPAD4-FLAG
YFP
α HA
OsEDS1 HA
α FLAG
OsPAD4 FLAG
α GFP
YFP

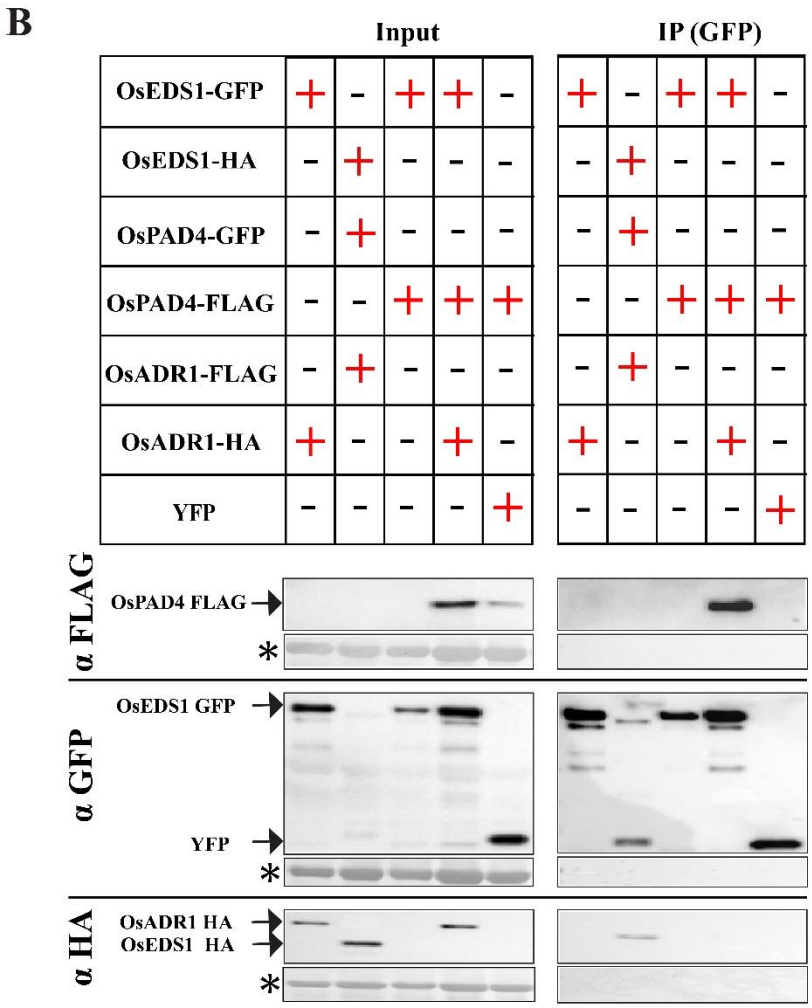
B
Input
IP (GFP)
OsEDS1-GFP
OsEDS1-HA
OsPAD4-GFP
OsPAD4-FLAG
OsADR1-FLAG
OsADR1-HA
YFP
α FLAG
OsPAD4 FLAG
α GFP
OsEDS1 GFP
YFP
α HA
OsADR1 HA
OsEDS1 HA

Figure 11: Transient protein expression in *N. benthamiana* to check associations by immuno-precipitation.

Coimmunoprecipitation assay (IP) to test interaction between *Os*EDS1, *Os*PAD4 and *Os*ADR1 using a p35S promoter driven *Os*EDS1-GFP, *Os*EDS1-HA, *Os*PAD4-FLAG, *Os*PAD4-GFP, *Os*ADR1-FLAG and *Os*ADR1-HA constructs were expressed using a *Agrobacterium tumefaciens* dependent transient expression assays in *N. benthamiana*. Samples were taken from infiltrated leaf areas at 2 d. The IP protocol for samples 1-7 was performed using α-GFP beads and for samples from 8-14 using α-HA beads. *Os*PAD4-FLAG interaction with YFP and *Os*EDS1-HA interaction with YFP were used as negative controls for α-GFP and α-HA IPs respectively. Experiments were performed two times independently with similar results. Ponceau S staining (mark with a ***** sign) of the input samples used for IP served as control for equal loading. The expected regions of the expressed proteins are marked using arrows.

A) Interaction of *Os*EDS1 and *Os*PAD4 proteins

B) Interaction of *Os*EDS1, *Os*PAD4 and *Os*ADR1 proteins

2.4 Explaining developmental phenotypes observed in *OsE3P3* mutants by probing the transcriptome

To search for potential differences in the transcriptomes of the *OsEDS1*, *OsPAD4* and *OsADR1* single, double and triple mutants, I performed an RNAseq analysis on the leaves of unstressed greenhouse grown 21-day-old soil-grown plants. Analysis of batch-corrected RNAseq data did not identify genes significantly upregulated in *OsE3P3* mutant vs other mutants or the wild type (data not shown). Since the samples were unstressed greenhouse grown plants, minor differences in gene expression over time that were identified may have contributed to the observed phenotypes. PCA analysis proved to be more informative and clearly separated the *OsE3P3* transcriptome in all three replicate samples from the other mutants and the wild-type (Figure 12).

2.4.1 Principal component analysis (PCA) distinguishes the *OsE3P3* mutant from other tested mutants and WT plant

In my RNAseq samples, the first principal component (PC1) explained 24% of the variance, whereas the PC2 samples only accounted for 10%, according to the PCA analysis (Fig. 12). The first principal component (PC1) in a PCA analysis is the linear combination of the original variables that accounts for the majority of the variation, while PC2 is the linear combination of the original variables that accounts for the majority of the remaining variation subject to being orthogonal (uncorrelated) to the first component. Between *OsE3P3* mutant and other mutants, the 24% PC1 explained variation (including WT). This explained variance is notably high given that the samples were not triggered. In the further section I will elaborate on the genes that contributed to PC1.

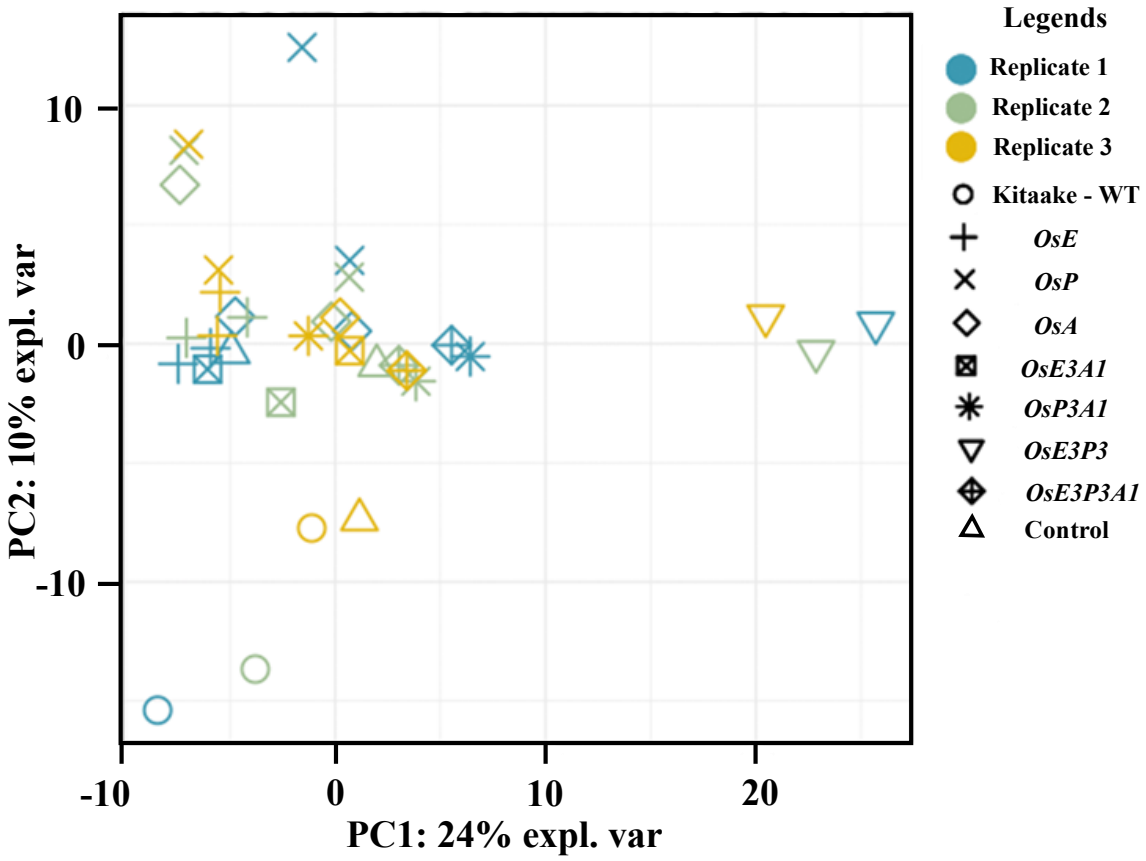

Figure 12: PCA of RNAseq data sets of non-stressed greenhouse grown plant leaves

Oseds1 (*OsE = OsE1 + OsE2*), *Ospad4* (*OsP =OsP1* and *OsP2*) *Osadr1* (*OsA =OsA1* and *OsA2*), double *Osedsadr1* (*OsE3A1-1*), *Ospad4adr1* (*OsP3A1-1*), *Oseds1pad4* (*OsE3P3-1*), triple *Oseds1pad4adr1* (*OsE3P3A1-1*) mutants and WT (Kitaake) plant RNAseq samples were used. The term "control" here pertains to a transgenic organism created specifically as a transformation control. In this context, a plasmid carrying the red fluorescent protein gene was introduced through the transformation process to validate that the procedure itself did not induce any unintended mutations.Using the mixOmics R-package a PCA analysis was performed on batch corrected samples. Three biological RNAseq sample replicates are indicated by 3 colours. The first PC (PC1), defined as the linear combination of the original variables that explains the greatest amount of variation while the second PC (PC2) is the linear combination of the original variables that accounts for the greatest amount of the remaining variation subject of being orthogonal (uncorrelated) to the first component.

2.4.2 PC1 contains genes involved in defence or growth and development

I selected the top 100 genes that explain the PC1 variance. Considering the annotation of the Kitaake variety is unique and relatively recent , I compared it to the more prevalent Nipponbare variety (RGAP and Rice annotation project database). Although a probable function for 100 of the genes was proposed, only 2 (LOC Os03g03810 and LOC Os11g31190) have been functionally characterized in rice (Table 1 and Table 2). To better understand their functions, I reverse BLASTed each of these genes to determine whether they play any roles in *A. thaliana*. On the basis of the putative annotations and the reverse BLAST protocol, I created two tables listing the genes necessary for growth and development and another list showing all the defence genes, which made up around 30% of the annotated genes.

The defence-related genes from the PC1 analysis included some predicted NLRs that have been well characterized in *A. thaliana*, including LOC Os08g29854 (homology to *A. thaliana RPM1*), LOC Os10g04090 (homology to *A. thaliana RPP13*), and LOC Os06g03500 (contains well characterized defence gene domains) (Table 1). Genes modulating defence hormones such as jasmonic acid pathway (LOC_Os11g29290, LOC_Os08g41780) and salicylic acid pathway (LOC_Os05g30454) were among the phytohormones that defined the *OsE3P3* group from the other mutants. Other notable genes that stood out were the *OsSWEET14* and LOC_Os08g07890 (homolog of *A. thaliana CIPK6*) (Table 1).

Among the developmental genes that explained the PC1 variance were genes involved in grain development and filling such as LOC_Os03g03810, LOC_Os08g07890. The cellulose synthase gene involved in the secondary cell wall formation was another gene that is contained in the PC1

PC1 ID	Locus ID	Putative function in *Oryza sativa*	Function in *Arabidopsis thaliana*
1	LOC_Os08g41780	triacylglycerol lipase precursor, putative, expressed	*AtMPL1*, Controlling green peach aphid (*Myzus persicae*) infestation on *A. thaliana* [114]
4	LOC_Os01g54670	coiled-coil domain-containing protein 25	
7	LOC_Os11g31190	nodulin *Mt*N3 family protein, putative, expressed *OsSWEET14* is negatively required for resistance to *Xoo* [115,116]	SWEET sucrose efflux transporter family proteins [117]
14	LOC_Os07g03000	Leucine-rich repeat protein kinase family protein	
17	LOC_Os05g30454	thiamin pyrophosphokinase 1, putative, expressed	Regulates the accumulation of Salicylic Acid and Immune Responses to *Pseudomonas syringae DC3000*[118]
36	LOC_Os01g16450	peroxidase precursor, putative, expressed	
43	LOC_Os10g03570	NB-ARC domain-containing disease resistance protein	
51	LOC_Os08g07890	NB-ARC domain containing protein, expressed	*AtCIPK6*, negatively regulates immunity [119]
55	LOC_Os11g29290	cytochrome P450, putative, expressed	catabolism of JA-Ile[120]
57	LOC_Os08g29854	NB-ARC domain-containing disease resistance protein	RPM1, RPS3[121]
67	LOC_Os10g04090	NB-ARC domain-containing disease resistance protein	disease resistance RPP13-like protein 1[122,123]
78	LOC_Os06g51060	CHIT8 - Chitinase family protein precursor, expressed	ATHCHIB, B-CHI, BASIC CHITINASE, CHI-B, HCHIB, PATHOGENESIS-RELATED 3, PR-3, PR3
79	LOC_Os06g03500	Disease resistance protein (CC-NBS-LRR class) family	

Table1: Defence genes explaining PC1.

The defence related genes annotated by the Rice Annotation Project Database (RAP-DB) were used to convert Kitaake annotations to RAP-DB annotations. The annotations between RAP-DB and Rice Genome Annotation Project (RGAP) can be interchanged. The current annotations are from RGAP. The PC1 ID column represents how likely the gene explains the variance (1 being most likely and 100 being less likely). Putative functions represent the possible function based on domain analysis. A reverse blast was performed to identify the *A. thaliana* genes and the last column represent the functions of the gene in *A. thaliana.*

PC1 ID	Locus ID	Putative function in *Oryza sativa*	Function in *A. thaliana*
2	LOC_Os06g1160	phosphate-induced protein 1 conserved	cell expansion in leaves [124]
5	LOC_Os03g03810	DEF8 - Defensin and Defensin-like DEFL family Grain filling Cd stress tolerance [125]	
8	LOC_Os02g09930	CSLA1 - cellulose synthase-like family A	Secondary wall formation [126]
18	LOC_Os01g65460	beta-galactosidase precursor	*At*BGAL10 β-galactosidase activity against xyloglucan[127]
20	LOC_Os01g06990	Pollen Ole e I allergen and extensin family protein precursor	elongation of root hairs [128]
31	LOC_Os02g49950	ARM repeat superfamily protein	Negatively regulates drought tolerance [129]
39	LOC_Os01g24480	DUF1399 containing protein	Arabidopsis development and stress response [130]
46	LOC_Os07g05960	expressed protein	meiotic homologous recombination[131]
50	LOC_Os08g07890	NB-ARC domain containing protein	somatic embryogenesis receptor-like kinase 1 [132,133]
74	LOC_Os07g16040	erythronate-4-phosphate dehydrogenase domain containing protein	Arabidopsis root development[134]
80	LOC_Os03g55420	peroxidase precursor	Root Epidermis Cell Differentiation [135]

Table2: Growth- and development- related genes explaining PC1

The growth- and development- related genes annotated from RGAP are listed. The PC1 ID column represents how likely the gene explains the variance (1 being most likely and 100 being less likely). Putative functions represent the possible function based on domain analysis. A reverse blast was performed to identify the *A. thaliana* genes and the last column represent the functions of the gene in *A. thaliana*

variance (Table 2). In summary, defence and development were the two major sectors affected by the mutations in *OsE3P3* mutants compared to the other mutants and WT.

2.5 Exploring contributions of *OsEDS1, OsPAD4* and *OsADR1* genes in rice ETI and basal immunity

OsEDS1 and *OsPAD4* have been previously shown to be involved in rice basal immunity towards *Mo* and *Xoo*[98,136]. The study further tested *Xoo* ETI and concluded that *OsEDS1* and *OsPAD4* are not essential for XA3/XA26 immunity [98]. When compared to WT, an overexpression line of P was found to be considerably more resistant to the *Mo* isolate Guy11 [136]. In my study I have tested the role of *OsEDS1*, *OsPAD4* and *OsADR1* in rice basal immunity towards *Mo*, *Xoo* and *Xoc* (Figure 13, 14A). Effector-triggered immunity against *Mo* was evaluated using the effectors AVRPia (Figure 14B), AVR1CO39, and AVRPikD. Partial requirement of *OsEDS1*, *OsPAD4* and *OsADR1* in CNL-triggered immunity was also tested using partially recognized effector mutant variants.

2.5.1 Role of *OsEDS1, OsPAD4* and *OsADR1* genes in *Mo* immunity

Mo is one of the most devastating and costly rice diseases causing pathogen in the world causing complete yield losses. My main goal was to investigate the basal and ETI of the rice mutants toward *Mo*. Basal immunity was investigated using the *Mo* isolate Guy11, which was isolated from French Guyana and has had its genome most extensively analysed. The Kitaake rice cultivar, which was employed in this study, has two integrated CNL pairs, RGA4/5 and Pikp1/2, which detect the effectors AVRPia and AVRPikD, respectively. I used these pairs to investigate ETI. I tested weakly recognized effector variants of AVRPia to determine whether *OsEDS1*, *OsPAD4*, and *OsADR1* play a redundant function in ETI in rice.

2.5.2 *OsE3P3* mutants display increased basal immunity to virulent *Mo*

To test the role of *OsEDS1*, *OsPAD4*, and *OsADR1* in basal immunity in rice, I used the extensively studied and fully sequenced *Mo* Guy11 strain to inoculate on my generated mutants. The method established in the Kroj lab was used to inoculate *Mo* and assess disease severity. Spore spray mimics inoculation in the wild but is highly variable. Percent lesion area (PLA) is the major published metric to determine disease susceptibility. While the single OsA1 and OsA2 mutants showed equal susceptibility to that of WT plants, the single *OsE1*, *OsE2*, *OsP1* and *OsP2* mutants (significantly for 2/3 mutants) were more susceptible to *Mo* Guy11 isolate (Figure 13A). Among the double mutants *OsP3A1-1*, *OsP3A1-2*, *OsE3A1-1* (higher susceptibility but not significant) were susceptible while the *OsE3P3-1* and *OsE3P3-2* mutants were less susceptible as compared to WT (Figure 13A). The *OsE3P3A1* triple mutant plants were susceptible as compared to WT suggesting a redundant role of *OsEDS1* and *OsPAD4* in regulating the *OsADR1* towards *Mo* basal immunity (Figure 13A).

2.5.3 *Mo* ETI towards full length effector AVRPia, AVR1CO39 and AVRPikD does not require *OsEDS1, OsPAD4* and *OsADR1*

To identify a role of *OsEDS1*, *OsPAD4*, *OsADR1* in *Mo* rice ETI, I tested the generated mutants with the published effectors AVRPia and AVRPikD which are recognized by RGA4/5 and Pikp1/2 NLR pairs respectively. I obtained the transformed effector in the Guy11 background to ensure relevant comparisons to the basal immunity results. Upon effector recognition a strong HR response is elicited towards the transformed *Mo* strain in WT plants as well as the generated mutants which negating the role of *Os*EDS1, *Os*PAD4, *Os*ADR1 proteins in rice ETI with respect to RGA4/5 and Pikp1/2 NLR pairs (Figure 13B). The positive controls were susceptible to Guy11:

AVRPia and Guy11: AVRPik-D inoculations (Data only shown for Guy11: AVRPia) (Figure 13B).

2.5.4 The *OsEDS1*, *OsPAD4* and *OsADR1* contribute partially to CNL-mediated ETI in *Mo*

In *A. thaliana* ETI triggered by the CNL receptor *AtRPS2*, *EDS1* and *ICS1*-dependent SA were found to act in a genetically redundant manner [61]. I wanted to know if *OsEDS1*, *OsPAD4*, and *OsADR1* gene functions are redundantly required to elicit ETI responses. In order to test these hypotheses, I sprayed previously published effector variants that are weakly recognized by their corresponding CNL receptors and elicit weak HR responses. The effector mutant strain Guy11:AVRPiaR43G (R43G) was transformed in the Guy11 background to ensure comparisons between FL effector and the mutant effector variant strains. Using this system, I was able to understand if there might be a role of these genes in systemic immunity as the avirulent pathogen is allowed to leave the HR sites, needed systemic immunity to arrest pathogen proliferation. The single *OsE1* and *OsE2* mutants were susceptible to the effector variant, the *OsP1* and *OsP2* mutants though susceptible were not significant while the *OsA1* and *OsA2* mutants were not significantly susceptible compared to WT (Figure 13C). These results further strengthen the role of *OsEDS1* and *OsPAD4* in basal immunity.

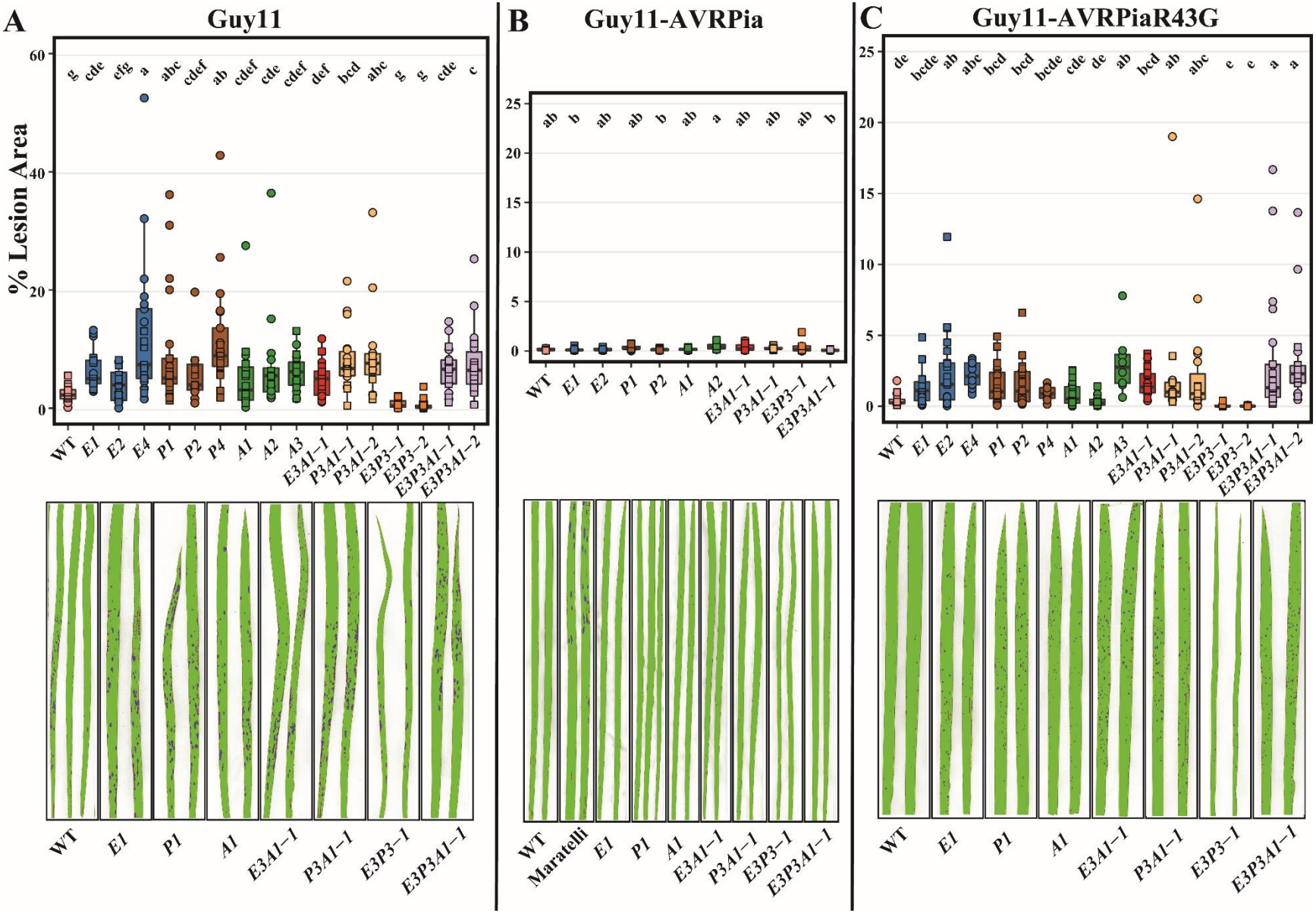
A
Guy11
% Lesion Area
WT E1 E2 E4 P1 P2 P4 A1 A2 A3 E3A1−1 P3A1−1 P3A1−2 E3P3−1 E3P3−2 E3P3A1−1 E3P3A1−2
WT E1 P1 A1 E3A1−1 P3A1−1 E3P3−1 E3P3A1−1
B
Guy11-AVRPia
WT E1 E2 P1 P2 A1 A2 E3A1−1 P3A1−1 E3P3−1 E3P3A1−1
WT Maratelli E1 P1 A1 E3A1−1 P3A1−1 E3P3−1 E3P3A1−1
C
Guy11-AVRPiaR43G
WT E1 E2 E4 P1 P2 P4 A1 A2 A3 E3A1−1 P3A1−1 P3A1−2 E3P3−1 E3P3−2 E3P3A1−1 E3P3A1−2
WT E1 P1 A1 E3A1−1 P3A1−1 E3P3−1 E3P3A1−1

Figure 13: Basal immunity but not CNL-mediated ETI requires *OsEDS1, OsPAD4* and *OsADR1* genes

A) 4-week-old LD grown single *Oseds1* (*OsE1* and *OsE2*), *Ospad4* (*OsP1* and *OsP2*) *Osadr1* (*OsA1* and *OsA2*), double *Osedsadr1* (*OsE3A1-1*), *Ospad4adr1* (*OsP3A1-1* and *OsP3A1-2*), *Oseds1pad4* (*OsE3P3-1* and *OsE3P3-2*), triple *Oseds1pad4adr1* (*OsE3P3A1-1* and *OsE3P3A1-2*) mutants and WT (Kitaake) plants were challenged with *Mo* strain Guy11. 5 days post spraying, the infected leaf was photographed and analysed using a program Leaf tool developed in INRAE, Montpellier to determine parameter such as PLA, lesion number and other lesion characteristics. The y-axis represents PLA which is the percentage of area occupied by the lesion on the leaf. Two independent experiments were performed which are indicated by two different shapes over the box-plots. Each respective shape over the box-plot represents a biological replicate (8/genotype). Genotype-treatment combinations sharing letters above boxplots do not show statistically significant differences (Tukey LSD test, $\alpha = 0.05$, $n = 5$). The bottom panel shows a representation leaf tool software generated false coloured leaf image where the lesions were indicated in blue.

B) 4-week-old LD grown plants described in A were challenged with an avirulent *Mo* strain Guy11 transformed with the Guy11: AVRPia effector to measure CNL-mediated ETI. PLA was plotted in the box plot. Two independent experiments were performed which are indicated by two different shapes over the box-plots. Each respective shape over the box-plot represents a biological replicate (8/genotype). Genotype-treatment combinations sharing letters above boxplots do not show statistically significant differences (Tukey LSD test, $\alpha = 0.05$, $n = 5$). The bottom panel shows a representation leaf tool software generated false coloured leaf image where the lesions were indicated in blue. A susceptible rice variety Maratelli is added to the panels as a positive control to the experiment.

C) 4-week-old LD grown plants described in A were challenged with AVRPia effector mutant variant Guy11:AVRPiaR43G. PLA was plotted in the box plot. Two independent experiments were performed which are indicated by two different shapes over the box-plots. Each respective shape over the box-plot represents a biological replicate (8/genotype). Genotype-treatment combinations sharing letters above boxplots do not show statistically significant differences (Tukey LSD test, $\alpha = 0.05$, $n = 5$). The bottom panel shows a representation leaf tool software generated false coloured leaf image where the lesions were indicated in blue.

The double *OsP3A1-1, OsP3A1-2* and *OsE3A1-1* (not significant) mutants were susceptible to Guy11:AVRPiaR43G while the *OsE3P3-1* and *OsE3P3-2* mutant susceptibility was similar to that of WT plants (Figure 13C). The *OsE3P3A1-1* and *OsE3P3A1-2* triple mutant plants were

susceptible as compared to WT (Figure 13C). *Os*ADR1 seems to induce auto activity in the absence of *Os*EDS1 and *Os*PAD4 . The double and triple mutant results reveal a possible role of *Os*ADR1 in systemic immunity which seems to be guarded by *Os*EDS1 and *Os*PAD4

2.5.5 Role of *OsEDS1, OsPAD4* and *OsADR1* genes in *Xanthomonas oryzae pv. oryzae (Xoo)* and *Xanthomonas oryzae pv. oryzicola (Xoc)* immunity

OsEDS1 plays an important role in disease resistance as evidenced by the susceptibility of *Oseds1* mutants to *Xoo* and *Xoc*. I expanded the previous study by testing the complete EPA module towards *Xoo* and *Xoc* basal immunity. I selected *Xoo* strains from two distinct genetic lineages based on their geographical distribution, African *Xoo* (strain MAI1) and Asian *Xoo* (strain PXO99). Despite being closely related to the African *Xoo* clade, the Asian *Xoc* strain BLS256 infects through the apoplast as opposed to the *Xoo*, which spreads through the vasculature. Together these selected *Xoo* strains represent a complete subset of the major genetic lineages and also incorporating different infection lifestyles of *Xoc*.

2.5.6 *OsE3P3* mutant is less susceptible to Asian *Xoo* than WT

I inoculated the rice mutants with the PXO99 Asian *Xoo* strain according to a standardized protocol from the Szurek lab (IRD, Montpellier, France). Pathogen disease progression is qualitatively assessed by the lesion length on the rice leaf. The Asian PXO99 *Xoo* strain was more virulent on single *OsE1, OsE2, OsP1, OsP2* mutants but not on *OsA1, OsA2* mutants as compared to WT plants (Fig. 11A). The double *OsE3A1-1*, *OsP3A1-1* and *OsP3A1-2* mutants were more susceptible as compared to WT plants while the *OsE3P3-1*, *OsE3P3-2* mutants were less susceptible to PXO99 (Figure 14A). The *OsE3P3A1-1* and *OsE3P3A1-2* mutants were susceptible

to PXO99 suggesting a possible auto-active role of *Os*ADR1 in the absence of both *Os*EDS1 and *Os*PAD4 in basal immunity towards Asian *Xoo* PXO99 (Figure 14A).

2.5.7 *OsE3P3A1* triple mutants are less susceptible to African *Xoo* vs WT plant

To understand whether the phenotypes observed towards Asian *Xoo* represent a common or clade-specific basal immunity response defect, I inoculated the rice mutants with the MAI1 African *Xoo* strain. As a negative control for lesion length water-clipped samples were used. The lesion length of the single *OsE1*, *OsE2*, *OsA1* and *OsA2* lines was longer than that of WT plants (Figure 14B). In contrast, the *OsP1* and *OsP2* mutants had significantly longer lesions than WT plants. The double *OsE3A1-1*, *OsP3A1-1* and *OsP3A1-2* mutants also showed a higher lesion length while the *OsE3P3* mutants had a lower lesion length as compared to WT plants (Figure 14A). Importantly, lesion length was higher in the *OsE3P3A1-1* and *OsE3P3A1-2* triple mutant lines compared to WT. This suggests a redundant role of *Os*EDS1 or *Os*PAD4 in regulating *Os*ADR1 basal immunity to African *Xoo* (Figure 14A).

2.5.8 *OsE3P3* mutant is less susceptible to *Xoc*

I subsequently investigated whether the EPA module is necessary for a different pathogen lifestyle with the *Xanthomonas oryzae* clade. To test this, I infiltrated the Asian *Xoc* BLS256 strain on the generated rice mutants. When compared to WT plants, the *OsA1* and *OsA2* mutants are not susceptible to *Xoc*, however the single *OsE1*, *OsE2*, *OsP1* and *OsP2* mutants are (Figure 15A). While the *OsE3P3-1* and *OsE3P3-2* mutant lesion length was comparable to that of WT plants, the *OsE3A1-1*, *OsP3A1-1* and *OsP3A1-2* double mutant lesion lengths were noticeably longer (Fig. 11C). The triple EPA mutants showed *Xoc* susceptibility, a pattern similar to *Xoo,* indicating that *Os*ADR1 might be auto-active in the absence of *Os*EDS1 and *Os*PAD4.

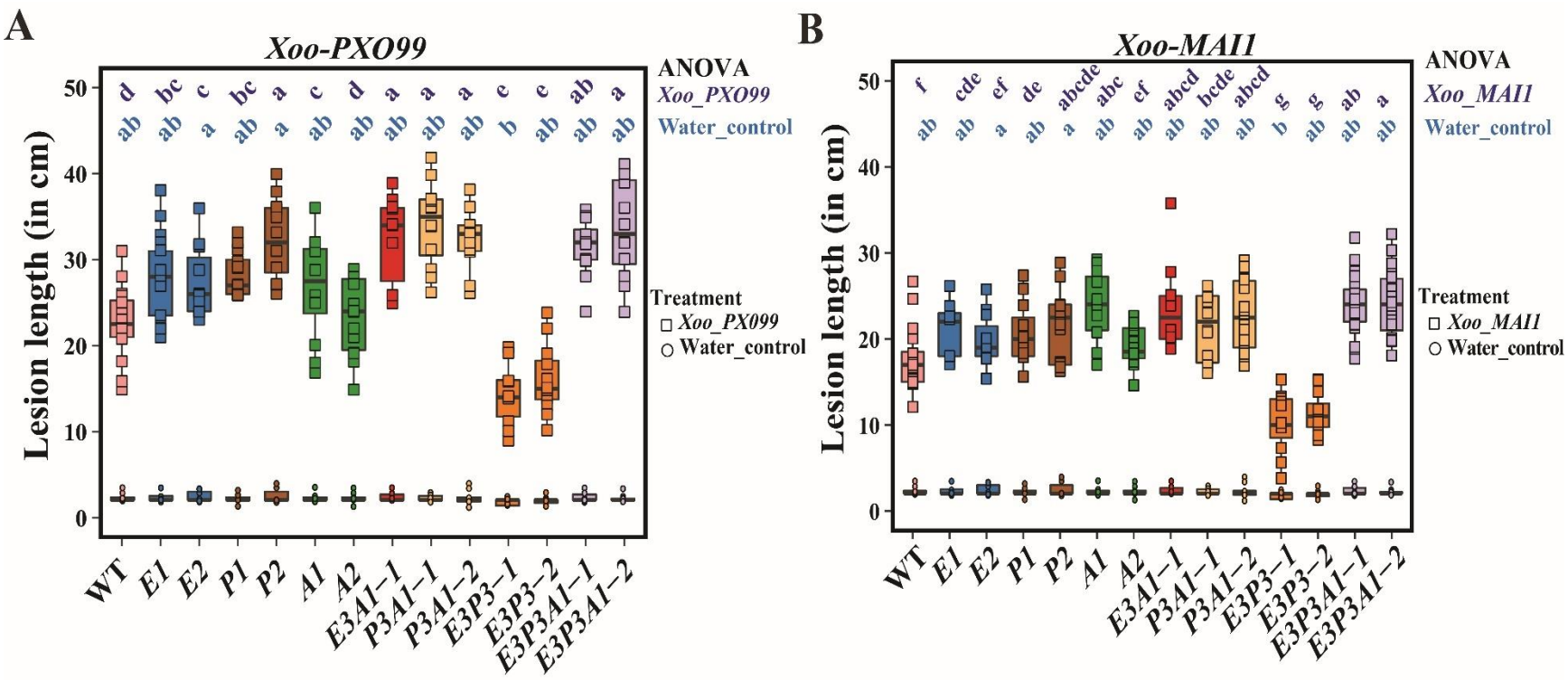

Figure14: Basal immunity towards African *Xoo* MAI1, Asian *Xoo* PXO99 and Asian *Xoc* BLS256 requires *OsEDS1*-family genes

4-5 week old single *Oseds1* (*OsE1* and *OsE2*), *Ospad4* (*OsP1* and *OsP2*) *Osadr1* (*OsA1* and *OsA2*), double *Osedsadr1* (*OsE3A1-1*), *Ospad4adr1* (*OsP3A1-1* and *OsP3A1-2*), *Oseds1pad4* (*OsE3P3-1* and *OsE3P3-2*), triple *Oseds1pad4adr1* (*OsE3P3A1-1* and *OsE3P3A1-2*) mutants and WT (Kitaake) greenhouse grown plants were leaf clipped with a 0.2 O.D of *Xoo* strain. Water leaf clipped samples were used as a negative experimental control. The lesion length was measured at 14 DPI. The box plots represent lesion length.

Each respective shape over the box-plot represents a biological replicate (16/genotype). Genotype-treatment combinations sharing letters above boxplots do not show statistically significant differences (Tukey LSD test, $\alpha = 0.05$, $n = 16$). The above and below lines of the ANOVA represent *Xoo* treated and water control significance values respectively.

I performed a bacterial CFU assay and observed that the *OsE3P3* mutants had fewer CFU values as compared to the other mutants and WT genotypes, a trend similar to that of the lesion length phenotypes (Figure 15B).

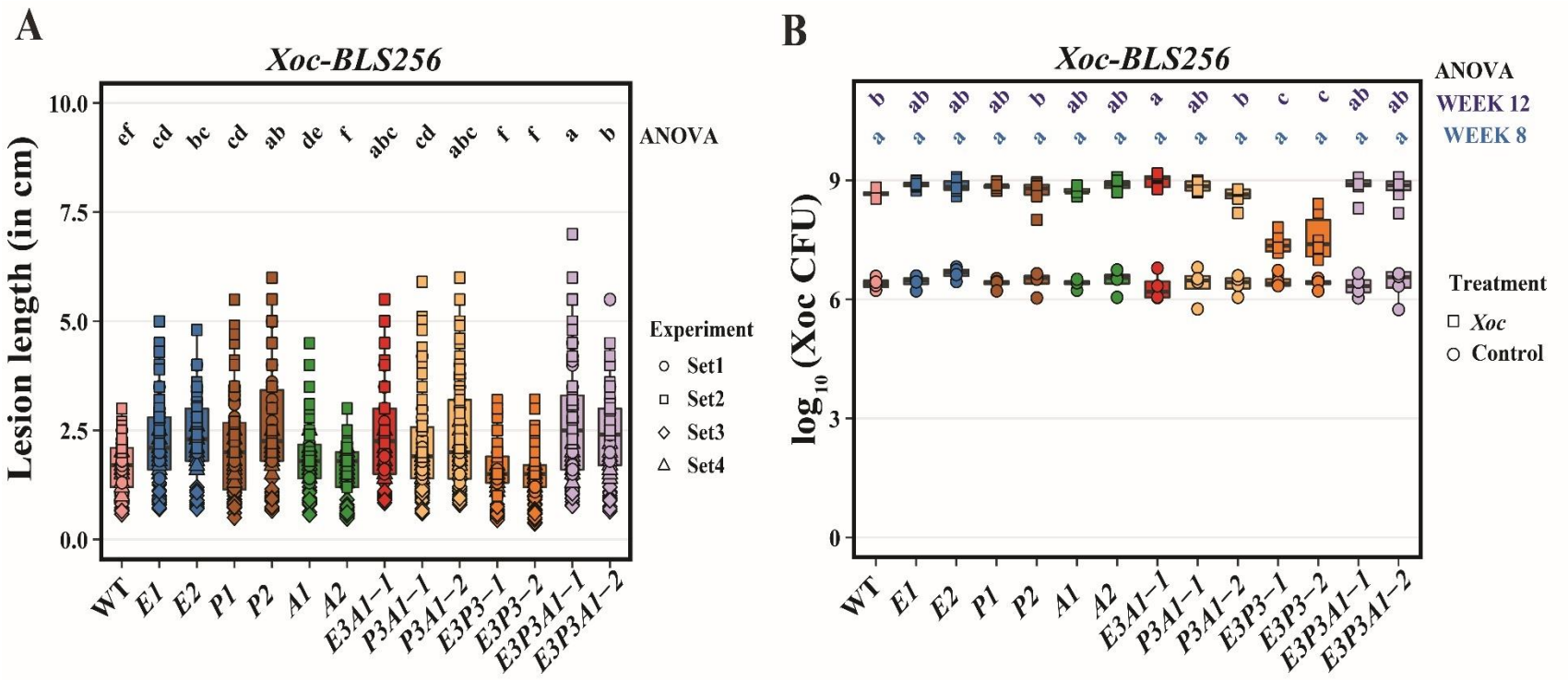

Figure 15: Basal immunity towards African *Xoo* MAI1, Asian *Xoo* PXO99 and Asian *Xoc* BLS256 requires *OsEDS1*-family and *ADR1* genes

4-5 week old single *Oseds1* (*OsE1* and *OsE2*), *Ospad4* (*OsP1* and *OsP2*) *Osadr1* (*OsA1* and *OsA2*), double *Osedsadr1* (*OsE3A1-1*), *Ospad4adr1* (*OsP3A1-1* and *OsP3A1-2*), *Oseds1pad4* (*OsE3P3-1* and *OsE3P3-2*), triple *Oseds1pad4adr1* (*OsE3P3A1-1* and *OsE3P3A1-2*) mutants and WT (Kitaake) greenhouse grown plants were infiltrated with a 0.5 O.D of *Xoc*-BLS256 strain.

A) *Xoc*-BLS256 (O.D 0.5) was infiltrated on the above-mentioned mutants. The water-soaked lesion was measured 5DPI. The box plots represent lesion length. Each respective shape over the box-plot represents a biological replicate (12/genotype). Genotype-treatment combinations sharing letters above boxplots do not show statistically significant differences (Tukey LSD test, $\alpha = 0.05$, $n = 12$).

B) *Xoc*-BLS256 at 0 DPI and 5 DPI (O.D 0.5) were infiltrated on the above-mentioned mutants. The box plots represent $\log_{10}$*Xoc* CFU. Each respective shape over the box-plot represents a biological replicate (12/genotype). Genotype-treatment combinations sharing letters above boxplots do not show statistically significant differences (Tukey LSD test, $\alpha = 0.05$, $n = 12$).

2.5.9 *OsE3P3* double mutant resistance phenotypes might be cell death independent

In *A. thaliana*, EDS1-PAD4 heterodimers controls a 'basal' resistance branch consisting of SA-dependent and SA-independent sub-branches, but contributing little to host cell death in ETI. EDS1-SAG101 heterodimer that works together with the NRG1 sub-family of signalling HeLo NLRs to induce host cell death (HR) at infection sites [5,13,31]. The *Mo, Xoo,* and *Xoc* pathogen data suggests that *Os*ADR1 in the absence of *Os*EDS1 and *Os*PAD4 is auto-active. However, it was not clear whether the lower pathogen titre is due to host cell death or another unknown resistance mechanism.

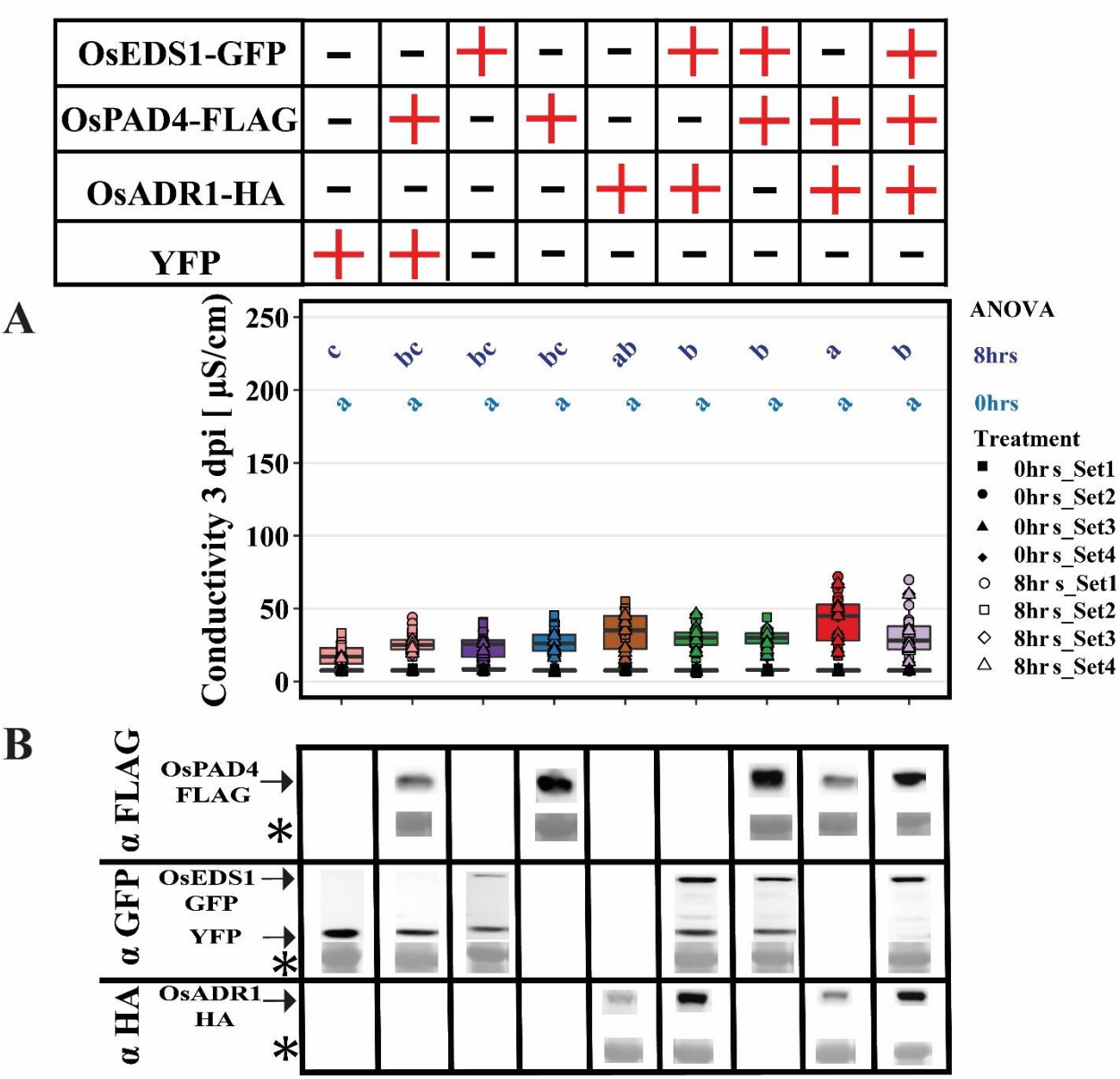

Figure 16: Assessment of ion leakage in *N. benthamiana* following *Agrobacterium*-mediated expression of *Os*EDS1, *Os*PAD4, and *Os*ADR1 did not trigger cell death reactions

EG refers to *Os*EDS1 CDS with a C-terminal GFP tag, PG refers to *Os*PAD4 CDS with a C-terminal GFP tag, PF refers to *Os*PAD4 CDS with a C-terminal FLAG tag, AF refers to *Os*ADR1 CDS with a C-terminal FLAG tag, EH refers to *Os*EDS1 CDS with a C-terminal HA tag and AH refers to *Os*ADR1 CDS with a C-terminal HA tag

A) Ion leakage assay to measure cell death in non-triggered tissues was determined by conductivity measurements three days after *Agrobacterium* infiltration. Overexpression of YFP and YFP co-expressed with *Os*PAD4-FLAG served as a negative control. Shapes plotted over boxplots indicate individual ion leakage measurements, representing a total of 8 biological replicates. Genotype-treatment combinations sharing letters above boxplots do not show statistically significant differences (Tukey HSD test, $\alpha = 0.05$, $n = 8$). All of the constructs were driven by a 35S promoter (please refer materials and methods for more details). YFP refers to expression of YFP CDS. Figure shows data from 4 independent experiments.

B) Western blots to detect expressed proteins which were used in the ion leakage assay in **A**. Experiments were performed 4 times independently. Ponceau S staining (mark with a ***** sign) served as control for equal loading. The expected regions of the expressed proteins are marked using arrows. The original file with the blots is in Appendix1.

To determine if *Os*ADR1 in presence/absence of *Os*EDS1 and *Os*PAD4 has a capacity to induce cell death, I cloned the *OsEDS1*, *OsPAD4*, and *OsADR1* gene CDS from rice into overexpression vectors appropriate for *Agrobacterium*-mediated transient expression in *N. benthamiana* as fusions to C-terminal YFP, HA, and FLAG tags. Overexpression of YFP alone and overexpression of YFP together with FLAG-tagged OsPAD4, serving as a negative control, did not induce cell death, as indicated by the basal ion leakage values. Overexpression of single *Os*EDS1, *Os*PAD4 or *Os*ADR1 constructs did not induce cell death (though the ion leakage values are significantly different, the values are too low to interpret the results as cell death). Co-expression of *Os*EDS1-*Os*ADR1, *Os*PAD4-*Os*ADR1, *Os*EDS1-*Os*PAD4, and *Os*EDS1-*Os*PAD4-*Os*ADR1 did not cause cell death, and the levels of ion leakage were comparable to those of the negative controls (Figure 16A). The cell death was not due to protein expression as shown by the westerns performed on the infiltrated tissues (Figure 16B, please also refer to Appendix figure 1 for the complete figure).

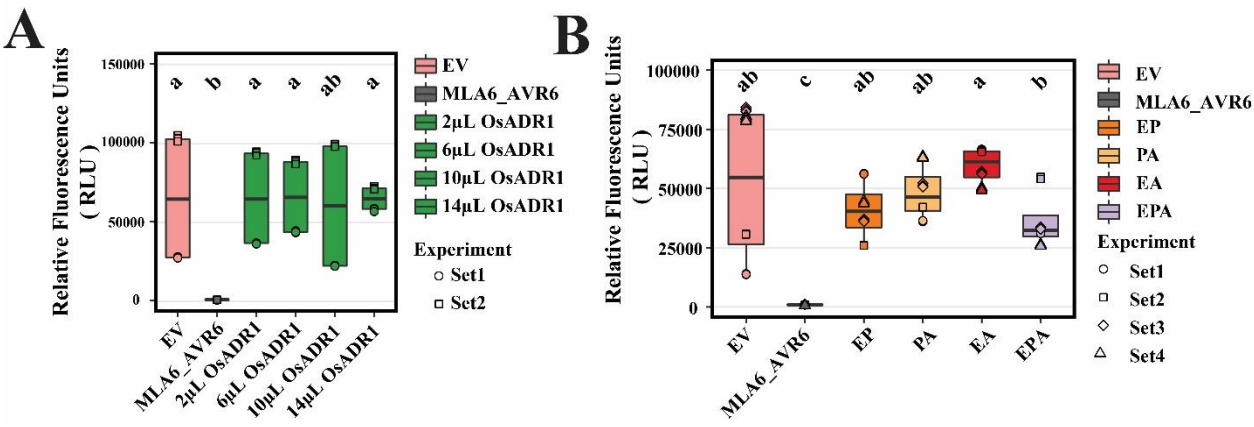

Figure 17: No detectable contribution of *Os*EDS1 *Os*PAD4 and *Os*ADR1 to cell death in non-triggered rice protoplasts

A) *Oseds1pad4adr1* triple mutant protoplasts were isolated and transfected with *pUBQ:luciferase* and either a *pIPKb002* empty vector (*EV*) control or *pIPKb002* vector with cDNAs of *OsADR1*. Luciferase activity was determined 16 h post transfection as proxy for cell death. Differences amongst all transfection samples were assessed by analysis of variance and subsequent Tukey post hoc test of luciferase measurements normalized to the *EV* sample for each construct (EV = 1). Box plots represent relative luminescence units (RLU). MLA6 and AVR6 was used a positive control for cell death. µL of OsADR1 refers to amount of untagged plasmid used (1µg/µL concentration).

B) *pIPKb002* vector with cDNA of *OsEDS1, OsPAD4 and OsADR1* was used to test combinations of *Os*EDS1, *Os*PAD4 and *Os*ADR1 proteins. E represents *Os*EDS1, P represents *Os*PAD4 and A represents *Os*ADR1 proteins in the figure. Combinations of two/three proteins such as EP, PA, EA and EPA were tested. The total concentration of the plasmids transfected was kept to 35µL (adjusted with EV). MLA6 and AVR6 was used a positive control for cell death. Each respective shape over the box-plot represents a biological replicate (3/combination). Genotype-treatment combinations sharing letters above boxplots do not show statistically significant differences (Tukey HSD test, $\alpha = 0.05$, $n = 3$).

In addition to the *N. benthamiana* ion leakage assays, I carried out a cell death assay using rice protoplasts. Using the *Oseds1pad4adr1* mutant protoplasts, I transfected plasmids capable of expressing *Os*EDS1, *Os*PAD4 and *Os*ADR1 proteins. A previously published MLA6-AVR6 interaction was used as a positive control [137]. I initially tested various *Os*ADR1 plasmid concentrations to check if in the absence of *Os*EDS1, and *Os*PAD4 proteins, *Os*ADR1 protein

induces cell death. Cell death was not observed upon *Os*ADR1 transfection (in various concentrations) in the *Oseds1pad4adr1* mutants (*OsE3P3A1*) as there was no significant decrease in RLU values as compared to EV transfections (Figure 17A). I further tested various double plasmids transfections of *Os*EDS1-*Os*ADR1, *Os*PAD4-*Os*ADR1, *Os*EDS1-*Os*PAD4 and triple plasmid transfections of *Os*EDS1-*Os*PAD4-*Os*ADR1 to test whether other combinations contribute to cell death phenotypes. The combinations' EV RLU values did not significantly differ from one another (Figure 17B). Together these data suggest that the *Os*ADR1-dependent resistance phenotypes might not be due to host cell death in rice.

Chapter 3: Discussion

The involvement of EDS1 and its interaction partners PAD4 and SAG101 for both TNL-triggered and basal immunity has been described in *A. thaliana*[13,19,31,32,63]. The EDS1-node, which acts as a crucial decision-making point and initiates downstream immune pathways, is necessary for all evaluated TNLs [52,53]. In TNL-triggered immunity of *A. thaliana* and a few other dicots, the presence of two different EDS1 family modules with specific co-functioning helper-CNLs has been clearly established. In *A. thaliana* EDS1-PAD4-ADR1 module contributes mainly to pathogen resistance and transcriptional defences, whereas the EDS1-SAG101-NRG1 module contributes mainly to cell death outputs[5,31,63]. The majority of tested CNLs but not all confer ETI without EDS1[54,61].

3.1 Comparative phylogenetic analysis with flowering plant genomes reveals a conserved subset of *EDS1*-family genes and NLRs in monocots

The EDS1-SAG101-NRG1 module cell death function is conserved in other eudicot genomes such as *N. benthamiana*, a knockout of *NbEDS1*, *NbSAG101* and *NbNRG1* abolished Roq1 mediated cell death response [63]. Though a redundant role of *NbPAD4* gene function in basal and ETI towards tested NLRs and pathogens the tomato *EDS1* and *PAD4* genes could compliment *AtEDS1* and *AtPAD4* functions[31]. Thus, though PAD4 is dispensable in some of the tested eudicots towards basal and ETI, it might not be the case in all of the eudicots. Phylogenetic analysis performed on available plant genomes reveals that the EDS1 gene family members arose in land plants. Comparative analysis between monocot and eudicot genomes reveals a loss of TNLs, SAG101 and NRG1 in monocot genomes while a conservation of EDS1, PAD4, ADR1 and CNLs

[4,58,89]. Based on this phylogenetic analysis it was tempting to hypothesize that monocot CNLs-mediated immunity signalling transduction could require *EDS1*, *PAD4* and the helper NLR *ADR1* genes.

3.2 Some CNLs in monocots could require *Os*EDS1 family proteins for disease resistance

Although all tested TNLs require EDS1 family proteins to confer ETI, barring a few tested CNLs that require EDS1 family genes (RPS2, HRT and RPP8) most CNLs function independent of EDS1-protein family in ETI [54]. Monocot wheat CNL Sr35, like *A. thaliana* CNL ZAR1 form a pentameric resistosome, moving to the PM and could function as a non-selective calcium channel inducing cell death independent of the EDS1 family proteins[17,50]. The structural and functional resemblance between CNL resistosomes in *A. thaliana* and wheat (*Triticum aestivum*) might represent a blue-print for other monocot CNLs. The tested monocot paired CNLs RGA4/5 and Pikp1/2, although not structurally solved might function similarly to CNL receptors ZAR1 and Sr35 and the helper CNL NRG1 to induce cell death upon activation by forming a resistosome and moving to the PM [51,60]. Unlike NRG1 which is a helper NLR, RGA4/5 and Pikp1/2 are both paired NLRs and in non-triggered conditions the sensor NLR regulates the signalling NLR, which if expressed alone is auto-active [90,138].These studied receptor pairs in rice are quite unlikely to require downstream *Os*EDS1, *Os*PAD4 and helper NLR *Os*ADR1 due to the presence of executor RGA4 and Pikp2 proteins [20,27,92]. The potential dependence of a cloned CNL gene in rice on *Os*EDS1 remains a plausible hypothesis warranting further investigation.

NAD^+ generated upon effector triggered TNL resistosome formation drives the generation of small molecules that activate EDS1 heterodimer formation with either PAD4 or SAG101 for immune responses in *A. thaliana* [139,140]. The EDS1-SAG101 and EDS1-PAD4 heterodimers are essential for immune signalling, because mutations impairing heterodimer formation or the pocket where TIR-generated small molecules bind to, cause disease susceptibility [139,140]. The absence of TNLs in monocots and an EDS1-independent mechanism of downstream signalling in CNL signalling suggests that monocot CNL-triggered ETI works independent of EDS1-family genes (Figure 13 B)

The expression of TIR-only domain proteins activating immune responses suggests that the TIR-domain only proteins in addition to TNLs are important for defence signalling [51,141–143]. The presence of TIR containing proteins in monocots suggests that some CNLs or all CNLs might relay a sensor CNL signal to these TIR-domain proteins, which upon activation generate a NAD^+ derived molecule that could trigger small molecule production thereby activating EDS1-family dependent signalling (Figure 18). A recent report in *A. thaliana* showed that a *Brachypodium distachyon* (a monocot) TIR domain containing protein (*Bd*TIR) when expressed in insect cells induced EDS1-PAD4 associations with ADR1-L1 in vitro [140]. Given the findings of these studies, it's tempting to explore whether rice TIRs can produce small molecules, marking the initial step in understanding this possibility. *Os*EDS1 and *Os*PAD4 associate to form a heterodimer (Figure 11), it would be interesting to test whether the generated small molecules could signal *Os*EDS1-*Os*PAD4 heterodimer-mediated downstream immune responses.

3.3 High order *OsEDS1, OsPAD4* and *OsADR1* mutants to identify potential roles in rice immunity

A. thaliana CNL triggered immunity required *At*EDS1, *At*PAD4, *At*ADR1 and SA phytohormone pathway towards ETI responses [13,144]. Using an established CRISPR-Cas9 mutagenesis system, I targeted rice *OsEDS1*, *OsPAD4*, *OsADR1* and *OsICS1* genes. Small insertions and deletions were added to the mutants in order to create frameshift mutants early in the genes, causing a STOP codon early in the proteins resulting in non-functional translated proteins. I generated mutants of *OsEDS1*, *OsPAD4* and *OsADR1*, however mutant generation of SA biosynthesis gene (*OsICS1)* knockout was successful but lethal to the plant as heterozygous *OsICS1* gene mutants were viable but not the homozygous mutants (Experiments performed but data not shown). A similar observation was observed in other labs (personal communication with Dr. Nakagami, Prof. Dr. Cui and Dr. Champion). In basal conditions, SA phytohormone levels in rice are notably elevated compared to *A. thaliana*, primarily attributed to the management of oxidative stress. Interestingly, pathogen treatment does not result in a significant increase in SA levels, indicating that defense mechanisms in rice might operate independently of SA signaling [94,96]. Preliminary basal and ETI assays on the generated single *Oseds1*, *Ospad4*, *Osadr1* and *Oseds1pad4* suggested the *OsEDS1* and *OsPAD4* was required for basal immunity while none of these genes were needed for ETI. This suggests that rice defence networks might work differently as compared to *A. thaliana* in CNL-triggered ETI, where the helper NLR *OsADR1* could be redundantly required for basal and ETI responses in rice. Hence, I generated combinatorial mutants of *OsEDS1*, *OsPAD4* and *OsADR1* genes in rice to rule out a possible deviant role of *OsADR1* as that of in *A. thaliana.*

Greenhouse grown CRISPR-Cas9 generated rice mutants grew to a similar height as WT plants except the *OsE3P3* mutants (Figure 6), which exhibited a short plant height reminiscent of an auto-immune plants. The leaf emergence (Huan index) measurements argued against the possibility of

OsE3P3 plants being developmentally impaired as all the plants developed equally. The fitness of the *OsE3P3* plants was also comparatively compromised as compared to the single, other double and triple mutant plants (Figure 8, 10). Auto-immune plants allocate more resources towards immunity which reduces the overall fitness of the plant [145–147]. Photosynthesis machinery was impaired, together with lower yields parameters corroborating with previous *A. thaliana* and rice auto-immune phenotypes. This result deviated from previous *A. thaliana* studies where knockout of *EDS1* and *PAD4* in eudicots (*A. thaliana* and *N. benthamiana*) did not produce an auto-immune phenotype [5,13,31,58,59] which suggest that *Os*EDS1 and *Os*PAD4 pathways might function differently in rice.

3.4 Principal component analysis on *OsE3P3* transcriptome reveals defence and developmental genes

RNAseq analysis on non-triggered tissues was performed to understand if there is a difference in the transcriptome between the CRISPR-Cas9 generated mutants. A principal component analysis (PCA) on the RNAseq samples showed that the transcriptome of the *OsE3P3* is different to other mutants. The majority of the annotated genes were defence and development related genes (Table 1 and 2). A prominent defense-associated gene accounting for 24% of the principal component 1 (PC1) variance in *OsE3P3* was identified as a triacylglycerol lipase precursor (LOC_Os08g41780), homologous to the A. thaliana AtMPL1 gene. In A. thaliana, this gene has been demonstrated to modulate defense responses against the green peach aphid in an AtPAD4-dependent manner, primarily by regulating the JA phytohormone pathway[114,148]. Another defence related gene that stood out was *OsSWEET14* gene (LOC_Os11g31190) encoding a well characterized susceptibility component for *Xoo* and *Xoc* infection [115,149–151]. Among the genes

explaining PC1 variance several genes encoding proteins containing domains important for defence responses such as LOC_Os10g04090, LOC_Os08g29854, LOC_Os01g54670, LOC_Os07g03000, LOC_Os10g03570 and LOC_Os06g03500. Several genes contributing to the variance observed in PC1 are involved in regulating phytohormones crucial for defense mechanisms (Table 1). These results together could explain the auto-immune like phenotypes observed in the *OsE3P3* mutants.

In addition to defence genes, several genes regulating developmental and yield characteristics were part of the PC1 explained variance. The LOC_Os06g11660 gene was characterized in *A. thaliana* to be required for cell expansion in leaves which could explain the smaller leaves in the *OsE3P3* mutants. The LOC_Os03g03810 gene was characterized in rice to be required in grain filling which could explain the poor seed weights and seed width in the *OsE3P3* mutants. Several other genes such as the LOC_Os07g16040, LOC_Os03g55420, LOC_Os01g65460 and LOC_Os02g09930 which are required for root and cell wall development could also explain the shorter phenotypes observed in the *OsE3P3* mutants.

Global gene expression in non-triggered tissues in the CRISPR-Cas9 mutants was not obviously differentially regulated between the *OsE (OsE1* and *OsE2), OsP (OsP1* and *OsP2), OsA (OsA1* and *OsA2), OsE3P3, OsP3A1, OsE3A1, OsE3P3A1* mutants and WT (Data not presented). Interestingly, the gene expression levels of *OsADR1* were found to be comparable between *OsE3P3* mutants and WT plants, showing no significant increase (Data not presented). This suggests that the possible regulation of *Os*ADR1 by *Os*EDS1 and *Os*PAD4 leading to an auto-immune phenotype in the *OsE3P3* mutants is not transcriptional and might be due to post-transcriptional or translational. Another possibility is that *OsADR1* gene regulates a set of CNLs

or defence-related genes (possibly genes shown in Table 1) in the absence of *OsEDS1* and *OsPAD4* gene expression. Both these possibilities could be addressed by assessing expression of these selected defence related genes in mock and pathogen treated samples. In conclusion, the loss of *Os*EDS1 and *Os*PAD4 proteins triggers an *Os*ADR1-dependent auto-immune response which is not linked to the transcription but more likely post-transcriptionally to *Os*ADR1-dependent resistance.

3.5 *EDS1*-family genes and *OsADR1* are required for basal immunity responses in rice

Using the virulent Guy11 *Mo* strain, *Xoo* strains PXO99 and MAI1, and *Xoc* strain BLS256 strain, I tested the generated CRISPR-Cas9 mutant basal immunity (Figures 13A, 14, 15). Individual mutants of *OsEDS1* and *OsPAD4* exhibited susceptibility to the virulent *Mo* strain Guy11, as depicted in Figure 13A. However, mutants lacking the *OsADR1* gene did not display susceptibility.. This trend was also observed in both tested *Xoo* strains (Fig. 14) and *Xoc* (Fig. 15) suggesting a conserved function of the *EDS1* and *PAD4* genes in both monocot and dicot basal immunity. The contribution of *Os*EDS1 and *Os*PAD4 towards basal immunity was similar to dicot *A. thaliana* basal immunity studies [13,58,61]. The similar susceptibility of *OsADR1* gene mutants as compared to WT plants corroborated to reports in *A. thaliana* where loss of single *AtADR1* gene was not as susceptible as WT plants. It is noteworthy that while the knockout of a single *AtADR1* gene in the A. thaliana genome did not result in an increase in susceptibility compared to WT plants, the presence of three *ADR1* genes contrasts with the single *ADR1* gene found in the rice genome. Despite this, the susceptibility observed in the *AtADR1* knockout was significantly lower than that seen in mutants lacking *AtEDS1* or *AtPAD4*[29,89]. *Os*EDS1 and *Os*PAD4 might form a

heterodimer similar to that in *A. thaliana* which is supported by the *Agrobacterium*-mediated heterologous expression assay of protein expression where *Os*EDS1 proteins immunoprecipitated with the *Os*PAD4 (Figure 11). Similar susceptibilities between the single *OsEDS1* and *OsPAD4* gene mutants suggests that the heterodimer formation and resistance signalling is conserved in rice.

Basal immunity is compromised in double *OsE3A1*, *OsP3A1* and triple mutants *OsE3P3A1* while the *OsE3P3* plants were less susceptible as compared to the WT plants (Figures 13-15). In *A. thaliana,At*EDS1 and *At*PAD4 heterodimer together with *AtADR1* drive basal defences [29,30,36,60]. *Os*ADR1 in absence of *Os*EDS1 and *Os*PAD4 shows an auto-active phenotype, an observation different from what is observed in *A. thaliana.* Based on the pathogen assays (*Mo*, *Xoo* and *Xoc*) a loss of either *Os*EDS1 or *Os*PAD4 increased susceptibility (Figures 13A, 14, 15) which suggests that *Os*EDS1 and *Os*PAD4 likely regulate Os*ADR1*. The heterodimer formation is vital as a loss of either *Os*EDS1 or *Os*PAD4 results in susceptibility. What signals and regulates *Os*EDS1 and *Os*PAD4 to OsADR1 is not known. One possibility is that *Os*ADR1 might be guarded from *Os*EDS1 and *Os*PAD4 by another CNL (since there are no TNLs present in monocots) which could likely trigger immune responses by forming a calcium channel just like the CNLs ZAR1 and Sr35 [16,50]. The RNAseq analysis revealed a few CNLs that might be initial candidates to screen (Table 1). Another possibility is that *Os*EDS1 and *Os*PAD4 might regulate *Os*ADR1 by another protein. These possibilities/theories could be tested by an RNAseq of pathogen triggered tissues to identify possible genes that might be differentially expressed in these *OsE3P3* mutant vs the single, WT and triple mutants. An IP-MS comparison of tagged proteins between pathogen triggered and mock tissues might help identify the possible candidates that might regulate *Os*ADR1. Another possibility is that a NAD^+ derived molecule from an activated

rice TIR-domain containing protein could trigger small molecule that could signal to downstream *Os*ADR1 Based on recently published literature, rice TIRs were shown to be temporally differentially expressed upon pathogen trigger [152]. It is likely that an active TIR trigger or a PAMP could induce *Os*EDS1-*Os*PAD4-*Os*ADR1 interaction. In conclusion, based on the pathogen and interaction assays, the *Os*EDS1, *Os*PAD4 and *Os*ADR1 interactions need to be investigated in triggered tissues (pathogen-/TIR-/PAMP-triggered) to understand how these genes might signal in rice immunity.

3.6 *Os*EDS1, *Os*PAD4 and *Os*ADR1 might be required to reinforce immunity around HR lesions by regulating phytohormone pathways

RGA4/5 and Pikp1/2 CNL triggered immunity was not impaired in any of the generated mutants which shows that *Os*EDS1, *Os*PAD4 and *Os*ADR1 singly or in combination are not required for CNL-triggered immunity corroborating with several CNLs working independent of EDS1 family genes in *A. thaliana*. The CNLs tested work in a pair where one of the CNLs detects the effector and the other executes downstream signalling, hence it is quite likely that the paired CNLs would function together with downstream helper NLR. It is possible to test single sensor NLRs and assess whether they would function with the *EDS1*-family genes in rice ETI.

Previously published studies at the Kroj lab helped me access *Mo* effector mutants that are weakly recognized by CNL pair RGA4/5. The *Mo* Guy11-AVRPiaR43G mutant variant when sprayed on the CRISPR-Cas9 generated mutants showed that *OsEDS1* and *OsPAD4* gene mutants were more susceptible as compared to WT plants while the *OsADR1* gene mutant susceptibility was similar to that of WT plants (Figure 13 C). This data suggests that *OsEDS1* and *OsPAD4* single mutants are needed to reinforce immunity around the HR lesions restricting the pathogen

growth in case the pathogen crosses the HR region. The combinatorial mutant phenotypes were similar to that of *Mo* basal immunity where the *OsE3A1*, *OsP3A1* and the *OSE3P3A1* mutants were susceptible while *OsE3P3* mutants showed resistant phenotype. These observations were in line with *A. thaliana* report where the systemic immunity with respect to CNL *At*RPM1 was *At*EDS1 and *At*PAD4 dependent [36,153–155]. In cells adjacent to the HR cell, the EDS1-PAD4-ADR1 module induces transcriptional reprogramming aiding accumulation of SA and antimicrobial molecules which restrict further progression of disease [29,36,57,156]. In this zone the EDS1-PAD4 promotes SA over JA responses which restricts pathogen growth [13,81].

The regulation of rice *EDS1* family gene might induce similar systemic resistance around the HR lesions, most likely regulating phytohormone pathways to restrict pathogen growth. SA is promoted towards biotrophic/hemi-biotrophic pathogen restriction in *A. thaliana*[5]. In rice, pathogen restriction mediated by phytohormones might be attributed to jasmonic acid (JA) rather than SA[96,99].. Unlike *OsICS1*, the JA biosynthesis gene mutations are not lethal [157,158] but show pleiotropic effects. It would be interesting to create combinatorial mutants of *Os*EDS1 family genes and the JA biosynthesis genes to address any redundancies towards basal immunity in rice. Assessing the phytohormone content of non-triggered and triggered tissues would also help assess whether there are any differences in phytohormone modulation.

In *A. thaliana,* EDS1-PAD4-ADR1 module is required for systemic immunity adjacent to HR cells. In these cells components such as LESIONS SIMULATING DISEASE 1 (LSD1) restrict cell death [29,57]. I tested host cell death inducing capabilities of *Os*EDS1, *Os*PAD4 and *Os*ADR1 to test two possibilities. Could the conserved EDS1-PAD4-ADR1 module in rice compensate the absence of EDS1-SAG101-NRG1 module to induce host cell death in CNL ETI or could this module be required for systemic immunity (host cell death independent). I did not observe host

cell death when *Os*EDS1, *Os*PAD4 and *Os*ADR1 were transiently expressed singly or in various double and triple expressed protein combinations in non-triggered tissues of *N. benthamiana* (non-native system but an excellent system to test host cell death)(Figure 16). No host cell death was observed in a native rice protoplast-based cell death assay (Figure 17). An absence of host cell death upon expression of *Os*EDS1, *Os*PAD4 and *Os*ADR1 singly and in various combinations suggests a conserved role of the EDS1-PAD4-ADR1 module in basal immunity by pathogen restriction (Figures 16 and 17). It is important to note that in the case of this experiment, I could have used a heat-killed pathogen or co-transfected an effector to rule out the possibility that this module is transiently activated upon effector/pathogen infection. Together these results further support a conservation of the EDS1-PAD4-ADR1 module function in mediating basal immunity responses.

3.7 Concluding remarks and outlook

My analysis lays a foundation to study a phylogenetically conserved EDS1-PAD4-ADR1 protein module in rice. Using CRISPR-Cas9 mutants I established that, individually, *Os*EDS1, *Os*PAD4 and *Os*ADR1 are essential for basal immunity to *Mo, Xoo* and *Xoc.* A putative rice EDS1-PAD4-ADR1 module is not essential for HR responses in CNL mediated ETI but these components do contribute to immunity reinforcement around CNL-induced HR sites to limit pathogen growth, an observation similar to that of *A. thaliana* CNL and TNL-mediated immunity. An auto-immune phenotype in the *OsE3P3* mutant and RNAseq analysis suggests a post-transcriptional/translational control of *Os*ADR1 by *Os*EDS1 and *Os*PAD4 [13] Future studies in other monocots such as barley, maize and wheat will help establish the role of *Os*EDS1-*Os*PAD4

dimers and their molecular and functional relationship with *Os*ADR1 to confer basal immunity in monocots.

How EDS1-family proteins and *Os*ADR1 are activated in rice is not known. A recent report showed that TIR-catalyzed small molecules induce EDS1 heterodimer formation in *A. thaliana*. *Bd*TIR domain was shown to induce *A. thaliana* EDS1-PAD4 heterodimer associations to ADR1-L1[140], consistent with *Bd*TIR producing appropriate nucleotide-based small molecules for EDS1-PAD4 activation Rice TIR-domain containing proteins have been shown to induce cell death in *N. benthamiana* in an *EDS1*-dependent manner[152]. Future experiments to test whether rice TIR-domain catalyzed small molecule in rice induce heterodimer formation *invitro* would help identify a mechanism of EDS1-PAD4 heterodimer activation and signalling in rice. Testing if rice TIR-domain proteins function in an *EDS1*-dependent pathway in rice could be easily tested in rice protoplasts with the genetic material available in my study. Together these experiments based on published literature would help identify EDS1-family protein activators in rice.

The mechanism of resistance and the downstream signalling in rice upon EDS1-family proteins and *Os*ADR1 activation is not known. Several studies have demonstrated a protein proximity-based labelling methods to identify potential interactors, a method that can be translated to rice protoplasts [159–161]. The resolution of Turbo-ID is higher which would in addition to identifying strong interactions also identify weak transient interactions helping build rice EDS1-PAD4 immune signalling pathway. A transcriptomic study in pathogen-triggered tissue in the generated CRISPR-Cas9 mutants would help parallelly identify signalling components aiding the proteomic studies. Together a transcriptomic and proteomic approach would help build a EDS1-family protein basal immunity network.

In our RNA-seq analysis, conducted as part of my study, we observed that several genes associated with phytohormone pathways contributed significantly to the variance observed in PC1. This finding suggests a potential involvement of phytohormones in the autoimmune phenotype observed in the *OsE3P3* mutants, as indicated in Table 1 and 2.*OsEDS1* mutants had a lower JA-Ile (bioactive JA) and JA signalling pathway component gene expression to WT suggesting a possible modulation of phytohormones in resistance to pathogens[98]. Comparing various phytohormone concentrations in mock vs pathogen inoculated plants would help identify phytohormones responsible for immune phenotypes. It would be tempting to assume that *Os*EDS1, *Os*PAD4 and *Os*ADR1 signalling converges, regulate and utilizes phytohormone pathways to resist pathogen growth.

Figure 18: A hypothetical model for *Os*EDS1, *Os*PAD4 and *Os*ADR1 function in rice innate immunity

Strong HR responses are generated in CNL-triggered immunity which likely induce ROS-promoted signalling could relay signals to adjacent cells[29,57]. These danger signals could

1) Activate TIR-only proteins in rice that could in a NAD^+ manner generate small molecules activating the *Os*EDS1-PAD4 heterodimer signalling through and unknown protein to activate *Os*ADR1 leading to an immune response
2) Signal to *Os*EDS1 and *Os*PAD4 likely interacting with *Os*ADR1 leading to an immune response

*Os*EDS1, *Os*PAD4 and *Os*ADR1 is likely important in regulating systemic immunity in rice which is supported by the basal and special ETI (Figures 13, 14, 15) experiments performed in my study.

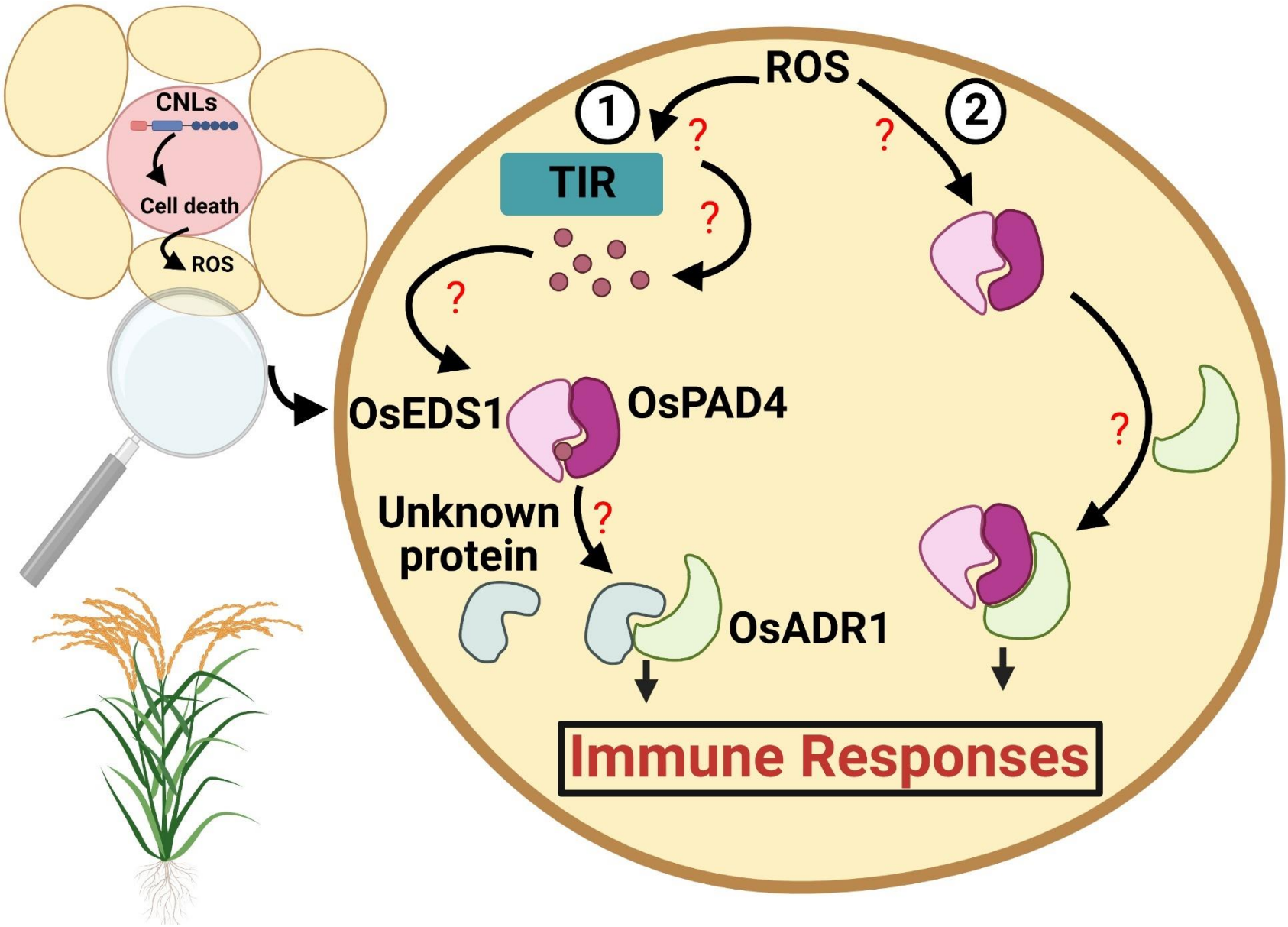
CNLs
Cell death
ROS
ROS
1
2
TIR
?
?
?
?
?
?
OsEDS1
OsPAD4
Unknown protein
OsADR1
Immune Responses

Chapter 4: Materials and Methods

Materials and methods are defined in two separate parts. The first Section, 4.1 lists materials used in this work including pathogen and bacterial strains, plant material, antibodies, chemicals, enzymes, media, etc. The second section consists of experimental procedures and peculiarities.

4.1 Materials

4.1.1 Pathogen Strains

Table 3: Pathogen strains used in this study

Species	Strain	Resistance	eLAB code	Source
Xanthomonas oryzae pv. oryzae	PXO99^{A} Asian strain	Rifampicin	dJF116	IRD, Montpellier France[162]
Xanthomonas oryzae pv. oryzae	MAI1 Malian strain race A3	NA	dJF119	IRD, Montpellier France[163]
Xanthomonas oryzae pv. oryzicola	BLS256 Asian strain	Rifampicin	dJF118	IRD, Montpellier France[164]
Magnaporthe oryzae	Guy11	NA	NA	INRAE, Montpellier
Magnaporthe oryzae	Guy11: AVR-Pia	NA	NA	INRAE, Montpellier France[165]
Magnaporthe oryzae	Guy11: AVR-Pia R43G	NA	NA	INRAE, Montpellier France [26]

4.1.2 Bacterial Strains

Table 4 - Bacterial strains utilized in this study

Species	Strain	Genotype
E.coli	DB3.1	F- gyrA462 endA Δ(sr1-recA) mcrB mrr hsdS20 (rBmB-) supE44 ara14 galK2 lacY1 proA2 rpsL20 (StrR) xyl5 λ- leu mtl1
E.coli	DH5α	F- Φ80dlacZΔM15 Δ(lacZYA-argF) U169 deoR recA1 endA1 hsdR17(rk -, mk+) phoA supE44 λ- thi-1 gyrA96 relA1
E.coli	DH10b	F- mcrA Δ(mrr-hsdRMS-mcrBC) Φ80lacZΔM15 ΔlacX74 deoR recA1 endA1 araΔ139 Δ(ara, leu)7697 galU galK λ- rpsL (StrR) nupG
A. tumefaciens	GV3101	pMP90RK[166]

4.1.3 Plant Materials

Table 5: *O. sativa* lines used in this study.

Genotype code	Gene mutant alleles present	Mutant generation protocol	Reference	eLAB reference
OsE1	*Oseds1-1*	CRISPR-Cas9 mutagenesis	Current study	stJF059
OsE2	*Oseds1-2*	CRISPR-Cas9 mutagenesis	Current study	stJF019
OsE4	*Oseds1-4*	CRISPR-Cas9 mutagenesis	Prof. Cui lab, China	stJF109
OsE5	*Oseds1-5*	CRISPR-Cas9 mutagenesis	Prof. Cui lab, China	stJF102
OsP1	*Ospad4-1*	CRISPR-Cas9 mutagenesis	Current study	stJF062
OsP2	*Ospad4-2*	CRISPR-Cas9 mutagenesis	Current study	stJF026

OsP4	*Ospad4-4*	CRISPR-Cas9 mutagenesis	Prof. Cui lab, China	stJF106
OsP5	*Ospad4-5*	CRISPR-Cas9 mutagenesis	Prof. Cui lab, China	stJF105
OsA1	*Osadr1-1*	CRISPR-Cas9 mutagenesis	Current study	stJF060
OsA2	*Osadr1-2*	CRISPR-Cas9 mutagenesis	Current study	stJF061
OsA3	*Osadr1-3*	CRISPR-Cas9 mutagenesis	Prof. Cui lab, China	stJF103
OsA4	*Osadr1-4*	CRISPR-Cas9 mutagenesis	Prof. Cui lab, China	stJF108
OsE3P3	*Oseds1-3* *Ospad4-3*	CRISPR-Cas9 mutagenesis	Current study	stJF063
OsE3A1-1	*Oseds1-3* *Osadr1-1*	Crossing (Segregated from *OsE3P3* X *OsA1*)	Current study	stJF187
OsP3A1-2	*Ospad4-3* *Osadr1-1*	Crossing (Segregated from *OsE3P3* X *OsA1*)	Current study	stJF188
OsP3A1-2	*Ospad4-3* *Osadr1-1*	Crossing (Segregated from *OsE3P3* X *OsA1*)	Current study	stJF189
OsE3P3-1	*Oseds1-3* *Ospad4-3*	Crossing (Segregated from *OsE3P3* X *OsA1*)	Current study	stJF190
OsE3P3-2	*Oseds1-3* *Ospad4-3*	Crossing (Segregated from *OsE3P3* X *OsA1*)	Current study	stJF191
OsE3P3A1-1	*Oseds1-3* *Ospad4-3* *Osadr1-1*	Crossing (Segregated from *OsE3P3* X *OsA1*)	Current study	stJF192
OsE3P3A1-2	*Oseds1-3* *Ospad4-3* *Osadr1-1*	Crossing (Segregated from *OsE3P3* X *OsA1*)	Current study	stJF193
Maratelli		Susceptible rice variety to Guy11, Guy11: AVR-Pia	INRAE, Montpellier	NA

4.1.4 Antibiotics

Table 6: Antibiotics used in this study.

Name	stock concentration (mg/ml)	Working concentration (µg/ml)	Dissolved in
Ampicillin	100	100	ddH2O
Carbenicillin	100	50	ddH2O
Kanamycin	50	25	ddH2O
Gentamycin	25	15	ddH2O
Rifampicin	40	100	DMSO
Spectinomycin	100	100	ddH2O

4.1.5 Antibodies

Table 7: List of antibodies used in this study

Antibody	Source	Dilution	Supplier	Group
α-flag	rabbit polyclonal	1:5000	Sigma-Aldrich	primary
α-GFP	rabbit monoclonal	1:5000	Cell Signaling Technology	primary
α-HA	rabbit monoclonal	1:5000	Cell Signaling Technology	primary
IgG-HRP	goat polyclonal	1:5000	Sigma-Aldrich	secondary

4.1.6 Chemicals

Laboratory grade chemicals used in this study met standard purity required for laboratory usage. They were obtained by various laboratory suppliers including Sigma-Aldrich (Hamburg, GER), Merck (Darmstadt, GER), Roth (Karlsruhe, GER), SERVA (Heidelberg, GER), ThermoFisher (MA, USA), and VWR (Langenfeld, GER).

4.1.7 Enzymes

4.1.7.1 Restriction Enzymes

For DNA digestion during cloning all restriction enzymes from either New England Biolabs (NEB, Frankfurt, GER) or ThermoFisher Scientific (MA, USA) were used as per the manufacturer's instructions.

4.1.7.2. DNA Polymerases

Choice for usage of different DNA Polymerases was done according to cloning requirements and complexity. An overview is given in Table 8.

Table 8 - DNA Polymerases used in this work

Name	Purpose	Supplier
Phire II	standard PCR	ThermoFisher
Phusion HF	HF,proof reading for cloning	ThermoFisher
Takara PrimeStar	HF, proofreading, for GC-rich templates	CloneTech

4.1.7.3 Other enzymes

Other enzymes used in this study include T4 DNA ligase (ThermoFisher), cDNA Synthesis SuperMix (Bimake, Munich, GER), Gateway® pENTR™/D-TOPO™ Kit (ThermoFisher), Gateway® LR Clonase® II Enzyme Mix (ThermoFisher), PhosSTOP™ Phosphatase Inhibitor (Merck, Darmstadt, GER), Lambda Protein Phosphatase (NEB), Cellulase Onozuka R-10, and Macerozyme R-10 (both SERVA, Heidelberg, GER) as per the manufacturer's instructions.

4.1.8 Oligonucleotides

Primers are given in Table 9. For regular oligo design the lasergene suite was used to analyze sequences and create primers (https://www.dnastar.com/software/lasergene/). Oligonucleotides were ordered at Sigma-Aldrich (Hamburg, GER). To make 100 µM stock concentration, lyophilised primers were resuspended in ddH2O and diluted 1:10 for a desired working concentration of 10 µM.

Table 9: Primers used in this study

eLAB ID	Orientation	Sequence Information	Purpose
nJF011	5' - 3'	GGTGGAAACCAAGAAGCTCAAATGCT	Genotyping: *OsPAD4* single mutants
nJF012	3' - 5'	CCTGGAATTCAGGGGATCTGCACA	Genotyping: *OsPAD4* single mutants
nJF015	5' - 3'	AGCAACTTGTGTTCATGGTGCCA	Genotyping: *OsADR1* single mutants
nJF016	3' - 5'	CACCCAGGGAACTTGAAGATGA	Genotyping: *OsADR1* single mutants
nJF019	5' - 3'	TCGACTATGTGGCCTATTCTTGT	Genotyping: *OsPAD4* double mutants
nJF020	3' - 5'	CTGTGAGACCACATGGCAGAAGTT	Genotyping: *OsPAD4* double mutants
nJF021	5' - 3'	GCCTTGGTGATCTCGGTGTTCA	Genotyping: Cas9 cassette mutants
nJF022	3' - 5'	CGGACAACTCCGATGTGGACAA	Genotyping: Cas9 cassette

nJF057	5' - 3'	ACCCACCCACCACACCACTCC	Genotyping: *OsEDS1* single/double mutants
nJF058	3' - 5'	AAACAGCAAAGCGCCGAAAAGA	Genotyping: *OsEDS1* single/double mutants
nJF091	3' - 5'	TTGAAGACAACGAACCCCAGGGCACAAGTTTCG	Golden gate cloning: Insert *OsEDS1* gene to Lev0
nJF093	3' - 5'	TTGAAGACAACGAACCCCTTCTCTCCCGGCCAT	Golden gate cloning: Insert *OsPAD4* gene to Lev0
nJF095	3' - 5'	TTGAAGACAACGAACCGTCTACAAGCCAGTCCA	Golden gate cloning: Insert *OsADR1* gene to Lev0
nJF102	5' - 3'	TTGAAGACAAAATGCCGGCGGCGGCGGCGCTGTC	Golden gate cloning: Insert *OsEDS1* gene to Lev0
nJF103	5' - 3'	TTGAAGACAAAATGCTTCTTCTTCGTCGTCGTCT	Golden gate cloning: Insert *OsPAD4* gene to Lev0
nJF104	5' - 3'	TTGAAGACAAAATGGAGAGGCTGTTCGAGGAGCT	Golden gate cloning: Insert *OsADR1* gene to Lev0
nJF144	5' - 3'	CACCATGCCGGCGGCGGCGGCGCTGTCC	Gateway cloning: c*OsEDS1* into pENTR vector for rice protoplast transformations
nJF145	3' - 5'	TTACCAGGGCACAAGTTTCGCGATGC	Gateway cloning: c*OsEDS1* into pENTR vector for rice protoplast transformations
nJF146	5' - 3'	CACCATGCTTCTTCTTCGTCGTCGTC	Gateway cloning: c*OsPAD4* into pENTR vector for rice protoplast transformations
nJF147	3' - 5'	CTACCTTCTCTCCCGGCCATGGGTGA	Gateway cloning: c*OsPAD4* into pENTR vector for rice protoplast transformations
nJF148	5' - 3'	CACCATGGAGAGGCTGTTCGAGGAGCTG	Gateway cloning: c*OsADR1* into pENTR vector for rice protoplast transformations
nJF149	3' - 5'	TCAGTCTACAAGCCAGTCCAGGTTAT	Gateway cloning: c*OsADR1* into pENTR vector for rice protoplast transformations

4.1.9 Vectors

Table 10: Vectors utilized for cloning in this study

eLAB ID	Vector	Purpose
	pENTR-D-TOPO	Empty Gateway ENTRY vector (ThermoFisher) used for TOPO recombination with amplified PCR products
JF064	pAGM1287_*Os*EDS1_Lev0	For further cloning
JF065	pAGM1287_*Os*PAD4_Lev0	For further cloning
JF066	pAGM1287_*Os*ADR1_Lev0	For further cloning

JF079	pICH47732_p35S_c*OsADR1*_HA	*Agrobacterium*-mediated transient expression in *N. benthamiana*
JF080	pICH47732_p35S_c*OsPAD4*_HA	*Agrobacterium*-mediated transient expression in *N. benthamiana*
JF081	pICH47732_p35S_c*OsADR1*_FLAG	*Agrobacterium*-mediated transient expression in *N. benthamiana*
JF082	pICH47732_p35S_c*OsPAD4*_FLAG	*Agrobacterium*-mediated transient expression in *N. benthamiana*
JF083	pICH47732_p35S_c*OsPAD4*_GFP	*Agrobacterium*-mediated transient expression in *N. benthamiana*
JF084	pICH47732_p35S_c*OsEDS1*_HA	*Agrobacterium*-mediated transient expression in *N. benthamiana*
JF085	pICH47732_p35S_c*OsEDS1*_GFP	*Agrobacterium*-mediated transient expression in *N. benthamiana*
JF106	pENTR _OsEDS1_STOP	For further cloning
JF107	pENTR _OsPAD4_STOP	For further cloning
JF108	pENTR _OsADR1_STOP	For further cloning
JF109	pIpKB002(pHL038) _*Os*EDS1_STOP	For transient expression in rice protoplasts
JF110	pIpKB002(pHL038)_*Os*PAD4_STOP	For transient expression in rice protoplasts
JF111	pIpKB002(pHL038)_*Os*ADR1_STOP	For transient expression in rice protoplasts

4.1.10 Media

All media were sterilized by autoclaving at 121 °C for 20 min after preparing as per the recipe provided in the table. In order to supplement heat sensitive additives like antibiotics in the media, their addition was performed once the media cooled down to approximately 50 °C. This procedure was followed throughout all media.

Table 11: Media used in this study

Name	Components
Luria-Bertani (LB) pH 7	0.5% yeast extract; 1% tryptone; 1% NaCl; 1.5% agar
YEB (Yeast Extract Beef)	0.5% beef extract; 1% yeast extract; 0.5% peptone; 0.5% sucrose; 0.5g/l $MgCl_2$; 1.5% agar

PSA (Peptone Sucrose Agar)	0.5% peptone, 2% sucrose, 0.05% K_2HPO_4, 0.025% $MgSO_4$. $7H_2O$, 1.6% agar

4.1.11 Buffers and Solutions

Following buffers along with the components used in this work are summarized in Table 8.

Table 8 - Buffers and Components

Application	Buffer	Components
DNA extraction (quick and dirty)	DNA extraction buffer	200 mM Tris pH 7.5, 250 mM NaCl, 25 mM EDTA pH 7.5, 0.5 % SDS
DNA extraction (sucrose prep)	sucrose solution	50 mM Tris pH 7.5, 300 mM NaCl, 300 mM sucrose
DNA electrophoresis	10x TAE running buffer	0.4 M Tris, 0.2 M acetic acid, 10 mM EDTA, pH 8.5
	6x DNA loading buffer	40 % (w/v) sucrose, 0.5 M EDTA, 0.2 %(w/v) bromophenol blue
	DNA ladder	10 %(v/v) 6× loading buffer, 5 %(v/v) 1 kb DNA ladder (ThermoFisher)
SDS-PAGE	10x Tris-glycine running buffer	250 mM Tris, 1.92 M glycine, 1 %(w/v) SDS
	2x SDS sample buffer (Lämmli buffer)	60 mM Tris pH6.8, 4 %(w/v) SDS, 200 mM DTT, 20 %(v/v) glycerol, 0.2 %(w/v) bromophenol blue
Immunoblotting	TBST buffer	10 mM Tris, 150 mM NaCl, 0.05 %(v/v) Tween 20, pH 7.5
	10x transfer buffer	250 mM Tris, 1.92 M glycine, 1 %(w/v) SDS, 20 %(v/v) Methanol
	Ponceau-S	Dilution of ATX Ponceau concentrate (Fluka) 1:5 in ddH2O

Protein Extraction	Extraction- and wash buffer	50 mM Tris (PH7.5), 150 mM NaCl, 10 % (v/v) Glycerol, 2 mM EDTA, 5 mM DTT, Protease inhibitor (Roche, 1 tablet per 50 mL), 0.1 % Triton
Rice protoplast preparation	Digestion enzyme solution	1.5% cellulose R10, 0.4% macerozyme R10 (SERVA), 0.6 M mannitol, 20 mM KCl, 10 mM MES (PH5.7), 55 °C for 10 min followed by cooling to room temperature before adding 10 mM CaCl2, 0.1% BSA (Sigma A-6793)
	Wash buffer	154 mM NaCl, 125 mM CaCl2, 5 mM KCl, 2 mM MES (pH 5.7)
	Transfection buffer 1	0.4 M mannitol, 15 mM MgCl2, 4 mM MES (pH 5.7)
	Transfection buffer 2	4 g PEG 4000 (Sigma-Aldrich, #81240), 0.2 M mannitol, 0.1 M CaCl2
	Regeneration buffer	4mM MES, 0.6M Mannitol, 20mM KCl
N. benthamiana transient expression	infiltration solution	10 mM MES, 10 mM MgCl2, pH5.6, 0.15 mM acetosyringone

4.2 Methods

4.2.1 Plant methods

4.2.1.1 Maintenance, cultivation and growth conditions of Rice plants

In a growth-chamber/greenhouse: Temperature 28°C; 60% humidity during the day, 60% humidity at night; Photoperiod of 12/12h.

4.2.1.2 Crossing of rice plants

To cross and obtain genetically desired backgrounds, rice plants were grown until inflorescence emergence. Flowers with immature pollen, but fully developed stigma were emasculated (dipped in 42°C for killing the pollen) and received donor pollen via dabbing donor stamen onto each stigma. Crosspollinated stigma were sealed in paper bags and left to set seeds. Progeny was then analyzed for segregation and desired gene combinations.

4.2.1.3 Isolation of Rice protoplasts

For preparation of rice protoplasts, an adapted version of the protocol published by the Saur et al., 2019 was used. Rice plants of desired genetic backgrounds were grown. Rice leaves were harvested 10-14 days after sowing. Different leaves were stacked and cut with a razor blade into 1 mm thin stripes on tissue paper. Cut leaves were then placed in enzyme solution (see section 4.1.11) immediately and were subjected to vacuum infiltrated for 45 min. This digestion mix was then incubated at RT for 3 h with continuous gentle shaking about 30 rpm. For isolating the

protoplasts, a nylon mesh (100 µm) was used to filter the solution and collected in a falcon tube. The washing steps were carried with the same volume wash buffer. After washing thoroughly, Cells were centrifuged at 100 g, RT, for 3 min. The supernatant was removed and 5 mL wash buffer was added. The protoplast concentration was measured with 0.5mL of solution and the remaining solution was incubated in the dark for 45min for the protoplasts to settle down. Remove the excess wash buffer and resuspend the protoplasts to a final concentration of $O.D_{600}$ of 0.4 using TB1.

4.2.1.4 Cell death assays

Cell death assays in *N. benthamiana* after agroinfiltration

N. benthamiana plants were placed under a 16 h light/8 h dark regime at 22°C. Six 8 mm leaf discs from *N. benthamiana* agroinfiltrated leaves were taken at 3 dpi, washed in 10-20 ml of MQ for 30-60 min, transferred to a 24-well plate with 1 ml MQ in each well and incubated at room temperature. Ion leakage was measured at 0 and 6 h with a conductometer Horiba Twin Model B-173. For statistical analysis, results of measurements at 8 h for individual leaf discs (each leaf disc represents a technical replicate) were combined from independent experiments (biological replicates). ANOVA was followed by Tukey's HSD posthoc test (α=0.05). For visual assessment of cell death symptoms, infiltrated leaves were covered in aluminum foil for 2 d and opened to "dry" the lesions and enhance visual symptoms at 3 dpi.

Luciferase based cell death assay in rice protoplasts

For protoplast transfections, 300 µl protoplasts were added to the desired plasmid combinations, mixed, and transformed by adding 350 µL Transfection 2 solution. Tubes were incubated at RT for 15 min in the dark after inverting thrice. Transformation was then stopped by adding 2 X 660µL Wash buffer. Mix by inverting the tubes about 8 times. Cells were centrifuged again (100 g, RT, 3 min), and 2 X 965µL supernatant was removed. Add 965µL of regeneration buffer and incubate at 14-16 hrs in dark at 22 °C. After incubation, centrifuge at 1000g for 3 min and remove 965 µL of supernatant and add 200 µL 2X Cell culture Lysis buffer (Promega E1531). Vortex and incubate on ice for 5 mins. 50 µL of this solution is mixed with 50µl LUC substrate solution (Promega E151A and E152A) and immediately measured using luminometer (Berthold Centro LB 960 luminometer). LUC activity of each sample was measured for 1 s/sample

4.2.1.5 *Agrobacterium tumefaciens* mediated transient expression assays in *N. benthamiana*

N. benthamiana plants were grown for 4-6 weeks in the greenhouse in the following conditions: 16 h light, 8 h dark and ~24 °C. Non-flowering and healthy plants were transferred to the lab for infiltration with A. tumefaciens (OD600 = 0.2-0.6; depending on the expression efficiency of the plasmid). Bacteria were grown for 2-3 days on YEB agar plates supplemented with respective antibiotics, dissolved in infiltration solution, and hand infiltrated using a needle-less syringe. Two mature leaves were selected per plant and infiltrated on the abaxial side of the leaf directly, or by first making a hole in the leaf with a needle. Samples were taken 2-3 days post-infiltration, snap frozen in liquid nitrogen, and stored at -80 °C for further downstream application.

4.2.1.6 Huan index (leaf emergence)

Leaf emergence was performed using the following equation.

Huan indice = $A + (\left(\frac{B}{C+20\%C}\right) * 100)$

Where, A refers to the number of fully expanded leaves,

B is the length of the last emerging leaf (youngest leaf) and,

C refers to the length of the last full expanded leaf

4.2.1.7 Plant height, tiller number TGW, seed length and seed width

Seed length and width measurement was performed using about 100-200 seeds/genotype. Seeds were imaged using an infrared imager and using a software developed in the Tsiantes department the seed length and width was measured. These measurements were repeated 5 times/genotype. Measurements were exported into a spreadsheet for further calculations.

TGW was measured by counting between 300-500 seeds/genotype using the same setup used for seed length measurement except here we counted the objects(seeds) and then weighing the counted seeds. Measurements were exported into a spreadsheet for further calculations.

Tiller number was measured 6 week and 12 weeks from the time of germination. The number of individual tillers were counted for 12 biological replicates. Measurements were exported into a spreadsheet for further analysis.

4.2.1.8 Measurement of Phi2

Phi2 measurements were performed to check the percentage of incoming light (excited electrons) that go into Photosystem II (photosynthetic processes) using MultispeQ V 2.0 handheld chlorophyll fluorometer. All the measurements were performed using the manufacturer's software (https://photosynq.org/) with manufacturer recommended programs (Photosynthesis RIDES protocol).

4.2.1.9 RNA sequencing and analysis

Samples for RNA-Seq and RNA isolation was performed as follows. Here, one biological replicate is the sum of 9 leaves from 9 plants from one treatment. Three biological replicates were used for each genotype for RNA sequencing. RNA was extracted by freezing in liquid nitrogen, grinding and adding 800 µL TRIzol. Add 160 uL Chloroform was added to the sample, vortex and spin down 10 min @ 14.000 g 4 °Tissue lysate was prepared in TRIzol® as indicated in the TRIzol® Reagent technical manual up to the point where phase separation would be performed. 35ul of isopropanol was added per 100ul of lysate and mixed by vortexing. 500µl of lysate was transferred to a ReliaPrep™ Minicolumn and centrifuge at 12,000. Centrifugatuion was again performed at 14,000 x g for 30 seconds at room temperature. ReliaPrep™ Minicolumn was removed and liquid was discarded in the Collection Tube. ReliaPrep™ Minicolumn was placed back into the Collection Tube. 500µl of RNA Wash Solution was added to the ReliaPrep™ Minicolumn. Centrifugation was again performed at 12,000–14,000 × g for 30 seconds. Collection Tube as was emptied before and placed in the microcentrifuge rack. Apply 30µl of freshly prepared DNase I incubation mix (containing 24µl

of Yellow Core Buffer, 3µl 0.09M MnCl2, 3µl of DNase I enzyme) was added directly to the membrane inside the column. After incubation for 15 minutes at room temperature, 200µl of Column Wash Solution was added to the ReliaPrep™ Minicolumn. Centrifugation was performed at 12,000–14,000 × g for 15 seconds. 500µl of RNA Wash Solution was added (with ethanol added) and centrifuge at 12,000–14,000 × g for 30 seconds. ReliaPrep™ Minicolumn was placed into a new Collection Tube. 300µl of RNA Wash Solution was added and centrifuged at high speed for 2 minutes. ReliaPrep™ Minicolumn was transferred from the Collection Tube to the Elution Tube. Nuclease-Free Water was added to the membrane according to the Elution volume and centrifuged at 12,000–14,000 × g for 1 minute. Column was removed and discard. The concentration of purified RNA was measured using a Nano drop and each sample was divided into two parts and stored at -80 °C. Upon quality testing the samples were shipped to Novogene for library preparation and RNA sequencing.

The mapping was performed using STAR (https://github.com/alexdobin/STAR). The counts after mapping were analyzed in R using the edgeR and MixOmics packages.

4.2.2 Bacterial/Fungal methods

4.2.2 1 *E. coli*

E. coli laboratory strains were grown in LB medium supplemented with the respective antibiotic at 37 °C to ensure plasmid maintenance. Transformation of chemically competent E. coli cells was performed as follows: 50 µl competent cells were thawed on ice and incubated with 2 - 10 ng plasmid DNA for 10 min on ice. The mixture was subjected to heat shock using a water bath at 42 °C for 30 sec and was snap chilled in ice for 2 min. After adding 800 µl LB medium, cells were incubated at 37 °C and 200 rpm for 1 h to allow expression of the resistance cassette. Cells were then centrifuged (5000 g, 1 min) and resuspended in 200 µl of which 100 µl were plated on selective LB media plates.

4.2.2 2 *A. tumefaciens*

Agrobacteria were grown in liquid or solid YEB medium with respective antibiotic resistance at 28 °C for 2 days. Transformation of Agrobacteria were performed via electroporation. Electro competent cells were incubated with 50 ng plasmid DNA for 10 min on ice before being transferred to a precooled electroporation cuvette (1 mm, Eurogentec, BE). The BioRad Gene Pulser Xcell™ with the following settings was used for electroporation. 25 µF, 2.5 kV, 5 ms, and 400 Ω. After pulsing, cells were supplied with 800 µl YEB medium immediately and incubated at 28 °C, 200 rpm for 2 h to allow resistance cassette expression. To obtain single colonies, 50 µl of cells were plated on selective LB media plates.

4.2.2 3 *Magnaporthe oryzae* inoculation

Mo isolates and transgenic strains Guy11-AVRPia and Guy11-EV were grown on rice flour agar for spore production (Berruyer et al., 2003). A suspension of fungal conidiospores (5 × 104 spores·mL−1) was spray-inoculated on the leaves of 3-week-old plants (Berruyer et al., 2003) for the determination of interaction phenotypes.

4.2.2 4 *Xoo/Xoc* patho-assays

Xoo/Xoc was grown on PSA media. Plates were incubated at 28 °C for two days, until single colonies were formed. Single colony was selected for subculturing it for 24h at 28°C on fresh PSA in order to obtain a patch of bacteria with little polysaccharides. A solution of 0.2 $O.D_{600}$ was used for *Xoo* and 0.5 OD_{600} for Xoc inoculations.

4-week-old plants week old plants were inoculated with Xoo by leaf clipping (scissors were dipped into OD_{600} = 0.2 for leaf-clipping. The second youngest leaf was cut 2- 3 cm from the leaf tip. Scissor was re-dipped the between each leaf, and one leaf per plant was clipped. Plants were allowed to grow in the greenhouse/growth chamber, and lesions lengths were measured after two weeks.

3-week-old plants were inoculated by syringe infiltrations. Youngest leave was infiltrated by using a needleless 1 mL syringe, applying tightly the tip of the syringe on the underside of the leaf and pressing the plunger. For basal resistance level evaluation, two infiltration spots were made each side of the midrib and water soaking symptoms 5 days after inoculation were evaluated.

4.2.2 5 *Xoc* CFU assays

4-week-old Kitaake plants were used for *Xoc* inoculation, *Xoc* bacterial culture was infiltrated with an $O.D_{600}$ of 0.5. The plants were transferred into the growth chamber and after 5 days the leaf samples containing the lesions were collected into a sterile microcentrifuge tube along with 2 sterile metal beads in each tube. The scissors were cleaned between each genotype. Samples were ground in TissueLyser for 1 min at a rate of 30 beats/second and 1 ml of sterile water was added (in fume hood). TissueLyser was run again twice for 1 min at 30 beats/second. A sterile water reservoir was prepared for multichannel pipette for making the dilutions. 90 µL of sterile H2O in was pipetted in each well (line A - E) using the multichannel pipette. Leaf suspensions were vortexed and placed into the well with 10µL sample in the line A, followed by homogenization with a multi-channel pipette. The serial dilutions of the same were prepared. Spot dilutions were performed on plates containing 40ml PSA + Rifampicin. Plates were then dried in the fume hood for about 15 mins, followed by their incubation in an oven for 72 hours. Colonies were then quantified at each spot in order to obtain the bacterial titers.

4.2.3 Biochemical methods

4.2.3.1 Total protein extraction for immunoblot analysis

Plant leaf tissue was collected from *N.benthamiana* plants and snap frozen in liquid nitrogen followed by homogenisation with the Qiagen TissueLyser II (Qiagen, Hilden, GER). 50 - 100 µl

Lämmli Buffer were added to the powder, vortexed, boiled at 95 °C for 10 min, and centrifuged at 14000 rpm, 4 °C, 5 min. Supernatant was transferred to a new tube and used for immunoblot analysis or stored at -20 °C.

4.2.3.2 Immunoprecipitation of transiently expressed protein

For immunoprecipitation of proteins expressed in rice protoplasts, cells were harvested by centrifugation (100 g, 1 min) followed by adding 600 µl extraction buffer directly to the cells. Samples were incubated on ice for 5 min with interspersed vortexing before being centrifuged for 2 min, 4 °C, 14000 rpm. 50 µl supernatant were taken as input sample. For immunoprecipitation, 12 µl of GFP-Trap or myc-Trap (Chromotek, Martinsried, GER) or ANTI-FLAG® M1 Gel (Sigma-Aldrich) were added to the supernatant and incubated on a rotating mixer for 2.5 h at 4 °C. After incubation, beads were spun down at 2500 g at 4 °C for 2 min and washed 4 times with 1 ml extraction buffer. To elute the protein, 100 µl of Lämmli buffer were added to the beads and heated to 95 °C, 10 min with 3 vortex steps. Finally, the eluted beads were collected at the bottom by centrifugation (14000 rpm, 4 °C, 1 min) and supernatant was transferred to a fresh tube and used for immunoblot analysis or stored at -20 °C. 4

4.2.3.3 SDS-polyacrylamide gel electrophoresis (SDS-PAGE)

To separate proteins based on their size via SDS-PAGE, the Mini-PROTEAN 3 SDS-PAGE system (BioRad) was used. Samples were extracted in Lämmli buffer and boiled at 95 °C for 10 min. Samples were loaded on discontinuous, self-cast polyacrylamide gels (8 - 10 % for running gel, see table 9, and 6 % for stacking gel, see table 10) with 1.5 mm width. Samples were subjected to electrophoresis in 1x Running buffer at 80 V for 15 min, followed by 120 V for 70 - 90 min. As

protein size marker 3 µl of the PageRuler™ Prestained Protein Ladder (ThermoFisher) were loaded.

Table 9 - Composition SDS PAGE running gels (for 4 1.5 mm gels)

Component	8 % running gel	10 % running gel
ddH2O	18.5 ml	15.7 ml
1.5 M Tris-HCl pH 8.8	10 ml	10 ml
10 % SDS	400 µl	400 µl
30 % Acrylamide/Bis solution 29:1	10.7 ml	13.3 ml
10 % APS	400 µl	400 µl
TEMED	25 µl	25 µl

Table 10 - Composition SDS-PAGE stacking gel (for 4 X 1.5 mm gels)

Component	6 % stacking gel
ddH2O	9 ml
0.5 M Tris-HCl pH 6.8	4 ml
10 % SDS	160 µl
30 % Acrylamide/Bis solution 29:1	2.6 ml
10 % APS	160 µl
TEMED	25 µl

4.2.3.4 Immunoblot analysis

After successful SDS-PAGE proteins were transferred to a Hybond™-ECL™ nitrocellulose membrane (GE Healthcare, Freiburg, GER). For this the BioRad Mini Trans-Blot® cell system was employed. Gels were submerged for 10 min in ice-cold 1x transfer buffer and transfer cassettes were assembled to the manufacturer's instructions. Transfer was performed at 110 V for 65 min at

4 °C. To avoid high background signal after immunoblotting, membranes were blocked with 5 % (w/v) low-fat milk TBST solution for 60 min at RT on a shaker (50 rpm). Primary antibodies were diluted in 2 % (w/v) milk TBST solution (see table 4) and blocked membranes were incubated with the primary antibody over night at 4 °C on a shaker (50 rpm). Next day, membranes were washed 3 times with TBST (5 min each) and then incubated with secondary antibody diluted in 2 % (w/v) milk TBST at RT for 60 min at 50 rpm. Primary antibodies bound by protein of interest were detected with a horseradish peroxidase (HRP) conjugated secondary antibody. After 4 washes with TBST (5 min each) membranes were supplied with the BioRad Clarity™ or Clarity Max™ Materials and Methods 88 Western ECL Substrate. For highly abundant proteins Clarity substrate was used. For low abundance proteins a 1:1 ratio of Clarity™:Clarity Max™ or pure Clarity Max™ was used. Chemiluminescence was detected with the BioRad ChemiDoc™ XRS+ system.

4.2.5 Molecular biological methods

4.2.5.1 Isolation of genomic DNA (sucrose prep)

For large numbers of DNA extraction (e.g. for genotyping) I used a method based on sucrose that allows DNA extraction in a 96 well plate format (Berendzen et al. 2005). Few mg of leaf material were collected in collection tubes (Qiagen) containing one metal bead. 200 µl sucrose solution were added to each tube and samples were homogenised with TissueLyser II (Qiagen). Tubes were then centrifuged at 1000 g, RT for 1 min and then placed in a water bath for 15 min at 97 °C. After this, samples were placed on ice for 30 min, before 1 µl of solution was used for PCR analysis. DNA extracted by this method should not be frozen and can be used for up to 7 days.

4.2.5.2 Polymerase Chain Reaction (PCR)

For standard PCRs I used non-proofreading Phire II DNA polymerase (ThermoFisher), while for cloning purposes I used proofreading Phusion HF polymerase (ThermoFisher) or Takara PrimeStar (CloneTech). An overview of used polymerases can be found in table 5. PCR mix was identical for all polymerases and is shown in table 11. The thermal cycling program was adjusted to each polymerase and is shown in Table 12.

Table 11 - PCR reaction mix

Component	Volume
10x PCR buffer	2 µl
dNTP mix (2.5 mM)	1.6 µl
forward primer (10 µM)	1 µl
reverse primer (10 µM)	1 µl
template DNA	0.2 - 10 ng
polymerase	0.2 - 0.5 µl
ddH2O	to 20 µl

Table 12 - Thermo-cycling programs

Stage	Temperature (°C)	Time (Phire II)	Time (Phusion, Takara)	Cycles
Initiation	95	30 sec	5 min	1x
Denaturation	95	10 sec	10 sec	
Annealing	55 - 60	15 sec	30 sec	30 - 35x
Elongation	72	15 sec/kb	30 sec/kb	
Final extension	72	5	5	1x

4.2.5.3 Site-directed Mutagenesis

To mutate specific nucleotides in a sequence of interest site-directed mutagenesis was performed with minor alterations according to the instructions of the QuickChange SiteDirected Mutagenesis Kit (Agilent, Waldbronn, GER). PCR mix can be seen in Table 11. To remove template plasmid from the reaction the methylation sensitive restriction enzyme DpnI (NEB) was used. 1 µl DpnI was added to 20 µl PCR mix and incubated for 1 h at 37 °C. As template DNA is methylated it will be digested, while the mutagenesis carrying nonmethylated DNA will not be affected. 5 µl of digested PCR mix were transformed into DH10b and plated on selective LB plates for colony isolation and further cloning.

4.2.5.4 cDNA Synthesis

Total RNA was isolated as described in section 4.2.4.3 and 250 - 1000 ng were used for cDNA synthesis. I used cDNA Synthesis SuperMix (Bimake) following manufacturer's instructions and diluted cDNA 1:1 when using 250 ng total RNA and 1:5 when using 1000 ng total RNA. cDNA was stored at -20 °C

4.2.5.5 Plasmid DNA Isolation from bacteria

For standard plasmid prep the NucleoSpin® Plasmid Kit (Macherey-Nagel, Düren, GER) was used as per the manufacturer's instructions. For Agrobacteria the low copy protocol was used. Protoplast transformation requires large amounts of high-quality DNA. For this purpose, the NucleoBond® Xtra Maxi Kit (Macherey-Nagel) was used. Typically, 250 ml of bacterial culture were grown and DNA was purified using NucleoBond® Finalizers yielding ~1 mg DNA.

4.2.5.6 Restriction endonuclease digestion of DNA

DNA digestion was performed to the respective enzyme manufacturer's instructions. Typically, 5 - 15 µl DNA were mixed with reaction buffer, 0.3 µl enzyme and brought to a final volume of 20 µl. The reaction was incubated at the correct temperature for 1 - 2 h and stored at 4 °C.

4.2.5.7 Agarose gel electrophoresis of DNA

DNA was mixed with DNA loading dye and loaded on a 0.8 - 3 % (w/v) agarose gel in TAE buffer. Typically, gels were run at 120 V for 30 - 45 min. Agarose gels were supplemented with 0.2 mg/l ethidium bromide and visualised on a 312 nm UV transilluminator.

4.2.5.8 DNA purification from agarose gels

Separated DNA fragments were illuminated on an UV trans-illuminator and cut out with a clean razor blade. For further processing the PCR clean-up and gel extraction kit (MachereyNagel) was used as per the manufacturer's instructions.

4.2.5.9 Golden Gate DNA cloning

Golden Gate cloning was performed as published (Engler et al. 2008, Weber et al. 2011, Engler et al. 2014, Patron et al. 2015). Concretely, for level 0 constructs, DNA was amplified using

primers with overhangs containing BpiI restriction sites, and a 4 nucleotide attachment overhang (5' “TACA” 3'). A typical Golden Gate reaction and the thermocycling conditions are shown in table 16 and table 17, respectively. 5 µl of reaction mix were transformed into chemically competent E. coli (DH10b) and plated on LB selection plates.

Table 16 - Golden Gate reaction mix

Component	Volume
10x FastDigest buffer	2 µl
10 mM ATP	2 µl
plasmid (insert)	50 ng
plasmid (backbone)	15 ng
ddH2O	to 20 µl
HF restriction enzyme	0.5 µl
T4 DNA ligase	0.5 µl

* For level 0 construction T4 DNA ligase, 1 U/µl was used. More complex assemblies like level 1 construction were performed with T4 DNA ligase, HC 30 U/µl

Table 17 - Thermo-cycling Golden Gate reaction

Stage	Temperature (°C)	Time	Cycles*
digestion	37	5 min	8-50x
ligation	16	5 min	8-50x
inactivation 1	55	5 min	1x
inactivation 2	85	5 min	1x

* For level 0 construction 8 cycles were sufficient. More complex assemblies like level 1 construction were performed with 30 - 50 cycles overnight.

4.2.5.10 DNA sequencing

DNA sequencing was carried out by Eurofins Genomics (Ebersberg, GER) using their Mix2Seq kit. Instructions were followed precisely as per the manufacturer's guidelines. The sequences were analyzed using the Laser-gene suite.

Appendix1

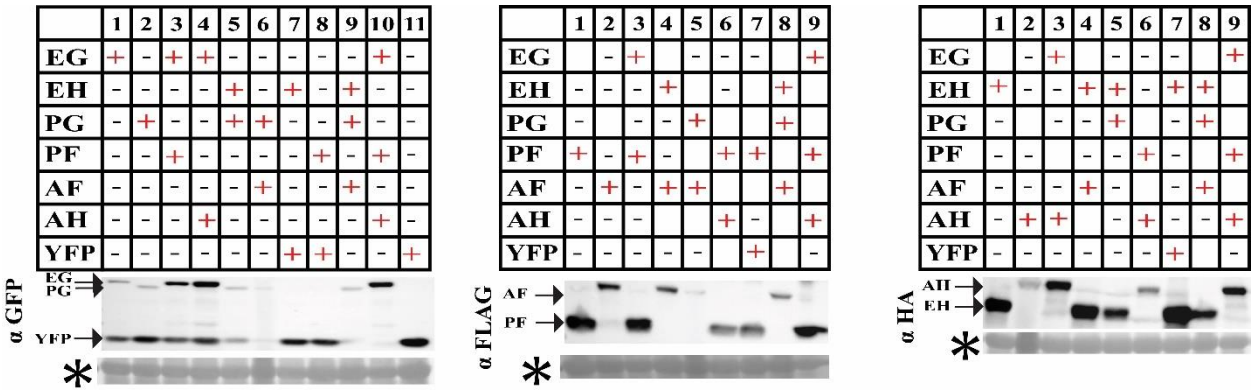

Appendix figure 1: Original protein blots of Figure 16.

The original protein blots of the cell death assay. Since I had cropped to ease the reader with a simpler figure the following original figure has been presented to show that the proteins were observed at the regions expected.

EG refers to *Os*EDS1 CDS with a C-terminal GFP tag, PG refers to *Os*PAD4 CDS with a C-terminal GFP tag, PF refers to *Os*PAD4 CDS with a C-terminal FLAG tag, AF refers to *Os*ADR1 CDS with a C-terminal FLAG tag, EH refers to *Os*EDS1 CDS with a C-terminal HA tag and AH refers to *Os*ADR1 CDS with a C-terminal HA tag

Western blots to detect expressed proteins which were used in the ion leakage assay in **A**. Experiments were performed 4 times independently. Ponceau S staining (mark with a ***** sign) served as control for equal loading. The expected regions of the expressed proteins are marked using arrows.

References

1. Jones, J. D. G. & Dangl, J. L. The plant immune system. *Nature* **444**, 323–329 (2006).

2. Cesari, S. Multiple strategies for pathogen perception by plant immune receptors. *New Phytologist* **219**, 17-24 (2018).

3. Baggs, E., Dagdas, G. & Krasileva, K. v. NLR diversity, helpers and integrated domains: making sense of the NLR IDentity. *Current Opinion in Plant Biology* **38**, 59-67 (2017).

4. Baggs, E. L. *et al.* Convergent loss of an EDS1/PAD4 signaling pathway in several plant lineages reveals coevolved components of plant immunity and drought response. *Plant Cell* **32**, 2158-2177 (2020).

5. Lapin, D., Bhandari, D. D. & Parker, J. E. Origins and Immunity Networking Functions of EDS1 Family Proteins. *Annual Review Phytopatholy* **58**, 253-276 (2020).

6. Hacquard, S., Spaepen, S., Garrido-Oter, R. & Schulze-Lefert, P. Interplay between Innate Immunity and the Plant Microbiota. *Annual Review Phytopatholy* **55**, 565-589 (2017).

7. Li, J., Wang, C., Liang, W. & Liu, S. Rhizosphere Microbiome: The Emerging Barrier in Plant-Pathogen Interactions. *Frontiers in Microbiology* **12**, 772420 (2021).

8. Dangl, J. L., Horvath, D. M. & Staskawicz, B. J. Pivoting the Plant Immune System from Dissection to Deployment. *Science* **341**, 746–751 (2013).

9. Couto, D. & Zipfel, C. Regulation of pattern recognition receptor signalling in plants. *Nat Rev Immunol* **16**, 537–552 (2016).

10. Yu, X., Feng, B., He, P. & Shan, L. From Chaos to Harmony: Responses and Signaling upon Microbial Pattern Recognition. *Annual Review of Phytopathology* **55**, 109-137 (2017).

11. Wan, W. L., Fröhlich, K., Pruitt, R. N., Nürnberger, T. & Zhang, L. Plant cell surface immune receptor complex signaling. *Current Opinion in Plant Biology* **50**, 18-28 (2019).

12. Saur, I. M. L., Panstruga, R. & Schulze-Lefert, P. NOD-like receptor-mediated plant immunity: from structure to cell death. *Nature Reviews Immunology* **5**, 305-318 (2021).

13. Bhandari, D. D. *et al.* An EDS1 heterodimer signalling surface enforces timely reprogramming of immunity genes in Arabidopsis. *Nat Communications* **10,** 772 (2019).

14. Cui, H., Tsuda, K. & Parker, J. E. Effector-Triggered Immunity: From Pathogen Perception to Robust Defense. *Annu Rev Plant Biol* **66**, 487–511 (2015).

15. Jonathan D. G. Jones, Russel E. Vance, J. L. D. Intracellular innate immune surveillance devices in plants and animals. **354(6316)** (2016).

16. Wang, J. *et al.* Ligand-triggered allosteric ADP release primes a plant NLR complex. *Science* **364(6435)** (2019).

17. Wang, J. *et al.* Reconstitution and structure of a plant NLR resistosome conferring immunity. *Science* **364(6435)** (2019).

18. Bernoux, M. *et al.* Structural and functional analysis of a plant resistance protein TIR domain reveals interfaces for self-association, signaling, and autoregulation. *Cell Host Microbe* **9(3)**, 200-211 (2011).

19. Feehan, J. M., Castel, B., Bentham, A. R. & Jones, J. D. Plant NLRs get by with a little help from their friends. *Current Opinion in Plant Biology* **56**, 99-108 (2020).

20. Cesari, S. *et al.* The Rice Resistance Protein Pair RGA4/RGA5 Recognizes the Magnaporthe oryzae Effectors AVR-Pia and AVR1-CO39 by Direct Binding. *Plant Cell* **25**, 1463–1481 (2013).

21. Maqbool, A. *et al.* Structural basis of pathogen recognition by an integrated HMA domain in a plant NLR immune receptor. *Elife* **4**, (2015).

22. le Roux, C. *et al.* A receptor pair with an integrated decoy converts pathogen disabling of transcription factors to immunity. *Cell* **161**, 1074–1088 (2015).

23. Sarris, P. F. *et al.* A plant immune receptor detects pathogen effectors that target WRKY transcription factors. *Cell* **161**, 1089–1100 (2015).

24. Maidment, J. H. R. *et al.* Multiple variants of the fungal effector AVR-Pik bind the HMA domain of the rice protein OsHIPP19, providing a foundation to engineer plant defense. *Journal of Biological Chemistry* **296**, 100371 (2021).

25. Oikawa, K. *et al.* The blast pathogen effector AVR-Pik binds and stabilizes rice heavy metal-associated (HMA) proteins to co-opt their function in immunity. *bioRxiv* 2020.12.01.406389 (2020) doi:10.1101/2020.12.01.406389

26. Ortiz, D. *et al.* Recognition of the magnaporthe oryzae effector AVR-pia by the decoy domain of the rice NLR immune receptor RGA5. *Plant Cell* **29**, 156-168 (2017).

27. Césari, S. *et al.* The NB-LRR proteins RGA4 and RGA5 interact functionally and physically to confer disease resistance. *EMBO J* **33**, 1941–1959 (2014).

28. Jubic, L. M., Saile, S., Furzer, O. J., el Kasmi, F. & Dangl, J. L. Help wanted: helper NLRs and plant immune responses. *Current Opinion in Plant Biology* **50**, 82–94 (2019).

29. Bonardi, V. *et al.* Expanded functions for a family of plant intracellular immune receptors beyond specific recognition of pathogen effectors. *Proceedings of the National Academy of Sciences* **108**, 16463–16468 (2011).

30. Dong, O. X. *et al.* TNL-mediated immunity in Arabidopsis requires complex regulation of the redundant ADR1 gene family. *New Phytologist* **210**, 960–973 (2016).

31. Lapin, D. *et al.* A coevolved EDS1-SAG101-NRG1 module mediates cell death signaling by TIR-domain immune receptors. *Plant Cell* **31 (10)**, 2430–2455 (2019).

32. Castel, B. *et al.* Diverse NLR immune receptors activate defence via the RPW8-NLR NRG1. *New Phytologist* **222**, 966–980 (2019).

33. Wu, Z. *et al.* Differential regulation of TNL-mediated immune signaling by redundant helper CNLs. *New Phytologist* **222(2)**, 938-953 (2019).

34. Peart, J. R., Mestre, P., Lu, R., Malcuit, I. & Baulcombe, D. C. NRG1, a CC-NB-LRR protein, together with N, a TIR-NB-LRR protein, mediates resistance against tobacco mosaic virus. *Current Biology* **15(10)**, 968-73 (2005).

35. Qi, G. *et al.* Pandemonium Breaks Out: Disruption of Salicylic Acid-Mediated Defense by Plant Pathogens. *Molecular Plant* **11**, 1427–1439 (2018).

36. Roberts, M., Tang, S., Stallmann, A., Dangl, J. L. & Bonardi, V. Genetic Requirements for Signaling from an Autoactive Plant NB-LRR Intracellular Innate Immune Receptor. *PLoS Genetics* **9(4)** (2013).

37. Ve, T., Williams, S. J. & Kobe, B. Structure and function of Toll/interleukin-1 receptor/resistance protein (TIR) domains. *Apoptosis* **20(2)**, 250-61 (2015).

38. Zhang, X. *et al.* Multiple functional self-association interfaces in plant TIR domains. *Proceedings of the National Academy of Sciences* **114(10)**, (2017).

39. Mestre, P. & Baulcombe, D. C. Elicitor-mediated oligomerization of the tobacco N disease resistance protein. *Plant Cell* **18(2)**, 491-501 (2006).

40. Bentham, A., Burdett, H., Anderson, P. A., Williams, S. J. & Kobe, B. Animal NLRs provide structural insights into plant NLR function. *Annals of Botany* **119(5)**, 827-702 (2017).

41. Williams, S. J. *et al.* Structural basis for assembly and function of a heterodimeric plant immune receptor. *Science* **344(6181)**, 299–303 (2014).

42. Ma, S. *et al.* Direct pathogen-induced assembly of an NLR immune receptor complex to form a holoenzyme. *Science* **370(6521)** (2020).

43. Martin, R. *et al.* Structure of the activated ROQ1 resistosome directly recognizing the pathogen effector XopQ. *Science* **370(6521)** (2020).

44. Williams, S. J. *et al.* Structure and function of the TIR domain from the grape NLR protein RPV1. *Front Plant Sci* **7**, 1850 (2016).

45. Nishimura, M. T. *et al.* TIR-only protein RBA1 recognizes a pathogen effector to regulate cell death in Arabidopsis. *Proceedings of the National Academy of Sciences* **114(10)**, E2053-E2062 (2017).

46. Swiderski, M. R., Birker, D. & Jones, J. D. G. The TIR domain of TIR-NB-LRR resistance proteins is a signaling domain involved in cell death induction. *Molecular Plant-Microbe Interactions* **22(2)**, 157-65 (2009).

47. Dinesh-Kumar, S. P., Tham, W. H. & Baker, B. J. Structure-function analysis of the tobacco mosaic virus resistance gene N. *Proceedings of the National Academy of Sciences* **97(26)**, 14789-94 (2000).

48. Krasileva, K. v., Dahlbeck, D. & Staskawicz, B. J. Activation of an Arabidopsis Resistance Protein Is Specified by the in Planta Association of Its Leucine-Rich Repeat Domain with the Cognate Oomycete Effector. *Plant Cell* **22**, 2444–2458 (2010).

49. Yu, D. *et al.* TIR domains of plant immune receptors are 2′,3′-cAMP/cGMP synthetases mediating cell death. *Cell* **185**, 2370-2386 (2022).

50. Förderer, A. *et al.* A wheat resistosome defines common principles of immune receptor channels. *Nature* **610**, 532–539 (2022).

51. Jacob, P. *et al.* Plant "helper" immune receptors are Ca2+-permeable nonselective cation channels. *Science* **373(6553)**, 420-425 (2021).

52. Aarts, N. *et al.* Different requirements for EDS1 and NDR1 by disease resistance genes define at least two R gene-mediated signaling pathways in *Arabidopsis*. *Proceedings of the National Academy of Sciences* **95**, 10306–10311 (1998).

53. Wirthmueller, L., Zhang, Y., Jones, J. D. G. & Parker, J. E. Nuclear Accumulation of the Arabidopsis Immune Receptor RPS4 Is Necessary for Triggering EDS1-Dependent Defense. *Current Biology* **17**, 2023–2029 (2007).

54. Venugopal, S. C. *et al.* Enhanced disease susceptibility 1 and salicylic acid act redundantly to regulate resistance gene-mediated signaling. *PLoS Genetics* **5**, (2009).

55. Feys, B. J. *et al.* Arabidopsis SENESCENCE-ASSOCIATED GENE101 stabilizes and signals within an ENHANCED DISEASE SUSCEPTIBILITY1 complex in plant innate immunity. *Plant Cell* **17(9)**, 2601-13 (2005).

56. Glazebrook, J. *et al.* Phytoalexin-deficient mutants of Arabidopsis reveal that PAD4 encodes a regulatory factor and that four PAD genes contribute to downy mildew resistance. *Genetics* **146(1)**, 381-92 (1997).

57. Wiermer, M., Feys, B. J. & Parker, J. E. Plant immunity: The EDS1 regulatory node. *Current Opinion in Plant Biology* **8**, 383–389 (2005).

58. Wagner, S. *et al.* Structural basis for signaling by exclusive EDS1 heteromeric complexes with SAG101 or PAD4 in plant innate immunity. *Cell Host Microbe* **14**, 619–630 (2013).

59. Rietz, S. *et al.* Different roles of Enhanced Disease Susceptibility1 (EDS1) bound to and dissociated from Phytoalexin Deficient4 (PAD4) in Arabidopsis immunity. *New Phytologist* **191**, 107–119 (2011).

60. Saile, S. C. *et al.* Two unequally redundant 'helper' immune receptor families mediate Arabidopsis thaliana intracellular 'sensor' immune receptor functions. *PLoS Biol* **18(9)**, e3000783 (2020).

61. Cui, H. *et al.* A core function of EDS1 with PAD4 is to protect the salicylic acid defense sector in Arabidopsis immunity. *New Phytologist* **213**, 1802–1817 (2017).

62. Tanaka, S., Han, X. & Kahmann, R. Microbial effectors target multiple steps in the salicylic acid production and signaling pathway. *Frontiers in Plant Science* **6**, 349 (2015).

63. Sun, X. *et al.* Pathogen effector recognition-dependent association of NRG1 with EDS1 and SAG101 in TNL receptor immunity. *Nature Communications* **12**, 3335 (2021).

64. Collier, S. M., Hamel, L.-P. & Moffett, P. Cell Death Mediated by the N-Terminal Domains of a Unique and Highly Conserved Class of NB-LRR Protein. *Molecular Plant-Microbe Interactions* **24**, 918–931 (2011).

65. Feys, B. J., Moisan, L. J., Newman, M. A. & Parker, J. E. Direct interaction between the Arabidopsis disease resistance signaling proteins, EDS1 and PAD4. *EMBO Journal* **20(19)**, 5400-11 (2001).

66. Glazebrook, J. Contrasting mechanisms of defense against biotrophic and necrotrophic pathogens. *Annual Review of Phytopathology* **43**, 205-27 (2005).

67. Zhou, N., Tootle, T. L., Tsui, F., Klessig, D. F. & Glazebrook, J. PAD4 functions upstream from salicylic acid to control defense responses in *Arabidopsis*. *Plant Cell* **10(6)**, 1021-30 (1998).

68. Wildermuth, M. C., Dewdney, J., Wu, G. & Ausubel, F. M. corrigendum: Isochorismate synthase is required to synthesize salicylic acid for plant defence. *Nature* **417**, 571–571 (2002).

69. Mine, A. *et al.* An incoherent feed-forward loop mediates robustness and tunability in a plant immune network. *EMBO Rep* **18(3)**, 464-476 (2017).

70. Liu, Y. *et al.* Diverse roles of the salicylic acid receptors NPR1 and NPR3/ NPR4 in plant immunity. *Plant Cell* **32(12)**, 4002-4016 (2020).

71. Backer, R., Naidoo, S. & van den Berg, N. The NONEXPRESSOR OF PATHOGENESIS-RELATED GENES 1 (NPR1) and related family: Mechanistic insights in plant disease resistance. *Frontiers in Plant Science* **10**, 102 (2019).

72. Ding, Y. *et al.* Opposite Roles of Salicylic Acid Receptors NPR1 and NPR3/NPR4 in Transcriptional Regulation of Plant Immunity. *Cell* **173(6)**, 1454-1467 (2018).

73. Kumar, S. *et al.* Structural basis of NPR1 in activating plant immunity. *Nature* **605**, 561–566 (2022).

74. Ding, P. & Ding, Y. Stories of Salicylic Acid: A Plant Defense Hormone. *Trends in Plant Science* **25(6)**, 549-565 (2020).

75. Chini, A., Gimenez-Ibanez, S., Goossens, A. & Solano, R. Redundancy and specificity in jasmonate signalling. *Current Opinion in Plant Biology* 33, 147-156 (2016).

76. Chini, A. *et al.* The JAZ family of repressors is the missing link in jasmonate signalling. *Nature* **448(7154)**, 666-71 (2007).

77. Dombrecht, B. *et al.* MYC2 differentially modulates diverse jasmonate-dependent functions in Arabidopsis. *Plant Cell* **19(7)**, 2225-45 (2007).

78. Chen, R. *et al.* The Arabidopsis Mediator Subunit MED25 Differentially Regulates Jasmonate and Abscisic Acid Signaling through Interacting with the MYC2 and ABI5 Transcription Factors. *Plant Cell* **24**, 2898–2916 (2012).

79. Kazan, K. & Manners, J. M. MYC2: The master in action. *Mol Plant* **6**, 686–703 (2013).

80. Sasaki-Sekimoto, Y. *et al.* Basic Helix-Loop-Helix Transcription Factors JASMONATE-ASSOCIATED MYC2-LIKE1 (JAM1), JAM2, and JAM3 Are Negative Regulators of Jasmonate Responses in Arabidopsis. *Plant Physiology* **163**, 291–304 (2013).

81. Cui, H. *et al.* Antagonism of Transcription Factor MYC2 by EDS1/PAD4 Complexes Bolsters Salicylic Acid Defense in Arabidopsis Effector-Triggered Immunity. *Molecular Plant* **11**, 1053–1066 (2018).

82. Pieterse, C. M. J., van der Does, D., Zamioudis, C., Leon-Reyes, A. & van Wees, S. C. M. Hormonal modulation of plant immunity. *Annual Reviews of Cell Developmental Biology* **28**, 489-521 (2012).

83. Uppalapati, S. R. *et al.* The phytotoxin coronatine contributes to pathogen fitness and is required for suppression of salicylic acid accumulation in tomato inoculated with Pseudomonas syringae pv. tomato DC3000. *Molecular Plant Microbe Interactions* **20**, 955–965 (2007).

84. Zheng, X. Y. *et al.* Coronatine promotes pseudomonas syringae virulence in plants by activating a signaling cascade that inhibits salicylic acid accumulation. *Cell Host Microbe* **11**, 587–596 (2012).

85. Mittal, S. & Davis, K. R. Role of the phytotoxin coronatine in the infection of Arabidopsis thaliana by Pseudomonas syringae pv. tomato. *Molecular plant-microbe interactions* **8**, 165–171 (1995).

86. Melotto, M., Underwood, W., Koczan, J., Nomura, K. & He, S. Y. Plant Stomata Function in Innate Immunity against Bacterial Invasion. *Cell* **126**, 969–980 (2006).

87. Maekawa, T., Kracher, B., Vernaldi, S., van Themaat, E. V. L. & Schulze-Lefert, P. Conservation of NLR-triggered immunity across plant lineages. *Proceedings of the National Academy of Sciences* **109(49)**, 20119-23 (2012).

88. Tarr, D. E. K. & Alexander, H. M. TIR-NBS-LRR genes are rare in monocots: Evidence from diverse monocot orders. *BMC Research Notes* **2**, 197 (2009).

89. Shao, Z. Q. *et al.* Large-scale analyses of angiosperm nucleotide-binding site-leucine-rich repeat genes reveal three anciently diverged classes with distinct evolutionary patterns. *Plant Physiol*ogy**170 (4)**, 2095-109 (2016).

90. Zdrzałek, R., Kamoun, S., Terauchi, R., Saitoh, H. & Banfield, M. J. The rice NLR pair Pikp-1/Pikp-2 initiates cell death through receptor cooperation rather than negative regulation. *PLoS One* **15(9)**, e0238616 (2020).

91. Yuan, B. *et al.* The Pik-p resistance to Magnaporthe oryzae in rice is mediated by a pair of closely linked CC-NBS-LRR genes. *Theoretical and Applied Genetics* **122(5)**, 1017-28 (2011).

92. Guo, L. *et al.* Specific recognition of two MAX effectors by integrated HMA domains in plant immune receptors involves distinct binding surfaces. *Proceedings of the National Academy of Sciences* **115**, 11637–11642 (2018).

93. Mine, A. *et al.* The defense phytohormone signaling network enables rapid, high-amplitude transcriptional reprogramming during effector-triggered immunity. *Plant Cell* **30(6)**, 1199-1219 (2018)

94. Silverman, P. Salicylic Acid in Rice. *Advances in Food Research* **108**, 633–639 (1995).

95. Yuan, Y. *et al.* Functional analysis of rice NPR1-like genes reveals that OsNPR1/NH1 is the rice orthologue conferring disease resistance with enhanced herbivore susceptibility. *Plant Biotechnology J* **5**, 313–324 (2007).

96. Yang, Y., Qi, M. & Mei, C. Endogenous salicylic acid protects rice plants from oxidative damage caused by aging as well as biotic and abiotic stress. *Plant Journal* **40**, 909–919 (2004).

97. Patkar, R. N. *et al.* A fungal monooxygenase-derived jasmonate attenuates host innate immunity. *Nature Chemical Biology* **11(9)**,733-40 (2015).

98. Ke, Y. *et al.* Jasmonic Acid-Involved OsEDS1 Signaling in Rice-Bacteria Interactions. *Rice* **12(1)**, 25 (2019).

99. Mei, C., Qi, M., Sheng, G. & Yang, Y. Inducible overexpression of a rice allene oxide synthase gene increases the endogenous jasmonic acid level, PR gene expression, and host resistance to fungal infection. *Molecular Plant-Microbe Interactions* **19(10)**, 1127-37 (2006).

100. Yamada, S. *et al.* Involvement of OsJAZ8 in jasmonate-induced resistance to bacterial blight in rice. *Plant Cell Physiology* **53(12)**, 2060-72 (2012).

101. Yang, D. L. *et al.* Plant hormone jasmonate prioritizes defense over growth by interfering with gibberellin signaling cascade. *Proceedings of the National Academy of Sciences* **109(19)**, E1192-200 (2012).

102. García, A. v. *et al.* Balanced nuclear and cytoplasmic activities of EDS1 are required for a complete plant innate immune response. *PLoS Pathogens* **6(7)**, e1000970 (2010).

103. Bhattacharjee, S., Halane, M. K., Kim, S. H. & Gassmann, W. Pathogen Effectors Target Arabidopsis EDS1 and Alter Its Interactions with Immune Regulators. *Science* **334**, 1405–1408 (2011).

104. Heidrich, K. *et al.* Arabidopsis EDS1 Connects Pathogen Effector Recognition to Cell Compartment-Specific Immune Responses. *Science (1979)* **334**, 1401–1404 (2011).

105. Miao, J. *et al.* Targeted mutagenesis in rice using CRISPR-Cas system. *Cell Research* **23**, 1233–1236 (2013).

106. Vo, K. T. X. *et al.* OsWRKY67 plays a positive role in basal and XA21-mediated resistance in rice. *Frontiers in Plant Science* **8**, 2220 (2018).

107. Peng, S., Cassman, K. G., Virmani, S. S., Sheehy, J. & Khush, G. S. Yield potential trends of tropical rice since the release of IR8 and the challenge of increasing rice yield potential. in *Crop Science* **39**, 1552-1559 (1999).

108. Cho, L. H., Yoon, J. & An, G. The control of flowering time by environmental factors. *Plant Journal* **90(4)**, 708-719 (2017).

109. Hori, K., Matsubara, K. & Yano, M. Genetic control of flowering time in rice: integration of Mendelian genetics and genomics. *Theoretical and Applied Genetics* **129(12)**, 2241-2252 (2016).

110. Korves, T. M. & Bergelson, J. A developmental response to pathogen infection in Arabidopsis. *Plant Physiology* **133(1)**, 339-47 (2003).

111. Lyons, R. *et al.* Investigating the association between flowering time and defense in the Arabidopsis thaliana-Fusarium oxysporum interaction. *PLoS One* **10(6)**, e0127699 (2015).

112. Veronese, P. *et al.* Identification of a locus controlling Verticillium disease symptom response in Arabidopsis thaliana. *Plant Journal* **35(5)**, 574-87 (2003).

113. Ye, T. *et al.* Nitrogen, phosphorus, and potassium fertilization affects the flowering time of rice (Oryza sativa L.). *Global Ecology and Conservation* **20**, e00753 (2019).

114. Louis, J. *et al.* Antibiosis against the green peach aphid requires the Arabidopsis thaliana MYZUS PERSICAE-INDUCED LIPASE1 gene. *Plant Journal* **64(5)**, 800-11 (2010).

115. Zeng, X. *et al.* CRISPR/Cas9-mediated mutation of OsSWEET14 in rice cv. Zhonghua11 confers resistance to Xanthomonas oryzae pv. oryzae without yield penalty. *BMC Plant Biology* **20(1)**, 313 (2020).

116. Oliva, R. *et al.* Broad-spectrum resistance to bacterial blight in rice using genome editing. *Nature Biotechnology* **37(11)**, 1344-1350 (2019).

117. Rouina, H., Tseng, Y. H., Nataraja, K. N., Uma Shaanker, R. & Oelmüller, R. Arabidopsis restricts sugar loss to a colonizing trichoderma harzianum strain by downregulating sweet11 and-12 and upregulation of suc1 and sweet2 in the roots. *Microorganisms* **9(6)**, 1246 (2021).

118. Yaeno, T. & Iba, K. BAH1/NLA, a RING-type ubiquitin E3 ligase, regulates the accumulation of salicylic acid and immune responses to Pseudomonas syringae DC3000. *Plant Physiology* **148(2)**, 1032-41 (2008).

119. Sardar, A., Nandi, A. K. & Chattopadhyay, D. CBL-interacting protein kinase 6 negatively regulates immune response to Pseudomonas syringae in Arabidopsis. *Journal of Experimental Botany* **125**, 749–760 (2017).

120. Kitaoka, N. *et al.* Arabidopsis CYP94B3 encodes jasmonyl-l-isoleucine 12-hydroxylase, a key enzyme in the oxidative catabolism of jasmonate. *Plant Cell Physiology* **52(10)**, 1757-65 (2011).

121. Mackey, D., Holt, B. F., Wiig, A. & Dangl, J. L. RIN4 interacts with Pseudomonas syringae type III effector molecules and is required for RPM1-mediated resistance in Arabidopsis. *Cell* **108(6)**, 743-54 (2002).

122. Bittner-Eddy, P. D. & Beynon, J. L. The Arabidopsis downy mildew resistance gene, RPP13-Nd, functions independently of NDR1 and EDS1 and does not require the accumulation of salicylic acid. *Molecular Plant-Microbe Interactions* **14(3)**, 416-21 (2001).

123. Bittner-Eddy, P. D., Crute, I. R., Holub, E. B. & Beynon, J. L. RPP13 is a simple locus in Arabidopsis thaliana for alleles that specify downy mildew resistance to different avirulence determinants in Peronospora parasitica. *Plant Journal* **21(2)**, 177-88 (2000).

124. Schröder, F., Lisso, J., Lange, P. & Müssig, C. The extracellular EXO protein mediates cell expansion in Arabidopsis leaves. *BMC Plant Biology* **9**, 20 (2009).

125. Gu, T.-Y. *et al.* Dual-function DEFENSIN 8 mediates phloem cadmium unloading and accumulation in rice grains. *Plant Physiology* **191(1),** 515-527 (2022)

126. Kim, W. C., Kim, J. Y., Ko, J. H., Kang, H. & Han, K. H. Identification of direct targets of transcription factor MYB46 provides insights into the transcriptional regulation of secondary wall biosynthesis. *Plant Molecular Biology* **85(6)**, 589-99 (2014).

127. Sampedro, J. *et al.* AtBGAL10 is the main xyloglucan β-galactosidase in arabidopsis, and its absence results in unusual xyloglucan subunits and growth defects. *Plant Physiology* **158(3)**, 1146-57 (2012).

128. Boron, A. K. *et al.* Proline-rich protein-like PRPL1 controls elongation of root hairs in Arabidopsis thaliana. *Journal of Experimental Botany* **65(18)**, 5485-95 (2014).

129. Chen, X. *et al.* Arabidopsis U-box E3 ubiquitin ligase PUB11 negatively regulates drought tolerance by degrading the receptor-like protein kinases LRR1 and KIN7. *Journal Integrative Plant Biology* **63(3)**, 494-50 (2021).

130. Ortega-Amaro, M. A. *et al.* Overexpression of AtGRDP2, a novel glycine-rich domain protein, accelerates plant growth and improves stress tolerance. *Frontiers of Plant Science* **5**, 782 (2015).

131. Kurzbauer, M. T. *et al.* Arabidopsis thaliana FANCD2 promotes meiotic crossover formation. *Plant Cell* **30(2)**, 415-428 (2018).

132. Fischer, W. N. *et al.* Low and high affinity amino acid H+-cotransporters for cellular import of neutral and charged amino acids. *Plant Journal* **29(6)**, 717-31 (2002).

133. Salaj, J. *et al.* AtSERK1 expression precedes and coincides with early somatic embryogenesis in Arabidopsis thaliana. *Plant Physiology and Biochemistry* **46(7)**, 709-714 (2008).

134. Yuan, H. & Liu, D. Genetic evidence that Arabidopsis ALTERED ROOT ARCHITECTURE encodes a putative dehydrogenase involved in homoserine biosynthesis. *Plant Cell Reports* **33(1)**, 25-33 (2014).

135. Bruex, A. *et al.* A gene regulatory network for root epidermis cell differentiation in Arabidopsis. *PLoS Genetics* **8(1)**, e1002446 (2012).

136. Ke, Y., Liu, H., Li, X., Xiao, J. & Wang, S. Rice OsPAD4 functions differently from Arabidopsis AtPAD4 in host-pathogen interactions. *Plant Journal* **78**, 619–631 (2014).

137. Saur, I. M. L., Bauer, S., Lu, X. & Schulze-Lefert, P. A cell death assay in barley and wheat protoplasts for identification and validation of matching pathogen AVR effector and plant NLR immune receptors. *Plant Methods* **15**, 118 (2019).

138. Cesari, S. *et al.* New recognition specificity in a plant immune receptor by molecular engineering of its integrated domain. *Nat Communications* **13(1)**, 1524 (2022).

139. Jia, A. *et al.* TIR-catalyzed ADP-ribosylation reactions produce signaling molecules for plant immunity. *Science* **377(6605)**, eabq8180 (2022).

140. Huang, S. *et al.* Identification and receptor mechanism of TIR-catalyzed small molecules in plant immunity. *Science* **377(6605)**, eabq3297 (2022).

141. Horsefield, S. *et al.* NAD+ cleavage activity by animal and plant TIR domains in cell death pathways. *Science* **365(6455)**, 793-799 (2019).

142. Wan, L. *et al.* TIR domains of plant immune receptors are NAD+-cleaving enzymes that promote cell death. *Science* **365(6455)**, 799-803 (2019).

143. Casey, L. W. *et al.* The CC domain structure from the wheat stem rust resistance protein Sr33 challenges paradigms for dimerization in plant NLR proteins. *Proceedings of the National Academy of Sciences* **113(45)**, 12856-12861 (2016).

144. Cui, H. *et al.* A core function of EDS1 with PAD4 is to protect the salicylic acid defense sector in Arabidopsis immunity. *New Phytologist* **213**, 1802–1817 (2017).

145. Bi, D. *et al.* Mutations in an atypical TIR-NB-LRR-LIM resistance protein confer autoimmunity. *Frontiers of Plant Science* **2**, 71 (2011).

146. Noutoshi, Y. *et al.* A single amino acid insertion in the WRKY domain of the Arabidopsis TIR-NBS-LRR-WRKY-type disease resistance protein SLH1 (sensitive to low humidity 1) causes activation of defense responses and hypersensitive cell death. *Plant Journal* **43(6)**, 873-88 (2005).

147. Li, X., Clarke, J. D., Zhang, Y. & Dong, X. Activation of an EDS1-mediated R-gene pathway in the snc1 mutant leads to constitutive, NPR1-independent pathogen resistance. *Molecular Plant-Microbe Interactions* **14(10)**, 1131-9 (2001).

148. Louis, J., Leung, Q., Pegadaraju, V., Reese, J. & Shah, J. P4D4-dependent antibiosis contributes to the ssi2-conferred hyper-resistance to the green peach aphid. *Molecular Plant-Microbe Interactions* **23(5)**, 618-27 (2010).

149. Zaka, A. *et al.* Natural variations in the promoter of OsSWEET13 and OsSWEET14 expand the range of resistance against Xanthomonas oryzae pv. Oryzae. *PLoS One* **13(9)**, e0203711 (2018).

150. Hutin, M., Sabot, F., Ghesquière, A., Koebnik, R. & Szurek, B. A knowledge-based molecular screen uncovers a broad-spectrum OsSWEET14 resistance allele to bacterial blight from wild rice. *Plant Journal* **84(4)**, 694-703 (2015).

151. Antony, G. *et al.* Rice xa13 recessive resistance to bacterial blight is defeated by induction of the disease susceptibility gene Os-11N3. *Plant Cell* **22(11)**, 3864-76 (2010).

152. Johanndrees, O. *et al.* Variation in plant Toll/Interleukin-1 receptor domain protein dependence on ENHANCED DISEASE SUSCEPTIBILITY 1 *Plant Physiology* **191(1)**, 626-642 (2022)

153. Riedlmeier, M. *et al.* Monoterpenes support systemic acquired resistance within and between plants. *Plant Cell* **29(6)**, 1440-1459 (2017).

154. Rustérucci, C., Aviv, D. H., Holt, B. F., Dangl, J. L. & Parker, J. E. The disease resistance signaling components EDS1 and PAD4 are essential regulators of the cell death pathway controlled by LSD1 in Arabidopsis. *Plant Cell* **13(10)**, 2211-24 (2001).

155. Breitenbach, H. H. *et al.* Contrasting roles of the apoplastic aspartyl protease APOPLASTIC, ENHANCED DISEASE SUSCEPTIBILITY1-DEPENDENT1 and LEGUME LECTIN-LIKE PROTEIN1 in arabidopsis systemic acquired resistance. *Plant Physiol* **165(2)**, 791-809 (2014).

156. Straus, M. R., Rietz, S., ver Loren Van Themaat, E., Bartsch, M. & Parker, J. E. Salicylic acid antagonism of EDS1-driven cell death is important for immune and oxidative stress responses in Arabidopsis. *Plant Journal* **62(4)**, 628-40 (2010).

157. Riemann, M. *et al.* Impaired Induction of the Jasmonate Pathway in the Rice Mutant hebiba. *Plant Physiology* **133(4)**, 1820-30 (2003).

158. Riemann, M. *et al.* Identification of rice Allene Oxide Cyclase mutants and the function of jasmonate for defence against Magnaporthe oryzae. *Plant Journal* **74**, 226–238 (2013).

159. Branon, T. C. *et al.* Efficient proximity labeling in living cells and organisms with TurboID. *Nature Biotechnology* **36**, 880–887 (2018).

160. Zhang, Y. *et al.* Turboid-based proximity labeling for in planta identification of protein-protein interaction networks. *Journal of Visualized Experiments* (2020) doi: 10.3791/60728.

161. Zhang, Y. *et al.* TurboID-based proximity labeling reveals that UBR7 is a regulator of N NLR immune receptor-mediated immunity. *Nature Communications* **10(1)**, 3252 (2019).

162. Hopkins, C. M., White, F. F., Choi, S. H., Guo, A. & Leach, J. E. Identification of a family of avirulence genes from Xanthomonas oryzae pv. oryzae. *Molecular Plant-Microbe Interactions* **5(6)**, 451-9 (1992).

163. Gonzalez, C. *et al.* Molecular and pathotypic characterization of new Xanthomonas oryzae strains from West Africa. *Molecular Plant-Microbe Interactions* **20(5)**, 534-46 (2007).

164. Bogdanove, A. J. *et al.* Two new complete genome sequences offer insight into host and tissue specificity of plant pathogenic Xanthomonas spp. *Journal of Bacteriology* **193(19)**, 5450-64 (2011).

165. Yoshida, K. *et al.* Association genetics reveals three novel avirulence genes from the rice blast fungal pathogen magnaporthe oryzae. *Plant Cell* **21(5)**, 1573-9 (2009).

166. Deak, M., Kiss, G. B., Koncz, C. & Dudits, D. Transformation of Medicago by Agrobacterium mediated gene transfer. *Plant Cell Reports* **5(2)**, 97-100 (1986).

Erklärung zur Dissertation

„Hiermit versichere ich an Eides statt, dass ich die vorliegende Dissertation selbstständig und ohne die Benutzung anderer als der angegebenen Hilfsmittel und Literatur angefertigt habe. Alle Stellen, die wörtlich oder sinngemäß aus veröffentlichten und nicht veröffentlichten Werken dem Wortlaut oder dem Sinn nach entnommen wurden, sind als solche kenntlich gemacht. Ich versichere an Eides statt, dass diese Dissertation noch keiner anderen Fakultät oder Universität zur Prüfung vorgelegen hat; dass sie - abgesehen von unten angegebenen Teilpublikationen und eingebundenen Artikeln und Manuskripten - noch nicht veröffentlicht worden ist sowie, dass ich eine Veröffentlichung der Dissertation vor Abschluss der Promotion nicht ohne Genehmigung des Promotionsausschusses vornehmen werde. Die Bestimmungen dieser Ordnung sind mir bekannt. Darüber hinaus erkläre ich hiermit, dass ich die Ordnung zur Sicherung guter wissenschaftlicher Praxis und zum Umgang mit wissenschaftlichem Fehlverhalten der Universität zu Köln gelesen und sie bei der Durchführung der Dissertation zugrundeliegenden Arbeiten und der schriftlich verfassten Dissertation beachtet habe und verpflichte mich hiermit, die dort genannten Vorgaben bei allen wissenschaftlichen Tätigkeiten zu beachten und umzusetzen. Ich versichere, dass die eingereichte elektronische Fassung der eingereichten Druckfassung vollständig entspricht."

Cologne, 19. December 2022

Joel Fernandes

Last but not the least

Plants are sessile organisms that are permanently restricted to their site of germination